

---

# Performance Optimisation of a Residential Wood Log Burning Stove

---

- Engineering Doctorate Innovation Report -

*Author:*

Adam AZENIC

*Primary supervisor:*

Gavin R. TABOR

*Contacts:*

adam.azenic@gmail.com

G.R.Tabor@exeter.ac.uk

January, 2023

**EPSRC**  
Pioneering research  
and skills

UNIVERSITY OF  
**EXETER**

CENTRE FOR DOCTORAL TRAINING  
IN **SUSTAINABLE**  
**MATERIALS AND**  
**MANUFACTURING**

 **WWMG**  
THE UNIVERSITY OF WARWICK

  
hunterstoves  
GROUP

*Cranfield*  
UNIVERSITY

I wish to show my sincere gratitude to my primary supervisor, Professor Gavin R. Tabor, for giving me very valuable guidance, advice and support in the entire research and in the writing of this thesis.

I would also like to extend my gratitude to my industrial mentor Mike Stoneman and Hunter Stoves' directors, Paul Grimes and Steve Clatworthy. Without their support and funding this project would not have been realised.

Lastly, I would like to express my deepest appreciation to my wife, Nikolina, who has given me love and relentless support over the entire duration of the project, and to my sons, Petar and Filip, who have constantly brought me joy and happiness.



## Abstract

Governments from around the world are committed to tighten the legal limits regarding pollutant emission levels from residential wood burning appliances. The European Union has decided to implement new Ecodesign pollutant emission limits from 1st January 2022, to which the United Kingdom is still committed, even after Brexit. This is the motivation for this doctorate project, whose aim is to minimise pollutant emission levels from commercial residential wood log burning stoves to below the required Ecodesign limits and, if possible, to below the pollutant levels from wood stoves present in the market today. Towards achieving this aim the relevant scientific and industrial literature has been reviewed, adequate formulae for calculation of important physical quantities have been derived, novel design of a down-draft gasification stove has been developed through iterative stove design, manufacturing, assembling, testing and analysis, the test data of the eight developed gasification stove variations and of seven extant conventional (up-draft) stoves have been analysed, and the developed gasification stove design has been optimised and compared to the performance data of the comparable counterparts. Statistical design of experiments was a method used for finding the statistically significant and influential design factors, or parameters, of the developed gasification stove design. The four tested design factors were i) primary chamber base area, ii) nozzle cover geometry, iii) secondary chamber glass area and iv) geometry of secondary chamber outlet (hole arrangement). Through analysis of variance it was shown that first two played the most influential and statistically significant role in emission factors of carbon monoxide and organic gaseous compounds. Distinct qualitative features of the tested gasification stove variants have been identified, tested and discussed: i) primary chamber sooting regime, ii) blow-back, iii) char bed channeling, iv) instability of secondary flame ignition, and v) the potential for leakage of air and, more importantly, of fuel rich pyrolytic gases into the otherwise clean flue gas stream. Important findings and conclusions of this project are: the tested gasification stove design is overall superior to the extant conventional designs in terms of pollutant emission levels and thermal efficiency; analysed conventional stoves can emit low particulate matter levels (2 to 15 mg/Nm<sup>3</sup> @ 13% O<sub>2</sub>) if the maximum volume fraction of CO<sub>2</sub> in flue gases is below 12%; such limit in maximum CO<sub>2</sub> concentration can be achieved by increasing the combustion chamber volume; alternatively, low pollutant levels can be achieved through increased slimness of the combustion chamber, even for increased CO<sub>2</sub>; tested gasification stoves feature two distinct regimes of elevated pollutant emissions: *oxygen deficient* and *char bed channeling* regime; oxygen deficient regime can be avoided if CO<sub>2</sub> in flue gases is kept below the effective mixing limit of a nozzle, whereas the char bed channeling regime can be minimised through adequate primary chamber design, wood log size, count and moisture content; two design factors in tested gasification stoves that were found to be most significant and influencing on the pollutant emissions during the char bed channeling regime were the surface area of a primary chamber stove base and the geometry of nozzle cover; the optimum gasification stove configuration featured following pollutant

emission levels:  $CO = 36.1 \text{ ppm}^1$ ,  $THC = 4.58^1 \text{ mgC/Nm}^3$ ,  $PM = 10.02^1 \text{ mg/Nm}^3$  (in some configurations down to  $5.62^1 \text{ mg/Nm}^3$ ) and efficiency = 92%. With such performance values, possibly excluding the PM, it is believed that the developed gasification stove is the lowest polluting one to come into the market, thus successfully achieving the project's aim.

---

<sup>1</sup> normalised to 13 vol% O<sub>2</sub>

# Contents

|  |           |
|--|-----------|
| <b>Nomenclature</b>                                    | <b>15</b> |
| <b>1 Introduction</b>                                  | <b>21</b> |
| 1.1 Motivation and Background . . . . .                | 22        |
| 1.2 Aims and Objectives . . . . .                      | 24        |
| 1.3 Document Outline . . . . .                         | 26        |
| <b>2 Literature Review</b>                             | <b>27</b> |
| 2.1 Studied Pollutant Gases and Particles . . . . .    | 27        |
| 2.1.1 Particulate Matter . . . . .                     | 28        |
| 2.1.2 Gaseous Emissions . . . . .                      | 28        |
| 2.2 Emission Factors of Pollutants . . . . .           | 29        |
| 2.3 Parameters Affecting Pollutant Emissions . . . . . | 30        |
| 2.3.1 Combustion Phases . . . . .                      | 30        |
| 2.3.2 Biomass Fuel Species . . . . .                   | 31        |
| 2.3.3 Fuel Moisture . . . . .                          | 31        |
| 2.3.4 Appliance/Fuel Type . . . . .                    | 32        |
| 2.3.5 Combustion Chamber Load . . . . .                | 34        |
| 2.3.6 User Influence . . . . .                         | 35        |

|          |   |           |
|----------|---|-----------|
| 2.4      | Measures for Reducing Pollutant Emissions                                   | 35        |
| 2.4.1    | Primary Measures  | 36        |
| 2.4.2    | Secondary Measures  | 37        |
| 2.5      | Limitation on Using Available Scientific Articles as Data Sources           | 38        |
| 2.6      | Overview of Pollutant Emissions from Commercial Wood Log Burning Appliances | 39        |
| 2.7      | Chapter Summary   | 40        |
| <b>3</b> | <b>Combustion Theory</b>  | <b>44</b> |
| 3.1      | Calculation of $CO_{2,max}$   | 45        |
| 3.2      | Concentration Normalisation to 13 % $O_2$                                   | 48        |
| 3.2.1    | Averaging Values  | 50        |
| 3.3      | Calculation of Normalised CO Volume Fraction                                | 51        |
| 3.4      | Calculation of Normalised OGC Concentration                                 | 51        |
| 3.5      | Calculation of Normalised Concentration of Particulate Matter in Flue Gas   | 53        |
| 3.6      | Flue Gas Mass Flow  | 54        |
| 3.6.1    | Calculation of Specific Volume of Dry Flue Gas                              | 55        |
| 3.6.2    | Calculation of Specific Volume of Water Vapour in Flue Gas                  | 58        |
| 3.6.3    | Final Formula for Flue Gas Mass Flow  | 60        |
| 3.7      | Thermal Heat Loss in Flue Gas   | 60        |
| 3.8      | Chemical Heat Loss in Flue Gas  | 61        |
| 3.9      | Efficiency  | 62        |
| 3.10     | Heat Output of the Appliance  | 63        |
| 3.11     | Conversion of Units of Pollutant EFs  | 63        |
| 3.12     | Chapter Summary   | 65        |

|          |   |           |
|----------|---|-----------|
| <b>4</b> | <b>Research Methodology</b>   | <b>66</b> |
| 4.1      | BS EN 16510-1:2018 Standard Specifications and Ecodesign Requirements . . . . . | 66        |
| 4.1.1    | Particulate Matter Sampling Procedure . . . . .                                 | 67        |
| 4.1.2    | Calculation Methods . . . . .   | 68        |
| 4.1.3    | Deviation from BS EN 16510-1 Procedure . . . . .                                | 69        |
| 4.2      | Testing Equipment Specifications . . . . .                                      | 69        |
| 4.3      | Statistical Design of Experiments . . . . .                                     | 72        |
| 4.4      | Firewood . . . . .  | 73        |
| 4.4.1    | Test Firewood Humidity Control . . . . .  | 73        |
| 4.5      | Chapter Summary . . . . .   | 73        |
| <b>5</b> | <b>Stove Design Development and Experimental Setup</b>                          | <b>75</b> |
| 5.1      | Basic Types of Residential Wood Burning Stoves . . . . .                        | 75        |
| 5.2      | Gasification Stove Prototypes . . . . .   | 80        |
| 5.2.1    | First prototype - 1.0 . . . . .   | 83        |
| 5.2.2    | Second prototype(s) - 2.0 and 2.1 . . . . .                                     | 84        |
| 5.2.3    | Third prototype - 3.0 and 3.1 . . . . .   | 85        |
| 5.2.4    | Fourth Prototype . . . . .  | 85        |
| 5.3      | Experimental Setup . . . . .  | 86        |
| 5.3.1    | Experiment Planning . . . . .   | 86        |
| 5.3.2    | Factorial Experiment . . . . .  | 87        |
| 5.4      | Comparison of Several Conventional Stove Models . . . . .                       | 88        |
| <b>6</b> | <b>Results</b>  | <b>91</b> |

|          |   |            |
|----------|---|------------|
| 6.1      | Emission Data Overview - Conventional versus Gasification Stoves Comparison . . . . .                               | 91         |
| 6.2      | Conventional Stoves' Test Results . . . . .   | 97         |
| 6.2.1    | Gaseous PIC Emissions of Tested Conventional Stoves . . . . .   | 97         |
| 6.2.2    | Particulate Matter Emission from Conventional Stoves . . . . .  | 98         |
| 6.2.3    | Influence of Combustion Chamber Volume on $CO_{2,max}$ . . . . .  | 100        |
| 6.3      | Gasification Stoves' Test Results . . . . .   | 104        |
| 6.3.1    | Significant Features of a Wood Gasification Stove . . . . .   | 104        |
| 6.3.2    | Gasification Stove Experimental Design Table and Results . . . . .  | 109        |
| 6.3.3    | Time evolution of $CO_2$ and $CO$ . . . . .   | 110        |
| 6.3.4    | Statistical Analysis . . . . .  | 122        |
| 6.3.5    | Assessment of Leakage into the Flue Way . . . . .   | 134        |
| 6.3.6    | EN 16510-1 Test Results of Optimal Stove Configuration . . . . .  | 139        |
| <b>7</b> | <b>Discussion</b>   | <b>140</b> |
| 7.1      | Discussion of Experimental Observations, Results, Analyses and Recommendations . . . . .                            | 143        |
| 7.1.1    | Comparison of Conventional and Gasification Stove Models . . . . .  | 143        |
| 7.1.2    | Discussion of Test Results from Conventional Stove Models . . . . .   | 144        |
| 7.1.3    | Discussion of Test Results from Gasification Stove Variations . . . . .   | 145        |
| 7.1.4    | Optimal Configuration of a Developed Gasification Stove . . . . .   | 155        |
| 7.1.5    | Comparison of PIC Levels of a Developed Gasification Stove to Other Stoves from the Literature & Industry . . . . . | 155        |
| 7.1.6    | Limitations of the reviewed scientific articles . . . . .   | 158        |
| 7.1.7    | Downsides of BS EN 16510-1, or similar, standard . . . . .  | 158        |

- 8 Conclusions & Recommendations** **162**
  
- Appendix A Results of Statistical Analyses** **176**
  
- A.1 Original Data Set - Data Set 1 . . . . . 176
  - A.1.1 Carbon Monoxide - Data Set 1 . . . . . 176
  - A.1.2 Particulate Matter - Data Set 1 . . . . . 178
  
- A.2 Data from Initial 15 Minutes of Every Charge - Data Set 2 . . . . . 180
  
- A.3 Data Without Initial 15 Minutes of Every Charge - Data Set 3 . . . . . 181
  - A.3.1 Carbon Monoxide - Data Set 3 . . . . . 181
  - A.3.2 Total Hydrocarbons - Data Set 3 . . . . . 183
  
- A.4 Data Without  $CO_2 > 15\%$  - Data Set 4 . . . . . 185
  - A.4.1 Carbon Monoxide - Data Set 4 . . . . . 185
  - A.4.2 Total Hydrocarbons - Data Set 4 . . . . . 187

# List of Figures

|     |  |    |
|-----|--|----|
| 1.1 | Emissions of particulate matter ( $PM_{2.5}$ ), from different sources, from 1990 until 2020, in the UK. Source: [1] . . . . .   | 23 |
| 1.2 | History of PM emissions from wood stoves tested in the Danish Technological Institute between 2004 and 2020. This data is provided by the Danish Terchnological Institute and is not in the public domain. . . . . | 24 |
| 5.1 | Basic designs for residential wood log burning appliances. . . . .   | 76 |
| 5.2 | Side cross-section of a gasification stove concept. . . . .  | 78 |
| 5.3 | Examples of commercially available natural drought down-flow domestic heating appliances. . . . .  | 79 |
| 5.5 | Two types of nozzle inlet covers - factor C. . . . .   | 87 |
| 5.6 | Two types of secondary chamber outlet geometries - factor D. . . . .   | 87 |
| 6.1 | Comparison of normalised $CO$ and $CO_2$ values between the conventional and gasification stove designs. . . . .   | 93 |
| 6.2 | Comparison of normalised $THC$ and $CO_2$ values between the conventional and gasification stove designs; semi-log plot. . . . .   | 94 |
| 6.3 | Comparison of normalised $THC$ and normalised $CO$ values between the conventional and gasification stove designs; log-log plot. . . . .   | 94 |
| 6.4 | Comparison of $THC_{avg}$ and $CO_{avg}$ values between the conventional and gasification stove designs. . . . .   | 95 |
| 6.5 | Normalised $CO$ and $THC$ versus $CO_2$ for 7 conventional stove models. . . . .   | 98 |



|      |   |     |
|------|---|-----|
| 6.6  | Scatter plot of $PM$ versus $CO_{2,max}$ values, with corresponding linear regression lines. . . . .                                    | 99  |
| 6.7  | Scatter plot of $CO_{2,max}$ (averaged across all charges) versus combustion chamber volume for every conventional stove model. . . . . | 100 |
| 6.8  | $CO_2$ versus normalised $CO$ and $THC$ values for stoves a (smallest one) and e (biggest one). . . . .                                 | 102 |
| 6.9  | Original $CO$ vs time data. Runs 1 and 2. . . . .   | 111 |
| 6.10 | Original $CO$ vs time data. Runs 3 and 4. . . . .   | 112 |
| 6.11 | Original $CO$ vs time data. Runs 5 and 6. . . . .   | 113 |
| 6.12 | Original $CO$ vs time data. Runs 7 and 8. . . . .   | 114 |
| 6.13 | Photographs of influencing events in a primary chamber in run 3. . . . .  | 118 |
| 6.14 | Photographs of influencing events in a primary chamber in run 5. . . . .  | 119 |
| 6.15 | Photograph of an influencing event in a primary chamber in run 8. . . . .   | 119 |
| 6.16 | Photographs of influencing events in a primary chamber in run 7. . . . .  | 120 |
| 6.17 | Comparison of time evolution of $CO$ and $THC$ between stove configurations with smaller and bigger char base areas. . . . .            | 121 |
| 6.18 | Adjusted $R^2$ and model p-values for PIC data from 3 data sets. . . . .  | 124 |
| 6.19 | Scatter plot of model p-values versus adjusted $R^2$ values. . . . .  | 125 |
| 6.20 | Scatter plot of $PM$ versus $CO_{2,max}$ during particulate matter sampling period of 30 minutes. . . . .                               | 128 |
| 6.21 | Charge averaged values of $CO$ versus $PM$ . . . . .  | 129 |
| 6.22 | Charge averaged values of $THC$ versus $PM$ . . . . .   | 130 |
| 6.23 | Time evolution of $CO_2$ values at EN and undiluted sampling points during a 3.5 hour burn time. . . . .                                | 135 |
| 6.24 | Period 1. Temperature, $CO_2$ , $CO$ and $\Delta CO$ versus time for both EN and undiluted sampling streams. . . . .                    | 136 |

|      |   |     |
|------|---|-----|
| 6.25 | Period 2. Temperature, $CO_2$ , $CO$ and $\Delta CO$ versus time for both EN and undiluted sampling streams. . . . .                  | 137 |
| 6.26 | Scatter plot of undiluted $CO$ versus $\Delta CO$ for both periods. . . . .   | 138 |
| 7.1  | Primary chamber geometry, with restricted depth and side clearances between the firewood and walls. . . . .                           | 149 |
| 7.2  | Comparison of PIC emission data and efficiency values between the developed gasification stove and other stoves and boilers . . . . . | 157 |
| A.1  | Normal probability plot . . . . .   | 177 |
| A.2  | Residual plot . . . . .   | 177 |
| A.3  | Normal probability plot . . . . .   | 179 |
| A.4  | Residual plot . . . . .   | 179 |
| A.5  | Normal probability plot . . . . .   | 182 |
| A.6  | Residual plot . . . . .   | 182 |
| A.7  | Normal probability plot . . . . .   | 184 |
| A.8  | Residual plot . . . . .   | 184 |
| A.9  | Normal probability plot of the residuals. . . . .   | 186 |
| A.10 | Plot of residuals versus predicted yield. . . . .   | 186 |
| A.11 | Normal probability plot . . . . .   | 188 |
| A.12 | Residual plot . . . . .   | 188 |

# List of Tables

|     |   |    |
|-----|---|----|
| 1.1 | Ecodesign limit values. . . . .   | 22 |
| 2.1 | <i>CO</i> , <i>TOC</i> and <i>PM</i> EFs obtained for three different types of boilers. . . . .   | 33 |
| 2.2 | Brunner et al results for optimised (secondary air included) and non-optimised (secondary air excluded) wood stove design. . . . .  | 36 |
| 2.3 | Representative list of stoves present on the European market. . . . .   | 41 |
| 2.4 | List of natural draft wood gasification stoves present on the European market, with corresponding performance values. All emission factors are normalised to 13% O <sub>2</sub> . . . . . | 42 |
| 2.5 | Representative list of gasification fan-assisted boilers with air valve regulation via lambda sensor. . . . .   | 43 |
| 3.1 | Relative molar contents of hydrogen, oxygen and sulphur in the test fuel with their formulae and units. . . . .   | 45 |
| 3.2 | Oxidation reactions of every main constituent of test fuel and their molar oxygen demand. . . . .   | 46 |
| 4.1 | Formulae for calculation of stove performance parameters defined by the BS EN 16510-1:2018 standard. . . . .  | 68 |
| 5.1 | Identified factors and their levels to be tested in a factorial experiment. . . . .   | 86 |
| 5.2 | Experimental design table. High level: +, Low level: -. . . . .   | 89 |

|      |   |     |
|------|---|-----|
| 5.3  | List of the seven conventional stoves with corresponding combustion chamber dimensions, volumes and top plate material. . . . . | 90  |
| 6.1  | $h/A$ ratio values for every conventional stove model. . . . .  | 98  |
| 6.2  | Experimental results from three data sets: 1, 3 and 4, with corresponding experimental design configurations. . . . .           | 109 |
| 6.3  | Photographs of all particulate matter sampling filters. . . . .   | 131 |
| 6.4  | Performance data of the - - - - stove configuration, tested according to BS EN 16510-1. . . . .                                 | 139 |
| A.1  | Effect estimates, aliases, regression coefficients and % contribution with $CO$ as response variable in data set 1 . . . . .    | 176 |
| A.2  | ANOVA table with $CO$ as response variable in data set 1 . . . . .  | 177 |
| A.3  | Regression model summary - $CO$ - data set 1 . . . . .  | 177 |
| A.4  | Effect estimates, aliases, regression coefficients and % contribution with $PM$ as response variable in data set 1 . . . . .    | 178 |
| A.5  | ANOVA table with $PM$ as response variable in data set 1 . . . . .  | 178 |
| A.6  | Regression model summary - $THC$ - data set 1 . . . . .   | 178 |
| A.7  | Effect estimates, aliases, regression coefficients and % contribution with $CO$ as response variable in data set 3 . . . . .    | 181 |
| A.8  | ANOVA table with $CO$ as response variable in data set 3 . . . . .  | 181 |
| A.9  | Regression model summary - $CO$ - data set 3 . . . . .  | 181 |
| A.10 | Effect estimates, aliases, regression coefficients and % contribution with $THC$ as response variable in data set 3 . . . . .   | 183 |
| A.11 | ANOVA table with $THC$ as response variable in data set 3 . . . . .   | 183 |
| A.12 | Regression model summary - $THC$ - data set 3 . . . . .   | 183 |
| A.13 | Effect estimates, aliases, regression coefficients and % contribution with $CO$ as response variable in data set 4 . . . . .    | 185 |

---

|  |     |
|--|-----|
| A.14 ANOVA table with <i>CO</i> as response variable in data set 4 . . . . .   | 185 |
| A.15 Regression model summary - <i>CO</i> - data set 4 . . . . .   | 186 |
| A.16 Effect estimates, aliases, regression coefficients and % contribution with<br><i>THC</i> as response variable in data set 4 . . . . . | 187 |
| A.17 ANOVA table with <i>THC</i> as response variable in data set 4 . . . . .  | 187 |
| A.18 Regression model summary - <i>THC</i> - data set 4 . . . . .  | 187 |

# Nomenclature

| <b>Greek letters</b>   |  | <b>Unit</b>  |
|------------------------|--|--|
| $\eta$                 | Thermal efficiency   | %  |
| $\lambda$              | Air excess ratio   | -  |
| $\nu$                  | Stoichiometric molar oxygen demand                               | (mol O <sub>2</sub> )/(mol C <sub>fuel</sub> )   |
| $\Phi_g$               | Flue gas mass flow   | (kg gas)/h   |
| $\rho$                 | Density  | kg/m <sup>3</sup>  |
| <b>Roman letters</b>   |  | <b>Unit</b>  |
| $\Delta H_{CO_{oxid}}$ | Enthalpy of oxidation of CO into CO <sub>2</sub>                 | kJ/mol kJ/Nm <sup>3</sup>  |
| $\Delta H_f$           | Enthalpy of formation  | kJ/mol   |
| $\Delta T$             | Temperature difference   | K  |
| $\dot{m}$              | Flue gas mass flow   | g/s or kg/h  |
| $C$                    | Heat capacity  | kJ/K   |
| $C_f$                  | Gas meter calibration factor                                     | -  |
| $C_f$                  | Mass fraction of carbon in fuel                                  | (kg C)/(kg fuel)   |
| $C_p$                  | Specific heat capacity per unit volume                           | kJ/(m <sup>3</sup> K)  |
| $CO$                   | Volume fraction of carbon monoxide                               | (m <sup>3</sup> CO)/(m <sup>3</sup> dfg) or vol ppm  |
| $CO_2$                 | Volume fraction of carbon dioxide                                | (m <sup>3</sup> CO <sub>2</sub> )/(m <sup>3</sup> dfg) or vol%   |
| $CO_{2,max}$           | Maximum possible volume fraction of carbon dioxide in flue gases | vol%   |
| $EF$                   | Emission factor  | %, vol ppm, $\frac{\text{mg pollutant}}{\text{Nm}^3}$ , $\frac{\text{mg pollutant}}{\text{MJ input energy}}$ |
| $FGV$                  | Flue gas volume  | m <sup>3</sup>   |

|           |   |  |
|-----------|---|--|
| $FW$      | Filter weight   | mg                                     |
| $G$       | Specific flue gas volume created by fuel combustion                         | $(Nm^3)/(kg \text{ fuel})$             |
| $G_C$     | Contribution to specific flue gas volume by fuel bound carbon per unit mass | $(Nm^3)/(kg \text{ C})$                |
| $G_d$     | Specific volume of dry flue gases per unit mass of fuel                     | $(Nm^3 \text{ dfg})/(kg \text{ fuel})$ |
| $G_H$     | Contribution to specific flue gas volume by fuel bound carbon per unit mass | $(Nm^3)/(kg \text{ H})$                |
| $G_N$     | Contribution to specific flue gas volume by fuel bound carbon per unit mass | $(Nm^3)/(kg \text{ N})$                |
| $G_O$     | Contribution to specific flue gas volume by fuel bound carbon per unit mass | $(Nm^3)/(kg \text{ O})$                |
| $G_S$     | Contribution to specific flue gas volume by fuel bound carbon per unit mass | $(Nm^3)/(kg \text{ S})$                |
| $G_w$     | Specific volume of wet flue gases per unit mass of fuel                     | $(Nm^3 \text{ wfg})/(kg \text{ fuel})$ |
| $G_{wv}$  | Specific volume of water vapour in flue gases per unit mass of fuel         | $(Nm^3 \text{ wv})/(kg \text{ fuel})$  |
| $H_f$     | Mass fraction of hydrogen in fuel   | $(kg \text{ H})/(kg \text{ fuel})$     |
| $H_{i,f}$ | Lower calorific value of fuel   | $kJ/(kg \text{ fuel})$                 |
| $i$       | iterator  | -                                      |
| $j$       | Molar content of hydrogen atoms relative to carbon atoms                    | $(kmol \text{ H})/(kmol \text{ C})$    |
| $k$       | Molar content of oxygen atoms relative to carbon atoms                      | $(kmol \text{ O})/(kmol \text{ C})$    |
| $l$       | Molar content of sulphur atoms relative to carbon atoms                     | $(kmol \text{ S})/(kmol \text{ C})$    |
| $M$       | Molar mass  | $(kg)/(kmol)$                          |
| $m$       | Mass  | kg or g                                |
| $N$       | Total number of sampled data points   | -                                      |
| $n$       | Amount of substance   | kmol or mol                            |
| $O_f$     | Mass fraction of oxygen in fuel   | $(kg \text{ O})/(kg \text{ fuel})$     |
| $p$       | Pressure  | Pa                                     |

|                        |   |                                   |
|------------------------|---|-----------------------------------|
| $Q$                    | Specific heat, per unit mass of fuel  | kJ/(kg fuel)                      |
| $Q^*$                  | Heat  | kJ                                |
| $Q_{\text{chem}}, Q_b$ | Chemical heat losses  | kJ/(kg fuel)                      |
| $Q_a$                  | Thermal heat losses   | kJ/(kg fuel)                      |
| $q_a$                  | Relative thermal heat losses  | %                                 |
| $q_b$                  | Relative chemical heat losses   | %                                 |
| $q_r$                  | Relative chemical heat losses due to char residue                                 | %                                 |
| $R^2$                  | R-squared   | -                                 |
| $R_u$                  | Universal gas constant; $R_u \approx 8.3145$                                      | (m <sup>3</sup> Pa)/(K mol)       |
| $S_f$                  | Mass fraction of sulphur in fuel  | (kg S)/(kg fuel)                  |
| $T$                    | Absolute temperature  | K                                 |
| $THC, C_{\text{OGC}}$  | Mass concentration of OGC, also referred to as THC                                | (mg C)/(Nm <sup>3</sup> dfg)      |
| $THC_{\text{propane}}$ | Total hydrocarbon volume fraction expressed in propane equivalents<br>ppm propane | vol<br>ppm propane                |
| $V$                    | Volume  | m <sup>3</sup>                    |
| $v, G$                 | Specific volume of a substance  | m <sup>3</sup> /kg                |
| $V_m$                  | Molar volume of any ideal gas at STP conditions; $V_m = 22.414$                   | (Nm <sup>3</sup> )/(kmol)         |
| $x$                    | Molar fraction of a constituent in a mixture                                      | (kmol constituent)/(kmol mixture) |
| $Y$                    | Mass fraction of a component in a mixture   | (kg component)/(kg mixture)       |
| FGV                    | Flue gas volume   | m <sup>3</sup>                    |

### Subscripts

|      |                |
|------|----------------|
| a    | After          |
| b    | Before         |
| C    | Celsius degree |
| chem | chemical       |
| conc | Concentration  |



daf Dry, ash free basis

dfg Dry flue gases

f Fuel

fir Fired basis

max Maximum

min Minimum

r Char residue

s Sampled

stoich stoichiometric

wfg Wet flue gases

wv Water vapour

### **Acronyms and Abbreviations**

$C_3H_8$  Propane molecule

ANOVA Analysis of Variance

avg Averaged emission value

BC Black carbon

C Carbon atom

CDT SMM Centre for Doctoral Training in Sustainable Materials and Manufacturing

CFD Computational Fluid Dynamics

CO Carbon monoxide

CO<sub>2</sub> Carbon dioxide

Defra Department for Environment, Food and Rural Affairs

DIN Deutsches Institut für Normung

DoE Design of experiments

DTI Danish Technological Institute

---

|  |  |
|--|--|
| EF   | Emission factor  |
| EngD   | Engineering Doctorate  |
| EPSRC  | Engineering and Physical Sciences Research Council                               |
| EU   | European Union   |
| FID  | Flame Ionisation Detector  |
| H  | Hydrogen atom  |
| KCl  | Potassium chloride   |
| MV   | Measured value   |
| N <sub>2</sub>   | Nitrogen molecule  |
| N <sub>2</sub> O                                       | Nitrous oxide  |
| N/A  | Not applicable   |
| Nm <sup>3</sup>  | Normal cubic metre, i.e. cubic metre of a substance at STP conditions            |
| NO   | Nitric oxide   |
| NO <sub>2</sub>  | Nitrogen dioxide   |
| NO <sub>x</sub>  | Nitric oxides  |
| norm   | Normalised emission value (to 13% O <sub>2</sub> )                               |
| NV   | Normalised value   |
| O  | Oxygen atom  |
| O <sub>2</sub>   | Oxygen molecule  |
| OC   | Organic Carbon   |
| OGC  | Organic Gaseous Carbon   |
| PAH  | Polycyclic Aromatic Hydrocarbons   |
| PIC  | Products of incomplete combustion  |
| PM   | Particulate Matter   |
| PM <sub>10</sub> , PM <sub>2.5</sub> , PM <sub>1</sub> | Particulate matter with particle size under 10 μm, 2.5 μm and 1 μm, respectively |

- S Sulphur atom
- SO<sub>x</sub> Sulphur oxides
- STP Standard temperature and pressure
- THC Total Hydrocarbons
- UK United Kingdom
- V Value
- VOC Volatile organic compounds

# Chapter 1

## Introduction

Residential wood combustion<sup>1</sup> is still often used as a renewable energy source in Europe [2], however it can be a major contributor to pollutant emissions into the atmosphere [3, 4]. Therefore, governments impose restrictions on pollutant emissions through legislation and standards. In the European Union, residential solid fuel appliances are currently regulated through the EN 13240 standard. However, from 1st January 2022, all EU countries will replace EN 13240 with the new one, EN 16510-1, and with new, stricter, Ecodesign pollutant emission limits [5, 6], shown in Table 1.1<sup>2</sup>. The UK has, as once an EU member country, also committed to implementing the Ecodesign emission limits for residential wood burning appliances. Even after Brexit, 'Defra<sup>3</sup> has confirmed its commitment to Ecodesign, as it will introduce stricter limits on emissions' [7, 8]. This engineering doctorate (EngD) project is, therefore, focused on finding ways to lower pollutant emissions to below Ecodesign limits, and, if possible, below emission values of most of appliances currently present on the market.

This EngD project was funded by the EPSRC<sup>4</sup> Centre for Doctoral Training in Sustainable Materials and Manufacturing (EP/L016389/1) and the company Hunter Stoves Limited<sup>5</sup>. Hunter Stoves designs, manufactures and wholesales wood log burning stoves for a wide market that includes the United Kingdom, the EU, New Zealand, Australia, and Japan.

---

<sup>1</sup> Residential wood combustion refers to combustion of wood, generally on a small scale (up to 50 kW of heat output), in residential environment, either for water heating (in furnaces or boilers) or for direct room heating - as wood log stoves.

<sup>2</sup> For comparison, the previous standard (BS EN 13240:2001 + A2:2004) only limits the efficiency to a minimum of 50 % and carbon monoxide emission to a maximum of 1 vol%, whereas the other pollutants, those covered by the Ecodesign limits, are not regulated by the EN 13240.

<sup>3</sup> Department for Environment, Food and Rural Affairs (in the UK government)

<sup>4</sup> Engineering and Physical Sciences Research Council

<sup>5</sup> Hunter Stoves Limited, 8 Emperor Way, Exeter Business Park, Exeter, EX1 3QS, United Kingdom

Table 1.1: Ecodesign limit values [9]. Each emission value is normalised to a standardised amount of oxygen (13 %).

|                                      |                          |
|--------------------------------------|--------------------------|
| CO @ 13% O <sub>2</sub>              | 1200 ppm                 |
| PM @ 13% O <sub>2</sub>              | 40 mg/Nm <sup>3</sup>    |
| THC @ 13% O <sub>2</sub>             | 120 mg C/Nm <sup>3</sup> |
| NO <sub>x</sub> @ 13% O <sub>2</sub> | 200 mg/Nm <sup>3</sup>   |
| Efficiency                           | > 65 %                   |

## 1.1 Motivation and Background

Like all biomass fuels, burning wood is a carbon neutral process [10], as the emitted carbon dioxide (CO<sub>2</sub>) is absorbed back into growing biomass through photosynthesis. By 'carbon neutral' it is meant that there is low<sup>6</sup> net addition of carbon dioxide into the atmosphere considering the process as a whole. Hence wood is considered a renewable energy source [10]. Nevertheless, burning wood, besides releasing CO<sub>2</sub>, also emits pollutants, some of which are gases, such as carbon monoxide (CO), unburnt hydrocarbons, nitrogen oxides, and particulate matter (PM), amongst others [10]. Reducing pollutant emissions from biomass burning appliances is not a trivial task and represents an everlasting challenge to the industry.

Figure 1.1 shows emissions of particulate matter in the UK, from various sources, including 'domestic combustion' [1]. The graph shows that the PM<sub>2.5</sub> emissions from domestic combustion in 2020 are comparable to those from manufacturing industries and construction, and approximately twice as large as the emissions from road transport and industrial processes. Similar trend can be observed if comparing PM<sub>10</sub> emissions [1]. Hence it can be concluded that PM emissions from domestic combustion are considerable<sup>7</sup> and need to be reduced, ideally through technological advancement - which will be the topic of this dissertation.

<sup>6</sup>Considering only wood combustion, it is a zero carbon process, however the whole process usually includes parts where fossil fuels are burnt, e.g. operation of firewood processing machinery, trucks, drying kilns, etc.

<sup>7</sup>Reader should note that 'domestic combustion' accounts for all domestic sources of particulate matter, including open fires and closed ones, i.e. wood stoves - which produce considerably less PM.

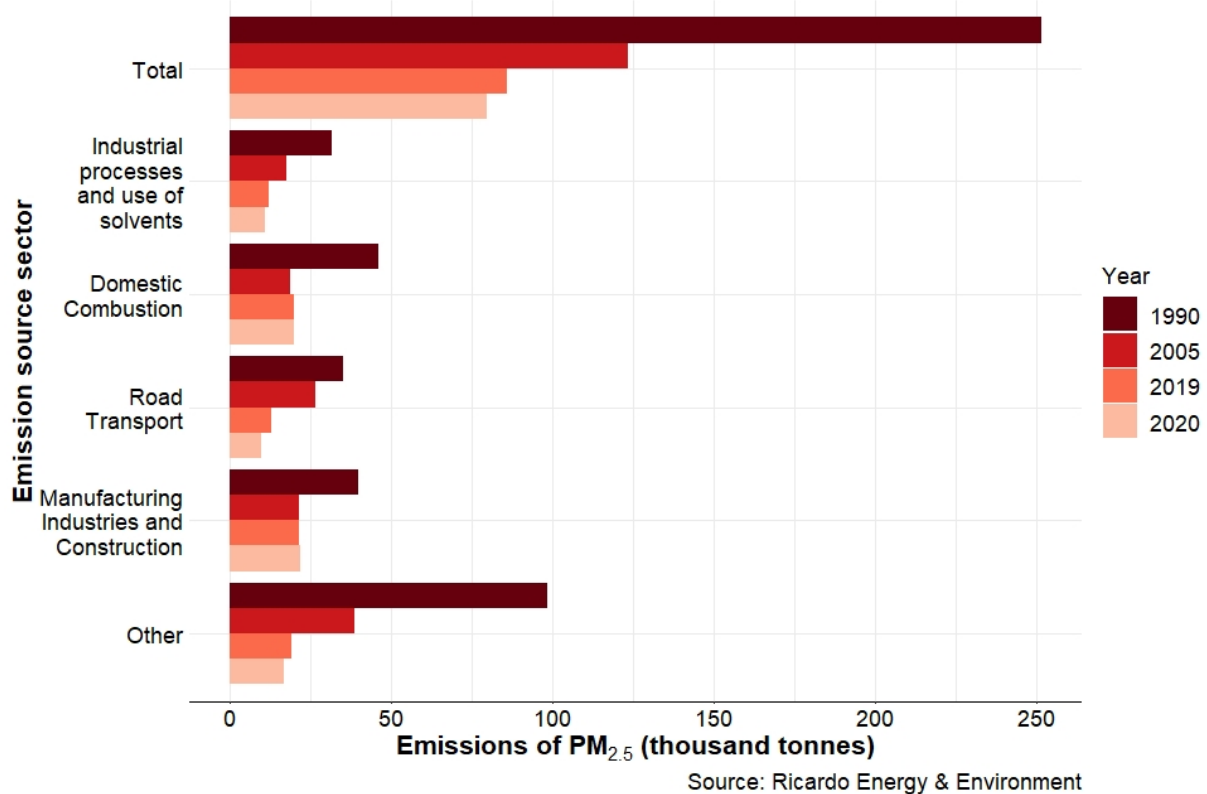


Figure 1.1: Emissions of particulate matter (PM<sub>2.5</sub>), from different sources, from 1990 until 2020, in the UK. Source: [1]

The Figure 1.2 shows the history of emissions of total particulate matter from wood stoves, type tested in the Danish Technological Institute between the years 2004 and 2020. Testing was done in accordance to NS3058 particle emission standard, meaning that PM sampling was done in a full flow dilution tunnel. Every datum point in the graph represents a weighted average of the total PM emission over up to four burn rates. The graph shows a declining trend in the PM emission between 2004 and 2012, while in later years the PM emission has flattened around 2 - 2.5 g/kg. This could indicate a limit of what the current stove technology is capable of. Hence, a novel wood stove technology might be needed in order to shift the emissions to lower levels.

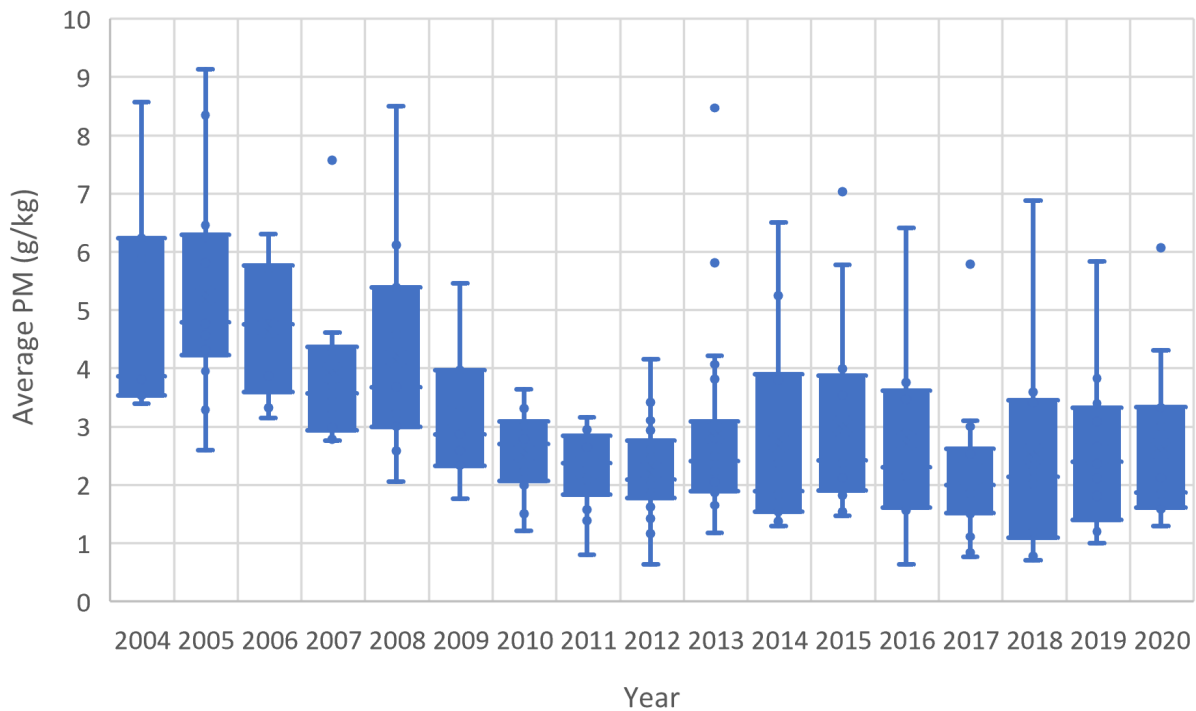


Figure 1.2: History of PM emissions from wood stoves tested in the Danish Technological Institute between 2004 and 2020. This data is provided by the Danish Technological Institute and is not in the public domain.

## 1.2 Aims and Objectives

The aim of this EngD project is to *minimise pollutant emissions from wood stoves* (i.e. any natural draft<sup>8</sup> driven wood log burning appliance) by numerical and experimental methods. The goal is to find ways to surpass the EU 'Ecodesign' emissions regulations [5, 6] and, if possible, to surpass the performance values of wood stoves present in the market today. In previous EngD reports the numerical methods have been reviewed [11] and evaluated [12], whereas in this thesis the physical experiments were the main methodology. The proximate objectives towards achieving the stated aim are:

1. To produce a literature review of the state-of-the-art in emission data and design of current stoves present on the market.
2. To identify and explain the industrial standard for construction, testing, limits of pollutant emission levels and calculation methods.
3. To design and fabricate a stove prototype or prototypes (as a proof-of-concept) for testing.

<sup>8</sup>Natural draft refers to the draft (pressure difference) in the range 10 - 20 Pa created by the chimney.

4. To identify important factors that influence performance of a stove through testing.
5. To design and conduct a factorial experiment in order to evaluate these previously identified factors, and to statistically analyse the experimental data.
6. To analyse test results of a commercial range of stoves, representative for the market, and of the developed stove model; and to produce guidance on designing a stove that emits minimal levels of pollutants.



## 1.3 Document Outline

The thesis is structured through the following eight chapters:

1. In the first chapter the introduction, motivation, aims and objectives of the thesis are given.
2. In the second chapter a review of the literature is provided. It covers categorisation of pollutant gases and particles that are of importance to this work, parameters affecting pollutant emissions, commonly used measures for reducing pollutant emissions, and finishes with an overview of pollutant emissions from different types of commercially available appliances.
3. Combustion theory is presented in the third chapter, in which formulae used in the EN 16510-1 standard are derived.
4. Research methods used in this project are explained in the fourth chapter. The chapter covers the important procedures and methods defined by the EN 16510-1 standard, specifications of testing equipment, a brief overview of statistical design of experiments methodology, and firewood specifications used in the experiments.
5. In the fifth chapter the design and development process of a gasification stove prototype is presented, as well as the experimental setup and features of tested conventional stoves. Gasification stove design is a specific design of a wood burning appliance where thermal decomposition of firewood and subsequent gaseous combustion occur in different reaction chambers. More detailed explanation is provided later in Section 5.1.
6. In the sixth chapter the testing data and results from analyses are presented. First the general comparison of emission data between the conventional and developed gasification stove models is provided. Then the testing data from the conventional stove range is analysed. Lastly, the experimental data and analyses of the gasification stove prototype are given.
7. A discussion of the results is presented in the seventh chapter.
8. In the last, eighth, chapter the conclusion to the thesis and recommendations for future development projects are provided.

In the next chapter the literature review is presented.

# Chapter 2

## Literature Review

In this chapter the review of relevant literature regarding residential wood combustion is presented. The literature review covers the following topics :

- different types of pollutant gases and particulates,
- different kinds of emission factors of pollutants, that is, what units are usually used when quantifying pollutant emission levels,
- different parameters affecting pollutant emissions,
- measures that are usually undertaken to lower pollutant emissions,
- limitations of using available scientific articles as sources of data for pollutant emission values, and
- different commercial models of conventional stoves, gasification stoves and gasification boilers.

### 2.1 Studied Pollutant Gases and Particles

There are many different kinds and categories of pollutant gases and particles being emitted from biomass burning appliances and these will be explored in this section. The emission factors will be presented in  $\text{mg}/\text{Nm}^3$  dry flue gas normalised to 13 % oxygen content, as these units are standard in the industry. If units from cited sources need to be converted, the assumptions taken into account will be reported.

### 2.1.1 Particulate Matter

Particulate matter (PM) is a mixture of particles in solid and liquid phases with various compositions and morphologies that are suspended in the flue gas or in the atmosphere. PM emitted from biomass combustion contains fly ash and soot, which in turn contains organic carbon (OC) and black carbon (BC). Generally, biomass burning appliances with more complete combustion emit less PM with higher relative content of inorganics (e.g. KCl), whereas the appliances with more incomplete combustion emit more PM with higher relative content of organics (e.g. OC and BC) [13].

PM is generally classified in three size categories:  $PM_{10}$  (particles under  $10\ \mu\text{m}$ ),  $PM_{2.5}$  (under  $2.5\ \mu\text{m}$ ) and  $PM_1$  (under  $1\ \mu\text{m}$ ). Smaller particles are considered more hazardous as they penetrate further into the lungs when inhaled [13].

There are several methods for measurement of PM, one of which is manual gravimetric method which measures total particulate matter content. It is described by EN 13284-1 [14] standard and required method for PM measurement during certification tests of wood stoves. Hence, the gravimetric method is the one used in this work.

### 2.1.2 Gaseous Emissions

Gaseous pollutants in the flue gases produced by biomass combustion include carbon monoxide (CO), nitric oxides ( $NO_x$ ), sulphur oxides ( $SO_x$ ), organic gaseous carbon (OGC), as well as several other pollutant gases that are of less importance for this work.

Carbon monoxide is a product of incomplete combustion of a carbon-containing fuel, e.g. biomass. CO emission from wood stoves ( $3077 - 7692\ \text{mg}/\text{Nm}^3$  at 13 % oxygen<sup>1</sup>) is generally much higher than that from natural gas boilers ( $40\ \text{mg}/\text{Nm}^3$  at 13 % oxygen<sup>1</sup>) [13].

$NO_x$  are pollutants formed during combustion and consist of nitric oxide (NO) and nitrogen dioxide ( $NO_2$ ). It is considered to be a major contributor to photochemical smog and ozone in the urban air (troposphere), and participates in a chain reaction removing ozone from the stratosphere, resulting in increased ultraviolet radiation reaching the surface of the earth.  $NO_x$  is produced through four different routes: thermal, prompt, from nitrous oxide ( $N_2O$ ) and fuel-bound nitrogen route, which is the primary source of  $NO_x$  during biomass combustion [15].

<sup>1</sup>The conversion from g/GJ is calculated according to formula (3.114).

Wood combustion emits low levels of  $\text{SO}_x$ , due to the low sulphur content of wood (<0.5 % on a dry basis).

Volatile organic compounds (VOC) refer to any organic compound with boiling temperature less than 250 °C at a pressure of 101325 Pa [13]. In the context of residential wood combustion, they are measured by a flame ionisation detector (FID) which is capable of measuring the amount of organically bound carbon atoms present in the VOC of the sampled flue gas stream (referred to as organic gaseous carbon (OGC)), ionised in a hydrogen flame within the detector [16]. FID responds strongly to organically bound carbon and has a negligible response to inorganic flue gas compounds (e.g. CO, CO<sub>2</sub>, NO, H<sub>2</sub>O). VOCs include a wide range of substances, such as hydrocarbons, halocarbons and oxygenates.

Polycyclic Aromatic Hydrocarbons (PAHs) are a type of hydrocarbon VOCs, which are often treated separately from other hydrocarbons due to their carcinogenic effects [13]. However, in this work, all VOCs were collectively measured through FID, as required by the BS EN 16510-1 standard which regulates design of and emissions from wood stoves. VOCs in the context of FID measurement are also often referred to as organic gaseous carbon (OGC) or total hydrocarbons (THC).

In this study, only CO, CO<sub>2</sub>, OGC and PM were measured as their measurement is required by BS EN 16510-1 standard<sup>2</sup>.

## 2.2 Emission Factors of Pollutants

Pollutant emission levels are quantified through emission factors (EFs), normally expressed in the following units:

- (mg pollutant)/(kg fuel)
- (mg pollutant)/(MJ energy input from fuel)
- (mg pollutant)/(m<sup>3</sup> flue gas) at reference conditions, e.g. STP conditions and standardised oxygen content in flue gas (in the case of wood stoves it is 13 vol% O<sub>2</sub>)
- percentage (or ppm) of pollutant by volume of the flue gas at reference (STP) conditions

---

<sup>2</sup>Measurement of NO<sub>x</sub> is also required by the standard, however the NO<sub>x</sub> measurement module was not available when the experiments were conducted.

When the emission factors of a pollutant is expressed for STP conditions, cubic metres are referred to as 'normal' cubic metres, abbreviated as Nm<sup>3</sup>.

In this study, according to BS EN 16510-1, pollutant emission factors are expressed in following units: PM in mg/Nm<sup>3</sup> of dry flue gas, CO<sub>2</sub> in vol% of dry flue gas, CO in vol ppm of dry flue gas and OGC is mg/Nm<sup>3</sup> dry flue gas (all at 13% oxygen content).

## 2.3 Parameters Affecting Pollutant Emissions

There are numerous parameters that affect pollutant EFs from biomass combustion, and the ones identified by the reviewed scientific literature will be presented in the following sections.

### 2.3.1 Combustion Phases

The burning cycle of a stove can be split into three stages:

1. The initial stage, when the first firewood batch is ignited. The first batch usually consists of kindling and, possibly, several normal sized wood logs. The objective in burning the ignition batch is to create enough char for the effective ignition of the next firewood batch, in a short period of time and, possibly with minimised sooting regime. However, this stage is usually the most polluting period of the entire heating duration of a stove [17, 18].
2. The middle stage which consists of multiple firewood batches (or charges, or refuelling cycles), with a usual burn duration of 45 minutes or more.
3. During the last stage, there is no more refuelling, only burnout of char that has been accumulated by all previous charges. This stage is characterised by elevated CO and OGC EFs.

During every charge cycle in the middle stage, three distinct combustion phases can be observed, as identified by many researchers (e.g. [19, 20, 21, 22, 23, 24, 25], and others)<sup>3</sup>:

1. Ignition phase - characterised with elevated PM, CO and OGC emissions; and high fuel mass loss rate

---

<sup>3</sup>Sometimes the researchers use slightly different terminology, but they refer to the same phenomena.

2. Flaming (intermediate) phase - efficiency is highest, lasts the longest and emissions are lowest in comparison, and
3. Char burnout (or glowing) stage - characterised with elevated CO and OGC emissions (see e.g. Olsson and Kjallstrand [22]); and low fuel mass loss rate.

The three phases are also evident from the test results obtained from experiments and will be identified in the Results chapter (6).

### 2.3.2 Biomass Fuel Species

Biomass fuel is available in a number of different forms: wood, straw or hay, or other grassy species, whilst wood can be further categorised as hardwood or softwood, or as individual wood species: spruce, birch, beech, oak, pine, etc.

Mitchel et al [26] have confirmed linear dependence of NO<sub>x</sub> EF and fuel-bound nitrogen content (which is universally low in wood, compared to other solid fuels, e.g. coal), and higher PM EFs for lower volatile content fuels, i.e. coal, compared to wood. Wood combustion data gave similar PM EFs for three different wood species. Much greater pollutant EF variance was found between different stages of combustion.

Krpec et al [27] have found low dependency of CO and PM EFs on fuel type, whereas Bignal et al [23] found no consistent effect of wood species on pollutant EFs. Petterson et al [18] have concluded that there is no significant difference between birch and other softwood fuels for most of the main pollutant EFs (except for terpenes,  $\delta$ -3-Carene, R-pinene, myrcene and limonene). Calvo et al [19] have reported higher EFs of CO, THC and PM for hardwood (eucalyptus) combustion than softwood (pine). However, concluding from Figure 6 of the same article, it can be seen that other parameters, such as the specific combustion phase, influence CO EF much more.

Hence, it can be concluded that there is no significant difference in EFs of pollutants such as CO, OGC and PM between burning different wood species, compared to the influence of other parameters.

### 2.3.3 Fuel Moisture

Many literature sources (e.g. Krpec et al [27], Johansson et al [28], Shen et al [25], Bignal et al [23]), have found that combustion of any biomass containing less moisture

will generally emit less CO, PM or OGC. However, the magnitude of impact of a fuel moisture content on emission levels, can depend on other factors (e.g. refuelling frequency). Therefore, in the following paragraph the qualitative observation of burning wood logs during testing with different moisture contents will be explained.

It was observed that a range of firewood moisture content of 12% to 20% provides optimum emission levels.

Burning drier firewood leads to very high variation in rates of thermal decomposition of firewood during a single charge. Hence it is very difficult to adjust the air inflow rate, which needs to be fixed<sup>4</sup> according to BS EN 16510-1. Apart from a great variation on decomposition rate, the peak decomposition rate is higher than that of a wetter firewood, for the same air inflow rates. It was observed that a very low emission regime (with CO @ 13% O<sub>2</sub> below 50 vol ppm (which is close to 63 mg/Nm<sup>3</sup>)) is achievable with dry firewood (with moisture content below 10%), in conventional, up draft burning stoves. However, the emission regime during other phases of combustion is much more polluting, which elevates overall PIC emission levels. Moreover, the decomposition rate is very sensitive to the air inflow rate into the char zone<sup>5</sup>. This is due to the fact that char burns at different rates for different air inflows, which has a large influence on the rate of firewood decomposition.

On the other hand wet firewood (where moisture content is above 20%) features a long ignition time (due to drying which is an endothermic process) and, hence, a prolonged elevated pollution regime. Moreover, soot (or smoke) is clearly visible throughout the entire charge burn time.

### 2.3.4 Appliance/Fuel Type

Appliance, or fuel type parameter refers to the biomass fuel being in the shape of either wood logs, wood chips, pellets, briquettes or similar, i.e. the appliance being designed to burn either one of these fuel types.

Johansson et al [28] tested i) two 'old-type' wood boilers, or conventional up-draft boiler design; ii) three 'modern' wood boilers, or gasification design; iii) four pellet boilers; and iv) two oil burners. The averaged EF values for CO, TOC and PM are presented in Table 2.1 (excluding oil burners). It is clear that pellet burning appliances gave lowest, and updraft stoves highest EFs for case of all pollutants.

<sup>4</sup>In absence of any automated air valve mechanism.

<sup>5</sup>The reader is referred to section 5.1 for explanation of stove operation and of different zones within the appliance.

Table 2.1: CO, TOC and PM EFs obtained for three different types of boilers. All EFs are shown in mg/Nm<sup>3</sup> @ 13% oxygen content - converted from mg/MJ through formula (3.114). Source: Johansson et al [28]

| Type       | CO           | TOC         | PM         |
|------------|--------------|-------------|------------|
| Up-draft   | 6300 - 25000 | 1000 - 7400 | 135 - 3400 |
| Down-draft | 780 - 5800   | 21 - 1050   | 28 - 137   |
| Pellets    | 46 - 1700    | 1.5 - 385   | 20 - 100   |

Lamberg et al [17] have tested both pellets and wood logs in the same hybrid stove and found that burning pellets emitted 92 % less PM and 65 % less CO.

However, Obernberger et al [29] reported that down-draft log wood boilers (also called gasification boilers) emit the lowest levels of PM<sub>10</sub>, compared to pellet and wood chip boilers: 5 to 14 mg/Nm<sup>3</sup>; pellet boilers emit around 15 mg/Nm<sup>3</sup>, whilst wood chip boilers emit the highest levels: 38 to 49 mg/Nm<sup>3</sup> of PM<sub>10</sub> (see Figure 9 in [20] and Figure 5 in [29]). The units are converted from mg/MJ according to formula (3.114).

Obaidullah et al [30], pp.155, reported in their review the PM levels for

- pellet stoves: 31 - 60 mg/Nm<sup>3</sup>,
- pellets boilers: 13 - 95 mg/Nm<sup>3</sup>,
- wood chip boilers: 28 - 75 mg/Nm<sup>3</sup> and
- wood log boilers: 6.8 - 59 mg/Nm<sup>3</sup>.

From the examples above (Johansson et al [28], Lamberg et al [17], Obernberger et al [29], Brunner et al [20] and Obaidullah et al [30]) it can be seen that the disparity in emission levels, even for the same fuel, or appliance category, is large. This is probably due to the fact that tested appliances by the researchers do not operate with identical levels of other, more fundamental, factors, such as stoichiometry (air excess ratio); number, position, orientation and jet velocity of secondary air holes; mixing conditions; human (operator) influence, etc. Nevertheless, it can also be concluded that very clean burning regimes are possible for down-draft wood log and pellet burning appliances.



### 2.3.5 Combustion Chamber Load

Combustion chamber load is the parameter often referred to as heat output, fuel load, or any similar metric which quantifies how the amount of fuel, or, consequently, the heat output, influences the emission factors. The most objective parameter to give this metric should be residence time of gases at sufficiently high temperature. However, this parameter is difficult to test in practice, hence alternative parameters are devised, such as heat output or fuel load, which are more dependant on a specific appliance.

Shen et al [25] have tested 0.5, 1 and 2 kg wood charge mass and found no significant difference in any measured pollutant EF.

Boman et al [31] found during testing of pellet appliances at different fuel loads (1.7 to 6 kW input energy) that higher fuel load lead to lower emissions of CO, OGC and PAH. On the other hand, in the second part of the study, where wood logs were tested, Petterson et al [18] found that increased heat output (achieved with dry and finely cleaved wood logs) lead to high emission levels due to oxygen deficiency. Those findings are opposite, and in authors opinion, both unrepresentative of the *combustion chamber load* parameter. Should Boman et al [31] have tested even higher heat output, they would have observed elevated pollutant EFs (due to either oxygen deficiency or lack of residence time), whereas if Petterson et al [18] had allowed for more air to enter the gaseous combustion zone (above the fuel bed), oxygen levels would be higher, hence pollutant EFs would be lower.

Signal et al [23] achieved lower heat output, i.e. lower combustion rate of wood by reducing the air flow rate - they called this 'slumber mode'. They observed higher CO EFs in slumber mode (521 - 6002 ppm) than in full flame mode (96 - 4744 ppm). Analogously to the case in the study of Boman et al [31] (mentioned in the paragraph above), low heat output leads to higher CO emissions. This could have been the case due to many other possible factors affecting the emissions: air excess ratio, low jet velocities at air entrainment holes affecting mixing, geometry of the combustion chamber, etc.

As already mentioned, residence time is probably the most objective parameter, but difficult to test in appliances; however, Boman et al [32] have shown in the reactor tube experiment that in the well mixed, air rich conditions (high air excess ratio) and high temperature conditions ( $> 850$  °C), combustion of softwood pellets gives very low levels of all gaseous products of incomplete combustion (PICs). It was also shown that residence time is of minor importance in minimizing gaseous PIC emission levels. Total PM, on the other hand, was not found to be correlated with either the combustion

chamber temperature or residence time.

### 2.3.6 User Influence

Pollutant EFs also depend on the way users operate their wood burning appliances [2, 33]. There are various factors that user can influence, e.g. [2, 20]:

- fuel related factors,
- different ways to ignite the fire,
- combustion air settings,
- frequency and intensity of use, or
- log wood orientation in a combustion chamber (vertical versus horizontal) [17]

It should be noted that any wood burning appliance which is not automated, i.e. where user is required to manually load fuel, or to manually adjust the air valve settings, will perform at different PIC emission levels, mostly above the levels tested in a laboratory by a very experienced engineer.

## 2.4 Measures for Reducing Pollutant Emissions

Measures for reducing pollutant emission levels are generally split into *primary* and *secondary* measures:

- Primary measures refer to the modifications to be made in the combustion process itself in order to minimise the emission levels, whereas
- secondary measures refer to the modifications (or processes) made on the flue gases, i.e. after the combustion process has taken place.

Both measures will be reviewed in the following subsections.

## 2.4.1 Primary Measures

Brunner et al [20] give an overview of several possible primary measures strategies for reducing pollutant emission levels. Regarding wood log devices they recommend the following:

- Ignition phase duration of a single charge cycle (which is the highest polluting phase) should be minimised, i.e. low oxygen concentrations should be achieved in a short period.
- Air staging is a very effective primary measure - according to online research, personal correspondence with people from the wood stove industry and the author's knowledge, nowadays the vast majority of stoves on the market feature three stages of air entrainment - primary (directly into the fuel bed), airwash (through a slot along the top edge of the door, oriented downwards, 5 or more mm wide), and secondary (above the fuel bed, oriented horizontally). Brunner et al [20] gave a comparison of CO, OGC and PM1 EFs between optimised (secondary air included) and non-optimised (secondary air excluded) stove variants, as reproduced in Table 2.2.

Table 2.2: Brunner et al [20] results for optimised (secondary air included) and non-optimised (secondary air excluded) wood stove design. All units is mg/Nm<sup>3</sup> @ 13% oxygen content - converted from mg/MJ through formula (3.114).

| Variant             | CO   | OGC | PM1 |
|---------------------|------|-----|-----|
| Secondary air excl. | 2900 | 338 | 54  |
| Secondary air incl. | 1030 | <46 | <31 |

- An automated air supply control system can ensure less variation of excess air ratio over time
- A gasification design (also called down-draft) of a wood log burning device is superior to the conventional updraft design. They also present data where such an appliance design is superior to wood chip and pellet burning appliances<sup>6</sup>. Such a design will be explained in more detail in section 5.1. The evidence of the superiority of the gasification design (with regard to PIC emissions) is given in section 6.1, where testing data from conventional stoves and a new gasification stove prototype are compared.

<sup>6</sup>see section 2.3.4, the paragraph with the Obernberger et al [29] study

Brunner et al [20] have also identified other primary measures, not necessarily directly related with stoves, that affect pollutant EFs:

- Fuel feeding - in automatic systems (pellets and chips) the fuel to air ratio should be kept at a constant level. This is also true for wood log burning appliances (operating in batch mode): the fuel pyrolysis to air ratio should ideally be kept constant, or having a minimal variation over time
- Fuel bed - Uneven distribution of air flow through the fuel (or char) bed can lead to channeling effects, which has proven to be of crucial importance in the stove tested in this study, as explained later in chapters 6 and 7.
- Combustion chamber design - division of the combustion chamber into two zones - i) the primary combustion zone where the fuel is located and primary combustion reactions take place, and ii) a secondary combustion zone where the rest of the gaseous combustion occurs through addition of secondary air.
- Process control - automation of fuel and of air addition is important in order to maintain the optimum amount of fuel and air present in the combustion chamber at any given time.
- User behaviour - different charging and ignition methods yield different pollutant emission levels.

## 2.4.2 Secondary Measures

Secondary measures for reducing the emission levels of PIC in the context of residential wood combustion mostly refer to the usage of a catalytic converter, or catalyst. This is a honeycomb structure placed downstream of a combustion chamber, whose function is to catalyse oxidation of unburned PICs. It is made out of a metal or ceramic substrate, washcoat and active catalytic coating material (e.g. [34]):

- Substrate gives the structure to the catalyst. If a metal substrate is used, it is often made out of very thin (50 microns) FeCrAlloy foil<sup>7</sup>.
- Washcoat is a porous refractory oxide layer (usually aluminium oxide) which serves as a carrier for the precious metal layer
- Precious metal coating - this is an active component for the oxidation catalysis. The most used metals are platinum, palladium and rhodium.

---

<sup>7</sup>This is an alloy made out of 74% iron, 21% chromium and 5% aluminium

Catalysts are effective tools to reduce pollutant emissions, especially during the ignition and burn-out phases, when primary measures have limited effectiveness [35]. Hukkanen et al [36] have found that appliances with installed catalysts showed 30 to 80 % improvement in PIC emissions over the case without the catalyst. Data obtained through experiments conducted by the author of this thesis show improvement of 90 - 95% (or more) for carbon monoxide emissions for a particular catalytic converter model, manufactured by Blackthorn Environmental Ltd<sup>8</sup> [37]. Similar improvement on similar catalyst model (made by the same manufacturer) was confirmed through tests conducted by the Energy Research Centre in Technical University of Ostrava<sup>9</sup>. In addition to carbon monoxide reduction, 50-65 % of organic gaseous carbon and 15-20 % of particulate matter reduction was recorded in that report.

The downside of catalyst usage could be the need for regular inspection and cleaning in order to ensure safe and efficient operating conditions.

Other secondary measures for reducing PIC emission levels generally in biomass burning appliances are the use of *inserts* upstream of a primary combustion zone (whose function is to enhance reactant mixing effectiveness) and *electrostatic precipitators* (ESPs) whose function is to electrically charge the particulate matter present in flue gases, pass them through an electric field and thus remove them from the stream of flue gases.

## 2.5 Limitation on Using Available Scientific Articles as Data Sources

There are several advantages and disadvantages for sourcing information from available scientific peer-reviewed journal articles for the specific topic of this thesis.

### *Advantages*

- Identification of the factors, or parameters, affecting biomass burning appliances' performance - it is beneficial to see researchers' agreement on influencing factors, e.g. fuel moisture, appliance type, or combustion phase.
- Any qualitative trends in comparative studies - e.g. adding secondary air into the gaseous zone above the fuel bed lowers PIC emission levels, or that gasification appliances generally emit less pollutants than conventional, up-draft appliances

<sup>8</sup>Blackthorn Environmental Limited, Kemp House, 152-160 City Road, London, EC1V 2NX, England

<sup>9</sup>This report is not in the public domain.

### *Disadvantages*

- Experiments conducted by researchers in the literature rarely follow any industrial standard. This thesis' goal is minimisation of emission levels measured under the rules and limitations of specific industrial standards, namely EN 13240 (current standard) or EN 16510 (similar to EN 13240 with regard to measurement procedures; to be applied from 1st Jan 2022). Moreover, many important features of burning appliances are often not reported in scientific articles, e.g. dimensions and specific geometry of the combustion chamber, location and distribution of different air inlets, baffling and gaps in the flue gas section between the combustion chamber and the chimney, combustion chamber wall material, door glass size, etc. Comparing data obtained through experiments of this study to the official data published in the brochures of commercial stoves<sup>10</sup> is much more objective than comparison to the data obtained by researchers under unknown conditions.
- Pollutant emission data available in scientific literature often does not satisfy Ecodesign limits, whereas the majority of currently commercially available appliances do. Hence, it is more meaningful to use emission levels from commercial products as a benchmark in the development of a cleaner burning product, than emission data from scientific literature.

Due to the presented disadvantages of the scientific articles as information sources, most quantitative comparisons of the experimental data obtained in this study are done with technical data from official brochures, or manuals, of commercial stove brands.

## **2.6 Overview of Pollutant Emissions from Commercial Wood Log Burning Appliances**

In this section the performance data, including pollutant emissions, efficiencies and heat output, of the commercially available wood log burning appliances are presented.

Table 2.3 shows performance data for the stoves of some European brands, that, in authors opinion are representative of the industry state-of-the-art. Their design is explained later in Section 5.1. Table 2.4 shows performance data for the natural draft gasification wood log burning appliances available on the market. Table 2.5 shows

---

<sup>10</sup>i.e. both data sets are obtained under the limitations of the same (or similar) industrial standard

the performance data for several fan-assisted<sup>11</sup> gasification boilers for one brand - as data from other brands were not available. It is to be noted that emission factors were available in different units, but are converted to the specific set of units so that quantitative comparisons are possible. Conventional stoves (presented in Table 2.3) and natural draft gasification stoves (presented in Table 2.5) belong in the same industrial category, i.e. they are tested according to the same industrial standard.

Comparing the data between i) conventional stoves, ii) natural draft gasification stoves and iii) fan-assisted lambda-sensor-regulated<sup>12</sup> gasification boilers, it can be concluded that gasification boilers emit lowest levels of PIC (CO: 21 - 154 ppm; PM: 9 - 23 mg/Nm<sup>3</sup>), natural draft gasification stoves intermediate levels (CO: 240 - 757 ppm; OGC: 37 - 47 mg/Nm<sup>3</sup>; PM: from 4 mg/Nm<sup>3</sup> above) whereas conventional stoves, in comparison, emit highest (CO: 400 - 1200 ppm; OGC: 29 - 82 mg/Nm<sup>3</sup>, PM: 6 - 23 mg/Nm<sup>3</sup>). Since the aim of this EngD project is minimisation of pollutant emission levels in wood stoves, i.e. natural draft wood burning appliances, the choice when designing a novel wood stove design is between the two options - conventional or natural draft gasification design - is obvious; the latter is preferred (as also recommended by Brunner et al [20]).

Data from all presented appliances will be used as a benchmark for comparison of experimental data from the developed stove prototype later in the discussion (Section 7).

## 2.7 Chapter Summary

In this chapter the review of scientific literature and industry state-of-the-art has been presented, including review of i) types of pollutant gases and particles, ii) usual emission factors of pollutants, iii) parameters that affect pollutant emissions from wood burning appliances, iv) measures for reducing pollutant emissions, v) limitations of scientific articles as sources of pollutant emission data and vi) commercial models of various types of wood burning appliances. In the following chapter the combustion theory necessary for understanding and calculation of important quantities is given.

---

<sup>11</sup>Fan-assisted wood boilers feature a fan, usually at the exit of a heat exchanger, whose function is to generate higher pressure difference in the system, than would be generated by natural chimney draft.

<sup>12</sup>Lambda sensor is located downstream of reaction chamber(s) and registers the level of oxygen in flue gases. Based on the registered oxygen levels the openings of air valves are adjusted in order to maintain optimal air excess ratio in the secondary combustion chamber.

Table 2.3: Representative list of stoves present on the European market.

| Stove                     | Source | Testing standard | CO, %              | THC, mg/Nm <sup>3</sup> | NOx, mg/Nm <sup>3</sup> | PM, mg/Nm <sup>3</sup> | Efficiency, % | Nominal heat output, kW |
|---------------------------|--------|------------------|--------------------|-------------------------|-------------------------|------------------------|---------------|-------------------------|
| Contura (C310, C310G)     | [38]   | EN 13240         | 0.07               | N/A                     | N/A                     | N/A                    | 77            | 7                       |
| Contura (C510)            | [39]   | EN 13240         | 0.09               | N/A                     | N/A                     | N/A                    | 80            | 5                       |
| Contura (C810, C810G)     | [40]   | EN 13240         | 0.12               | N/A                     | N/A                     | N/A                    | 81            | 5                       |
| Rais (600 MAX, 600 MAX/E) | [41]   | N/A              | 0.0915<br>(0.1927) | N/A                     | 69 (76)                 | 15 (15)                | 76 (81)       | 5.8 (7.8)               |
| Rais (Q-Tee, Q-Tee C)     | [42]   | N/A              | 0.0987<br>(0.0987) | N/A                     | 79 (79)                 | 20 (20)                | 80 (80)       | 4.7 (4.7)               |
| Rais (Viva L series)      | [43]   | N/A              | 0.0602             | N/A                     | 80                      | 6                      | 80            | 5.6                     |
| Scan 41-1                 | [44]   | EN 13240         | 0.08               | 81                      | 104                     | 20                     | 82            | 6                       |
| Scan 41-2                 | [45]   | EN 13240         | 0.1                | 82                      | 117                     | 20                     | 79            | 6                       |
| Scan 83-4 Maxi            | [46]   | EN 13240         | 0.08               | N/A                     | 98                      | 23                     | 81            | 5                       |
| Scan 68-14                | [47]   | EN 13240         | 0.04               | 29                      | 85                      | 14                     | 80            | 5.5                     |



Table 2.4: List of natural draft wood gasification stoves present on the European market, with corresponding performance values. All emission factors are normalised to 13% O<sub>2</sub>.

| Stove                       | Source | Testing standard     | CO, vol ppm | THC, mg/Nm <sup>3</sup> | NOx, mg/Nm <sup>3</sup> | PM, mg/Nm <sup>3</sup> | Efficiency, % | Nominal heat output, kW |
|-----------------------------|--------|----------------------|-------------|-------------------------|-------------------------|------------------------|---------------|-------------------------|
| Rais Bionic Fire            | [48]   | EN 13240 & NS 3058-1 | 240         | 11                      | N/A                     | <4 (0.635 g/kg****)    | 86            | 4.6                     |
| Xeoos TwinFire 5kW          | [49]   | N/A                  | 600         | N/A                     | N/A                     | 20                     | 83.7          | 5                       |
| Xeoos TwinFire 8kW          | [50]   | N/A                  | 500         | N/A                     | N/A                     | 22                     | 83.6          | 8                       |
| Walltherm AIR               | [51]   | EN 13240             | <320 [52]*  | N/A                     | N/A                     | 12.4                   | >87           | 12                      |
| Pyro Nemo 6 kW              | [53]   | EN 13240             | 890         | N/A                     | N/A                     | N/A                    | 82            | 6                       |
| Pyro Nemo 9 kW              | [54]   | EN 13240             | 615         | N/A                     | N/A                     | N/A                    | 83            | 9                       |
| Pyro Nemo 12 kW             | [55]   | EN 13240             | 340         | N/A                     | N/A                     | N/A                    | 83            | 12                      |
| Pyro Magic 6 kW             | [56]   | EN 13240             | 757         | N/A                     | N/A                     | N/A                    | 82            | 6                       |
| Pyro Magic 10 kW            | [57]   | EN 13240             | 757         | N/A                     | N/A                     | N/A                    | 83            | 10                      |
| Pyro Magic 14 kW            | [58]   | EN 13240             | 704         | N/A                     | N/A                     | N/A                    | 83            | 14                      |
| Hektos Aqua II              | [59]   | EN 13240             | 496**       | 47                      | 74                      | 17                     | 91            | 10.5                    |
| LUUMA Luvano Touch          | [60]   | N/A                  | <400**      | N/A                     | N/A                     | <20                    | >91           | 15                      |
| Pertinger 100 Reverse Flame | [61]   | N/A                  | 260**       | 37                      | 61                      | 15                     | 90.5          | 10.5                    |
| Jayline UL200               | [62]   | AS/NZ 2918:2001      | N/A         | N/A                     | N/A                     | 37***                  | 75            | N/A                     |
| (Same as above)             | [62]   | ECAN-CM1             | N/A         | N/A                     | N/A                     | 52***                  | 79            | N/A                     |

\*CO data presented for Walltherm Vajolet, as none was found for Walltherm AIR; 0.032% corresponds to 400 mg/Nm<sup>3</sup> - given in [52]

\*\* CO converted from mg/Nm<sup>3</sup>; CO density is 1.25 kg/Nm<sup>3</sup> [63]

\*\*\* PM converted from mg/MJ according to the equation (3.114) \*\*\*\* Tested according to NS 3058-1 (dilution tunnel test method)

Table 2.5: Representative list of gasification fan-assisted boilers with air valve regulation via lambda sensor. Testing standards: EN ISO 17225-5:2014 and DIN EN 303-5:2012-10.

| Appliance                    | Source | Testing standard     | CO, vol ppm | OGC, mg/Nm <sup>3</sup> | NO <sub>x</sub> , mg/Nm <sup>3</sup> | PM, mg/Nm <sup>3</sup> | Efficiency, % | Nominal heat output, kW |
|------------------------------|--------|----------------------|-------------|-------------------------|--------------------------------------|------------------------|---------------|-------------------------|
| Hargassner Neo-HV 20         | [64]   | EN ISO 17225-5:2014  | 30*         | N/A                     | 117**                                | 9**                    | 93.7          | 25.4                    |
| Same as above (partial load) | [64]   | EN ISO 17225-5:2014  | 37*         | N/A                     | 105**                                | 11**                   | 92.8          | 12.2                    |
| Hargassner MV 49             | [64]   | EN ISO 17225-5:2014  | 154*        | N/A                     | N/A                                  | 12**                   | 90            | 47                      |
| Same as above (partial load) | [64]   | EN ISO 17225-5:2014  | 134*        | N/A                     | N/A                                  | 23**                   | 92.6          | 39                      |
| Solarbayer BioX 15           | [65]   | DIN EN 303-5:2012-10 | 22***       | 1                       | 115                                  | 10                     | 90.6          | 16.6                    |
| Solarbayer BioX 20           | [65]   | DIN EN 303-5:2012-10 | 22***       | 1                       | 116                                  | 10                     | 90.9          | 19.4                    |
| Solarbayer BioX 25           | [65]   | DIN EN 303-5:2012-10 | 21***       | 1                       | 130                                  | 11                     | 90.7          | 25                      |
| Solarbayer BioX 35           | [65]   | DIN EN 303-5:2012-10 | 21***       | 1                       | 130                                  | 11                     | 90.7          | 33.6                    |
| Solarbayer BioX 45           | [65]   | DIN EN 303-5:2012-10 | 21***       | 1                       | 126                                  | 10                     | 90.5          | 43.2                    |

\* conversion from mg/MJ done through equations (3.110) and (3.114); CO density is 1.25 kg/Nm<sup>3</sup> [63]

\*\* conversion from mg/MJ done through equation (3.114)

\*\*\* conversion from mg/Nm<sup>3</sup> done through equation (3.110)

# Chapter 3

## Combustion Theory

In the previous chapter a literature review was presented, while in this chapter the combustion theory is given. This chapter mostly covers the derivation of formulae defined in the BS EN 16510-1:2018 standard. This includes the derivation of equations for calculation of following quantities:

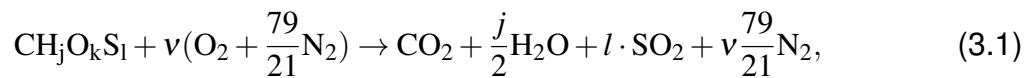
- Maximum concentration of CO<sub>2</sub> in the flue gas:  $CO_{2,max}$
- Flue gas mass flow,
- Thermal heat loss in flue gas,
- Chemical heat loss in flue gas,
- Concentration of pollutant gases (CO and OGC), normalised to 13% O<sub>2</sub>
- Concentration of particulate matter (PM), normalised to 13% O<sub>2</sub>
- Efficiency of a stove
- Heat output of a stove

The formulae provided in the BS EN 16510-1:2018 standard are simply stated without derivation, or any physical clarification of specific factors and terms present in the equations. The majority of the formulae in this chapter were derived by the author, unless otherwise stated. To the author's knowledge this represents the first time that these derivations and analysis have been presented in a single source, and this represents a significant contribution to the subject in its own right.

In order to derive equations for the flue gas mass flow, heat losses and normalised concentrations, first the equations for  $CO_{2,max}$  and for gas or PM concentration normalisation to 13%  $O_2$  need to be derived.

### 3.1 Calculation of $CO_{2,max}$

Given that the combustible part of the test fuel is composed of mainly carbon, hydrogen, oxygen and sulfur, a generic empirical formula for the test fuel can be written as:  $CH_jO_kS_l$ . Therefore, the chemical reaction equation with the stoichiometric amount of air reads



where  $v$  is the stoichiometric coefficient of  $O_2$  in  $(\text{kmol } O_2)/(\text{kmol } CH_jO_kS_l)$  and  $j$ ,  $k$  and  $l$  denote molar contents of hydrogen, oxygen and sulphur atoms in the test fuel relative to carbon atoms, respectively. The stoichiometric coefficient of  $N_2$  is  $79/21$ , because there is always  $79/21$  times more nitrogen than oxygen in the air (by volume). Since these relative molar contents of carbon, hydrogen, oxygen and sulphur in the test fuel  $C_{(1)}H_aO_bS_c$  are  $1 : j : k : l$ , their formulae and units are shown in Table 3.1.

Table 3.1: Relative molar contents of hydrogen, oxygen and sulphur in the test fuel with their formulae and units.

| Constituent | Molar content of the constituent | Formula                 | Unit  |
|-------------|----------------------------------|-------------------------|---|
| Hydrogen    | $j$                              | $n_{H,fuel}/n_{C,fuel}$ | $\frac{\text{kmol atoms } H_{fuel}}{\text{kmol atoms } C_{fuel}}$ |
| Oxygen      | $k$                              | $n_{O,fuel}/n_{C,fuel}$ | $\frac{\text{kmol atoms } O_{fuel}}{\text{kmol atoms } C_{fuel}}$ |
| Sulphur     | $l$                              | $n_{S,fuel}/n_{C,fuel}$ | $\frac{\text{kmol atoms } S_{fuel}}{\text{kmol atoms } C_{fuel}}$ |

Calculation of  $j$ ,  $k$  and  $l$  occurs through following relations:

$$j = \frac{n_{H,fuel}}{n_{C,fuel}} = \frac{m_H/M_h}{m_C/M_C} = \frac{M_C m_H}{M_H m_c} = \frac{M_C m_H/m_f}{M_H m_C/m_f} = \frac{M_C H_{daf}}{M_H C_{daf}} = \frac{12.01 H_{daf}}{1.01 C_{daf}} \quad (3.2)$$

$$\approx 12 \frac{H_{daf}}{C_{daf}}, \quad (3.3)$$

$$k = \frac{n_{O,fuel}}{n_{C,fuel}} = \dots = \frac{M_C O_{daf}}{M_O C_{daf}} = \frac{12.01 O_{daf}}{16 C_{daf}} \quad (3.4)$$

$$\approx \frac{12 O_{daf}}{16 C_{daf}}, \quad (3.5)$$

$$l = \frac{n_{S,fuel}}{n_{C,fuel}} = \dots = \frac{M_C S_{daf}}{M_S C_{daf}} = \frac{12.01 S_{daf}}{32.07 C_{daf}} \quad (3.6)$$

$$\approx \frac{12 S_{daf}}{32 C_{daf}}, \quad (3.7)$$

where  $n$  denotes substance amount in kmol,  $m$  denotes mass of a constituent in kg,  $m_f$  is the mass of fuel in kg,  $M$  denotes molar mass of a constituent in kg/kmol, and  $C_{daf}$ ,  $H_{daf}$ ,  $O_{daf}$  and  $S_{daf}$  denote mass fractions of carbon, hydrogen, oxygen and sulphur in fuel (in (kg constituent)/(kg fuel)) on a dry, ash-free basis, respectively, which should be known from an ultimate analysis of the firewood before calculation.

Equations (3.3), (3.5) and (3.7) are defined in BS EN 16510-1, presented later.

The oxidation reactions of every constituent in the test fuel and its molar oxygen demand are shown in Table 3.2.

Table 3.2: Oxidation reactions of every main constituent of test fuel and their molar oxygen demand.

| Oxidation reaction                    | Molar oxygen demand $n_{O_2}/n_{constituent}$       |
|---------------------------------------|---|
| $C_{fuel} + O_2 \rightarrow CO_2$     | $n_{O_2}/n_C = 1$ (mol $O_2$ )/(mol $C_{fuel}$ )    |
| $H_{fuel} + 0.25O_2 \rightarrow H_2O$ | $n_{O_2}/n_H = 1/4$ (mol $O_2$ )/(mol $H_{fuel}$ )  |
| $S_{fuel} + O_2 \rightarrow SO_2$     | $n_{O_2}/n_S = 1$ (mol $O_2$ )/(mol $S_{fuel}$ )    |
| $O_{fuel} - 0.5O_2 \rightarrow 0$     | $n_{O_2}/n_O = -0.5$ (mol $O_2$ )/(mol $O_{fuel}$ ) |

Therefore, the stoichiometric molar oxygen coefficient  $\nu$  (present in the equation (3.1)) for the oxidation of the test fuel represented with empirical formula  $CH_jO_kS_l$ , is calculated by using data from the Table 3.2, as follows:

$$\begin{aligned}
v \left[ \frac{\text{mol } O_2}{\text{mol } C_{\text{fuel}}} \right] &= n_{O_2}/n_C \left[ \frac{\text{mol } O_2}{\text{mol } C_{\text{fuel}}} \right] \cdot 1 \left[ \frac{\text{mol } C_{\text{fuel}}}{\text{mol } C_{\text{fuel}}} \right] \\
&+ n_{O_2}/n_H \left[ \frac{\text{mol } O_2}{\text{mol } H_{\text{fuel}}} \right] \cdot j \left[ \frac{\text{mol } H_{\text{fuel}}}{\text{mol } C_{\text{fuel}}} \right] + \\
&n_{O_2}/n_O \left[ \frac{\text{mol } O_2}{\text{mol } O_{\text{fuel}}} \right] \cdot k \left[ \frac{\text{mol } O_{\text{fuel}}}{\text{mol } C_{\text{fuel}}} \right] \\
&+ n_{O_2}/n_S \left[ \frac{\text{mol } O_2}{\text{mol } S_{\text{fuel}}} \right] \cdot l \left[ \frac{\text{mol } S_{\text{fuel}}}{\text{mol } C_{\text{fuel}}} \right]
\end{aligned} \tag{3.8}$$

which gives the formula defined in BS EN 16510-1:

$$v = 1 + \frac{j}{4} - \frac{k}{2} + l \tag{3.9}$$

Taking into account the ideal gas law [66], pp.134:

$$pV = nR_uT, \tag{3.10}$$

where  $p$  is pressure in Pa,  $V$  is volume in  $\text{m}^3$ ,  $n$  is amount of substance in kmol,  $R_u \approx 8.3145 \text{ (m}^3 \text{ Pa)/(K mol)}$  is the universal gas constant and  $T$  is the absolute temperature in K, of an ideal gas, one gets that molar fraction and volume fraction are identical quantities:

$$x_i = \frac{n_i}{\sum_{j=1}^N n_j} = \frac{\frac{pV_i}{R_uT}}{\sum_{j=1}^N \frac{pV_j}{R_uT}} = \frac{V_i}{\sum_{j=1}^N V_j} \tag{3.11}$$

Hence, by substituting the stoichiometric coefficients of products<sup>1</sup> (flue gases) from equation (3.1) into equation (3.11), one gets

$$x_{CO_2,stoich.} = CO_{2\max} = \frac{1 \text{ mol } CO_2}{1 \text{ mol } CO_2 + l \text{ mol } SO_2 + v(79/21) \text{ mol } N_2} \tag{3.12}$$

$$= \frac{1}{1 + l + v(79/21)} \left[ \frac{\text{m}^3 CO_2}{\text{m}^3 \text{ dry flue gas}} \right] \tag{3.13}$$

The equation (3.13) is defined in standard BS EN 16510-1.

<sup>1</sup>Excluding water vapour, as  $CO_{2,\max}$  is defined as  $CO_2$  content in  $(\text{m}^3 \text{ } CO_2)/(\text{m}^3 \text{ dry flue gas})$

### 3.2 Concentration Normalisation to 13 % O<sub>2</sub>

Any actual (or measured) content or concentration of a component in the flue gas stream can be normalised to a specific value of oxygen in the flue gases. This is done in order to obtain an objective criterion of comparison between measured concentration and limited concentration (Ecodesign limits [9] in this case). The calculation of the normalised value is accomplished through the following generic formula:

$$\text{Normalised Value} = \text{Measured Value} \cdot \lambda \cdot \frac{21 - O_{2,\text{standardised}}}{21}, \quad (3.14)$$

where  $\lambda$  is the air excess ratio and  $O_{2,\text{standardised}}$  is the standardised value of oxygen volume fraction in the dry flue gas mixture in vol%. By multiplying measured value by  $\lambda$  one obtains a value normalised to 0 % oxygen, i.e. to stoichiometric conditions. By further multiplication by a factor  $\frac{21 - O_{2,\text{standardised}}}{21}$ , one obtains the value normalised to  $O_{2,\text{standardised}}$  (which is 13 % O<sub>2</sub> in the case of BS EN 16510-1 standard).

The air excess ratio  $\lambda$  can be calculated from the measured value of either O<sub>2</sub> or CO<sub>2</sub>. There are two different ways to calculate  $\lambda$ .

1. The first way is to use the instantaneous values<sup>2</sup> of  $O_{2,i}$  or  $CO_{2,i}$ , in which case one of the following two formulae are to be used:

$$\lambda_i = \frac{21}{21 - O_{2,i}}, \quad \text{or} \quad (3.15)$$

$$\lambda_i = \frac{CO_{2,\text{max}}}{CO_{2,i}}, \quad (3.16)$$

where  $O_{2,i}$  and  $CO_{2,i}$  denote the instantaneous volume fractions of oxygen and carbon dioxide in vol% of dry flue gases respectively, whereas  $\lambda_i$  is the instantaneous excess air ratio. Instantaneous quantities are calculated for each data point, measured with 5 s interval in the case of experiments conducted in this study<sup>3</sup>.

2. The second way to calculate  $\lambda$  is to use averaged values  $O_{2,\text{avg}}$  or  $CO_{2,\text{avg}}$ , in

<sup>2</sup>In this study 5 s interval was used. Maximum interval permitted (and mostly used) by the BS EN 16510-1 standard is 30 s.

<sup>3</sup>For comparison, EN 13240 and EN 16510-1 standards define maximum allowed gas sampling interval of 30 seconds.

which case one of the following two formulae are to be used:

$$\lambda_{\text{avg}} = \frac{21}{21 - O_{2,\text{avg}}}, \quad \text{or} \quad (3.17)$$

$$\lambda_{\text{avg}} = \frac{CO_{2,\text{max}}}{CO_{2,\text{avg}}}. \quad (3.18)$$

Here averaged values are calculated as the arithmetic mean of all measured data over a given test period (typically a single refuelling period).

Hence, equation (3.14) can be expressed by taking into account equations (3.15), (3.16), (3.17), (3.18), in one of the following four forms:

1. Instantaneous values of  $O_{2,i}$  or  $CO_{2,i}$ :

$$NV = MV \cdot \frac{21 - O_{2,\text{standardised}}}{21 - O_{2,i}}, \quad \text{or} \quad (3.19)$$

$$NV = MV \cdot \frac{CO_{2,\text{max}}}{CO_{2,i}} \cdot \frac{21 - O_{2,\text{standardised}}}{21}. \quad (3.20)$$

2. Average values of  $O_{2,\text{avg}}$  or  $CO_{2,\text{avg}}$ :

$$NV = MV \cdot \frac{21 - O_{2,\text{standardised}}}{21 - O_{2,\text{avg}}}, \quad \text{or} \quad (3.21)$$

$$NV = MV \cdot \frac{CO_{2,\text{max}}}{CO_{2,\text{avg}}} \cdot \frac{21 - O_{2,\text{standardised}}}{21}, \quad (3.22)$$

where NV and MV denote normalised and measured values.

The first (3.19) and third (3.21) forms are to be used if oxygen is being measured by the gas analyser, whereas the second (3.20) and fourth (3.22) form should be used if carbon dioxide is measured.

In the following text only value normalisation formulae containing  $CO_2$  data will be used as  $CO_2$  was measured in the experiments of this study.



### 3.2.1 Averaging Values

The averaged value  $V$  is calculated as an arithmetic mean of all data available for a single test period (refuelling period):

$$V_{\text{avg}} = \sum_{i=1}^N V_i, \quad (3.23)$$

where  $N$  is the total number of sampled data. Formulae for normalisation of instantaneous values can be written in two different ways:

1. by using instantaneous  $CO_2$  data:

$$NV_i = MV_i \cdot \frac{CO_{2,\text{max}}}{CO_{2,i}} \cdot \frac{21 - O_{2,\text{standardised}}}{21}, \quad \text{and} \quad (3.24)$$

2. by using averaged  $CO_{2,\text{avg}}$  data:

$$NV_i = MV_i \cdot \frac{CO_{2,\text{max}}}{CO_{2,\text{avg}}} \cdot \frac{21 - O_{2,\text{standardised}}}{21}. \quad (3.25)$$

In the equations above (3.24) and (3.25)  $MV_i$  denotes single measured data point at  $i$ th time instant and  $NV_i$  corresponding normalised value. By combining equations (3.23) and (3.24), following equation for averaged normalised value is obtained:

$$NV_{\text{norm, avg}} = CO_{2,\text{max}} \cdot \frac{21 - O_{2,\text{standardised}}}{21} \cdot \sum_{i=1}^N \frac{MV_i}{CO_{2,i}}, \quad (3.26)$$

whereas by combining equations (3.23) and (3.25), following equation for averaged normalised value is obtained:

$$NV_{\text{norm, avg}} = \frac{CO_{2,\text{max}}}{CO_{2,\text{avg}}} \cdot \frac{21 - O_{2,\text{standardised}}}{21} \cdot \sum_{i=1}^N MV_i \quad (3.27)$$

$$= \frac{CO_{2,\text{max}}}{CO_{2,\text{avg}}} \cdot \frac{21 - O_{2,\text{standardised}}}{21} \cdot MV_{\text{avg}} \quad (3.28)$$

Therefore, one is left with two different ways of calculating the average of a normalised value - equation (3.26), where instantaneous  $CO_2$  data is used and equation (3.28), where the average  $CO_{2,\text{avg}}$  is used.

Even though the calculation method with instantaneous  $CO_2$  data (equations (3.24) and (3.26)) gives better estimate of pollutant emissions, the alternative one with averaged  $CO_{2,\text{avg}}$  data (equations (3.25) and (3.28)) is used in the standard BS EN 16510-1. In

most analyses the EN 16510-1 normalisation formula is used in order for the comparison to emission data of other stoves is possible. However, in case of assessment of flap seal or missed weld leakage (presented in Section 6.3.5) the more accurate formula (3.26) is used.

### 3.3 Calculation of Normalised CO Volume Fraction

The normalised value of carbon monoxide can be calculated by using either instantaneous  $CO_2$  data (equations (3.24) and (3.26)):

$$CO_{norm,i} = CO_i \cdot \frac{CO_{2,max}}{CO_{2,i}} \cdot \frac{21 - O_{2,standardised}}{21}, \quad \text{and} \quad (3.29)$$

$$CO_{norm, avg} = CO_{2,max} \cdot \frac{21 - O_{2,standardised}}{21} \cdot \sum_{i=1}^N \frac{CO_i}{CO_{2,i}}, \quad (3.30)$$

or averaged  $CO_{2,avg}$  data (equations (3.25) and (3.28)):

$$CO_{norm,i} = CO_i \cdot \frac{CO_{2,max}}{CO_{2,avg}} \cdot \frac{21 - O_{2,standardised}}{21}, \quad (3.31)$$

$$CO_{norm, avg} = CO_{avg} \cdot \frac{CO_{2,max}}{CO_{2,avg}} \cdot \frac{21 - O_{2,standardised}}{21}. \quad (3.32)$$

Standard BS EN 16510-1 uses equation (3.32) for calculation of averaged  $CO$  @ 13 %  $O_2$  ( $O_{2,standardised} = 13$  %). If the equation (3.31) is averaged one gets equation (3.32) - which is defined in BS EN 16510-1. Hence, formula (3.31) is used in all the graphs in this document (apart from section 6.3.5) as it is consistent with the formula defined by the standard. The reason for using formula (3.31) in section 6.3.5 which explains the leakage of the tested stove is the fact that it provides a more objective, or true, instantaneous level of normalised  $CO$ .

### 3.4 Calculation of Normalised OGC Concentration

Total organic gaseous carbon (OGC) is measured continuously with the flame ionisation detector (FID) [63]. It can measure the volume fraction of total hydrocarbon content in the flue gas. This measurement method cannot detect specific hydrocarbon gases, but rather the total amount of hydrocarbon, usually expressed as equivalents of a reference substance, that being propane ( $C_3H_8$ ). As the measurement system is heated to 195 °C in order to minimise loss of material in the sampling system, the flue gases

in the system contain water vapour, therefore they are referred to as wet flue gases.

It is to be noted that OGC and THC often refer to the same quantity. The term OGC is used in the BS EN 16510-1 standard, while THC is used in the rest of this thesis.

The formula for the calculation of the mass concentration of OGC, or THC (in (mg C)/(Nm<sup>3</sup> dry flue gas)), based on the measured volume fraction of total hydrocarbon content  $THC_{\text{propane}}$  (in vol ppm propane equivalents of wet flue gas) is as follows:

$$THC \left[ \frac{\text{mg C}}{\text{Nm}^3 \text{ dry flue gas}} \right] = \frac{THC_{\text{propane}} \left[ 10^{-6} \frac{\text{m}^3 \text{C}_3\text{H}_8}{\text{m}^3 \text{ wet flue gas}} \right] \cdot 3 \left[ \frac{\text{kmol C}}{\text{kmol C}_3\text{H}_8} \right] \cdot M_C \left[ \frac{\text{kg C}}{\text{kmol C}} \right]}{V_m \left[ \frac{\text{Nm}^3}{\text{kmol}} \right]} \cdot \frac{CO_{2,\text{max}}}{CO_{2,\text{avg}}} [-] \cdot \frac{21 - O_{2,\text{standardised}}}{21} [-] \cdot \frac{G_W \left[ \frac{\text{Nm}^3 \text{ wet flue gas}}{\text{kg fuel}} \right]}{G_D \left[ \frac{\text{Nm}^3 \text{ dry flue gas}}{\text{kg fuel}} \right]}, \quad (3.33)$$

since

$$THC_{\text{propane}} \left[ 10^{-6} \frac{\text{m}^3 \text{C}_3\text{H}_8}{\text{m}^3 \text{ wet flue gas}} \right] = THC_{\text{propane}} [\text{vol ppm C}_3\text{H}_8 \text{ in wet flue gas}]. \quad (3.34)$$

In equation (3.33),  $V_m = 22.414 \text{ Nm}^3/\text{kmol}$  is the molar volume of any ideal gas at standard conditions, whereas  $M_C = 12.01 \text{ kg/kmol}$  is the molar mass of carbon. Derivation of  $G_W$  and  $G_D$  will be shown later in section 3.6.  $V_m$  is calculated from the ideal gas law, considering standard conditions (273.15 K and 101325 Pa):

$$V_m = \frac{V}{n} = \frac{R_u T}{p} = \frac{8.31 \text{ Pa} \cdot \text{m}^3 / (\text{mol} \cdot \text{K}) \cdot 273.15 \text{ K}}{101325 \text{ Pa}} = 22.41 \text{ m}^3 / \text{kmol} \quad (3.35)$$

Hence the final formula for calculation of normalised mass concentration of organic gaseous carbon in dry flue gases reads as follows:

$$C_{\text{OGC}} = THC = \frac{THC_{\text{propane}} \cdot 36}{22.41} \cdot \frac{CO_{2,\text{max}}}{CO_{2,\text{avg}}} \cdot \frac{21 - O_{2,\text{standardised}}}{21} \cdot \frac{G_w}{G_d}, \quad (3.36)$$

which is also defined in standard BS EN 16510-1.

### 3.5 Calculation of Normalised Concentration of Particulate Matter in Flue Gas

Measurement of particulate matter concentration is done with the heated filter method, explained later in section 4.1.1. A portion of the flue gas stream is sampled and particulate matter is filtered through a glass fiber filter. Based on the mass of the particulate matter on the filter and the corresponding sampled flue gas volume, the PM concentration can be determined.

Sampled volume is calculated as the difference between the gas meter reading before and after sampling:

$$FGV_s = FGV_a - FGV_b. \quad (3.37)$$

This volume then needs to be normalised to standard conditions. This is done through the ideal gas law (3.10):

$$nR_u = \frac{m}{M}R_u = m\frac{R_u}{M} = mR = \frac{p_1V_1}{T_1} = \frac{p_2V_2}{T_2} \quad \longrightarrow \quad V_2 = V_1\frac{T_2 p_1}{T_1 p_2}, \quad (3.38)$$

where  $R$  is the gas constant of a specific gas (or gas mixture), and 1 and 2 refer to two different states. Therefore, when normalising the sampled volume at recorded temperature and ambient pressure to standard conditions, one gets:

$$FGV_{STP} = FGV_s \cdot \frac{T_{STP}}{T_{measured}} \cdot \frac{p_{measured}}{p_{STP}} \quad (3.39)$$

$$FGV_{STP} = (FGV_a - FGV_b) \cdot \frac{273.15}{273.15 + T_{C, measured}} \cdot \frac{p_{measured}}{1013}, \quad (3.40)$$

where  $T_{C, measured}$  is measured temperature at the gas meter in °C and  $p_{measured}$  is measured ambient pressure at the gas meter in hPa.

When the gas meter calibration factor is accounted for, one gets the expression defined in BS NE 16510-1:

$$FGV_{STP} = FGV = (FGV_a - FGV_b) \cdot \frac{273.15}{273.15 + T_{C, measured}} \cdot \frac{p_{measured}}{1013} \cdot C_f \quad (3.41)$$

Solid matter concentration (in (mg PM)/(Nm<sup>3</sup> dry flue gas)) is calculated as follows:

$$PM_{conc} = \frac{m_{PM}}{FGV} = \frac{FW_a - FW_b}{FGV}, \quad (3.42)$$

where  $FW_a$  and  $FW_b$  are filter weights after and before the sampling in mg, respectively.

Lastly, solid matter concentration is to be normalised to 13 % oxygen according to formula (3.28):

$$PM_{HF} = PM_{conc} \cdot \frac{CO_{2,max}}{CO_{2,avg}} \cdot \frac{21 - O_{2,standardised}}{21} \quad (3.43)$$

Equations (3.41), (3.42) and (3.43) are defined in BS EN 16510-1.

## 3.6 Flue Gas Mass Flow

The mass flow of flue gas (under standard conditions) depends on several factors:

- consumption rate of fuel,
- chemical composition of fuel
- fuel moisture, and
- air excess ratio.

The flue gas mass flow  $\Phi_g$  can be calculated through the following equation:

$$\Phi_g = \dot{m}_f \cdot \rho_g \cdot G_w, \quad (3.44)$$

where  $\dot{m}_f$  is the fuel consumption rate in kg/h and  $\rho_g$  is the density of flue gas in (kg gas)/Nm<sup>3</sup> and  $G_w$  is the specific volume of wet flue gas expressed per unit mass of fuel: (Nm<sup>3</sup> flue gas)/(kg fuel).

The fuel consumption rate  $\dot{m}_f$  is calculated from the following expression:

$$\dot{m}_f = m_f / t, \quad (3.45)$$

where  $m_f$  is the mass of test fuel in kg and  $t$  is the duration of the test period in hours.

The density of the flue gas  $\rho_g$  is between the air density  $\rho_{air}$  (i.e. theoretical case of the flue gas density when air excess ratio is  $\infty$ ) and the density of the flue gas at stoichiometric conditions (no excess air)  $\rho_{g,stoich}$ . Air density at standard conditions is

1.293 kg/Nm<sup>3</sup>, whereas  $\rho_{g,stoich}$  is

$$\rho_{g,stoich} = x_{N_2} \cdot \rho_{N_2} + x_{CO_2} \cdot \rho_{CO_2} \quad (3.46)$$

$$= 0.79 \frac{\text{m}^3 \text{N}_2}{\text{m}^3 \text{g}} \cdot 1.25 \frac{\text{kgN}_2}{\text{m}^3 \text{N}_2} + 0.21 \frac{\text{m}^3 \text{O}_2}{\text{m}^3 \text{g}} \cdot 1.98 \frac{\text{kgCO}_2}{\text{m}^3 \text{CO}_2} \quad (3.47)$$

$$= 1.40 \frac{\text{kg}}{\text{m}^3 \text{g}}. \quad (3.48)$$

In the equation above (3.46)  $x_{N_2}$  and  $x_{CO_2}$  denote volume fractions of N<sub>2</sub> and CO<sub>2</sub> in the flue gas, respectively, whereas  $\rho_{N_2}$  and  $\rho_{CO_2}$  denote densities of N<sub>2</sub> and CO<sub>2</sub>, respectively. Hence,  $1.29 < \rho_g < 1.40$  [ kg/Nm<sup>3</sup> ]. In BS EN 16510-1, the value of 1.3 kg/Nm<sup>3</sup> is chosen.

If the flue gas mass flow is to be expressed in g/s, rather than kg/h, the following calculation is needed:

$$\dot{m}_{f \text{ in g/s}} \left[ \frac{\text{g}}{\text{s}} \right] = \dot{m}_{f \text{ in g/s}} \left[ \frac{10^{-3} \text{ kg}}{1/3600 \text{ h}} \right] = 3.6 \cdot \dot{m}_{f \text{ in g/s}} \left[ \frac{\text{kg}}{\text{h}} \right] = \dot{m}_{f \text{ in kg/h}} \left[ \frac{\text{kg}}{\text{h}} \right]. \quad (3.49)$$

Hence

$$\dot{m}_{f \text{ in g/s}} \left[ \frac{\text{g}}{\text{s}} \right] = \frac{1}{3.6} \cdot \dot{m}_{f \text{ in kg/h}} \left[ \frac{\text{kg}}{\text{h}} \right]. \quad (3.50)$$

Specific volume of wet flue gas  $G_w$  can be split into dry flue gas part  $G_d$  and water vapour part  $G_{wv}$ :

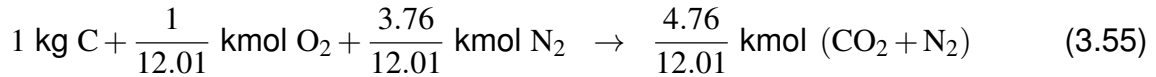
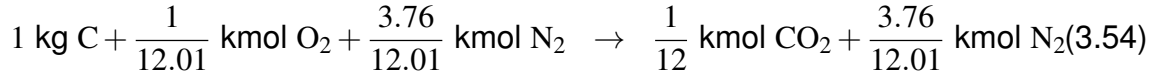
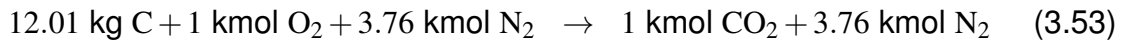
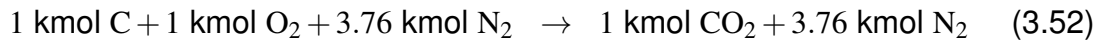
$$G_w \left[ \frac{\text{Nm}^3 \text{ wet flue gas}}{\text{kg fuel}} \right] = G_d \left[ \frac{\text{Nm}^3 \text{ dry flue gas}}{\text{kg fuel}} \right] + G_{wv} \left[ \frac{\text{Nm}^3 \text{ water vapour}}{\text{kg fuel}} \right]. \quad (3.51)$$

In the following two subsections, equations for specific volumes of dry flue gas  $G_d$  and of water vapour  $G_{wv}$  will be derived.

### 3.6.1 Calculation of Specific Volume of Dry Flue Gas

Specific dry flue gas volume quantifies how much volume (in standard conditions) of flue gas is produced per mass unit of burned fuel. Fuel is composed of its basic constituents: carbon, nitrogen, oxygen and sulphur. For example, the oxidation of carbon

with a stoichiometric amount of air can be shown as:



In equation (3.53) 1 kmol of C is substituted by 12.01 kg of C, as the molar mass of carbon is 12.01 kg/kmol. From equation (3.55) it is clear that 1 kg of C gives 4.76/12.01 kmol of (CO<sub>2</sub> + N<sub>2</sub>) mixture. In standard conditions this amount of substance occupies a uniquely defined volume:

$$V_C = n \cdot V_m = \frac{4.76}{12.01} [\text{kmol}] \cdot 22.41 \left[ \frac{\text{Nm}^3}{\text{kmol}} \right] = 8.88 \text{ Nm}^3. \quad (3.56)$$

Since 1 kg of carbon gives 8.88 Nm<sup>3</sup> of flue gas, one can determine the specific flue gas volume from carbon oxidation  $G_C = 8.88 \text{ Nm}^3/(\text{kg C})$ .

An analogous procedure can be followed for hydrogen<sup>4</sup> and sulphur, the two other combustible constituents. Their specific flue gas volume values are  $G_H = 20.97 \text{ Nm}^3/(\text{kg H})$  and  $G_S = 3.32 \text{ Nm}^3/(\text{kg S})$ .

The specific flue gas volume from fuel bound nitrogen is calculated as follows:



$$G_N = \frac{0.5}{14.01} \frac{\text{kmol N}_2}{\text{kg N}} \cdot 22.41 \frac{\text{Nm}^3}{\text{kmol}} = 0.80 \frac{\text{Nm}^3}{\text{kg N}} \quad (3.60)$$

The specific flue gas volume from fuel bound oxygen is negative as its presence reduces the demand of air for combustion. Every atom of O from fuel replaces another

<sup>4</sup>In the products of hydrogen (right-hand-side of the chemical balance equation), water is to be ignored as the specific volume of *dry* flue gas is being determined.

atom of O from air. Hence

$$1 \text{ kmol } O_{\text{fuel}} - 0.5 \text{ kmol } O_{2,\text{air}} - 0.5 \cdot 3.76 \text{ kmol } N_{2,\text{air}} \rightarrow -0.5 \cdot 3.76 \text{ kmol } N_{2,\text{air}} \quad (3.61)$$

$$16 \text{ kg } O_{\text{fuel}} - 0.5 \text{ kmol } O_{2,\text{air}} - 0.5 \cdot 3.76 \text{ kmol } N_{2,\text{air}} \rightarrow -0.5 \cdot 3.76 \text{ kmol } N_{2,\text{air}} \quad (3.62)$$

$$1 \text{ kg } O_{\text{fuel}} - \frac{0.5}{16} \text{ kmol } O_{2,\text{air}} - \frac{0.5}{16} \cdot 3.76 \text{ kmol } N_{2,\text{air}} \rightarrow -\frac{0.5}{16} \cdot 3.76 \text{ kmol } N_{2,\text{air}} \quad (3.63)$$

Thus the specific flue gas volume from fuel bound oxygen is

$$G_O = -\frac{0.5 \cdot 3.76}{16} \frac{\text{kmol } N_{2,\text{air}}}{\text{kg } O_{\text{fuel}}} \cdot 22.41 \frac{\text{Nm}^3}{\text{kmol}} = -2.63 \frac{\text{Nm}^3}{\text{kg } O_{\text{fuel}}}. \quad (3.64)$$

Therefore, the formula for specific flue gas volume from combustion of fuel with  $C_f$ ,  $H_f$ ,  $N_f$ ,  $O_f$  and  $S_f$  contents of carbon, hydrogen, oxygen and sulphur (on fired basis) reads

$$G \left[ \frac{\text{Nm}^3}{\text{kg fuel}} \right] = 8.88C_f + 20.97H_f + 0.80N_f - 2.63O_f + 3.32S_f \quad (3.65)$$

With the data from the ultimate analysis of wood used in this study, equation (3.65) gives  $G = 3.932 \text{ Nm}^3/(\text{kg fuel})$ .

If equation (3.65) is modified so that only carbon content is taken into account, the equation would read

$$G \left[ \frac{\text{Nm}^3}{\text{kg fuel}} \right] = 8.88 \cdot C_f \quad (3.66)$$

and  $G$  would amount to  $G = 3.838 \text{ Nm}^3/(\text{kg fuel})$ , which is only 2.37 % less.

If there is excess air present in the flue gas, the specific dry flue gas volume would read

$$G_d = G \cdot \lambda \quad (3.67)$$

Through the combination of equations (3.66), (3.18) and (3.70), one gets

$$G_d = 8.88 \cdot C_f \cdot \frac{CO_{2,\text{max}}}{CO_2}, \quad (3.68)$$

Taking the  $CO_{2,\text{max}}$  value from this study  $CO_{2,\text{max}} = 0.2046 (= 20.46\%)$  one gets

$$G_d = \frac{C_f}{0.55 \cdot CO_2}. \quad (3.69)$$

Taking into account the unburnt carbon content in the residue and potential cases with significant incomplete combustion, where a significant proportion of CO is being



produced, one gets

$$G_d = \frac{C_f - C_r}{0.55 \cdot (CO_2 + CO)} \approx \frac{C_f - C_r}{0.536 \cdot (CO_2 + CO)}, \quad (3.70)$$

which is identical to the  $G_d$  term present in equations (??), (3.99) and (3.90), as given by BS EN 16510-1. The relative difference between the factors in the numerator (0.55 vs 0.536) is 2.6 %.

Alternatively, if  $G = 3.93 \text{ Nm}^3/(\text{kg fuel})$  is to be kept constant, while leaving only  $C_f$  in calculation, one obtains

$$G = 9.10 \cdot C_f. \quad (3.71)$$

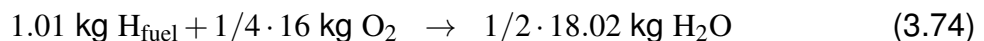
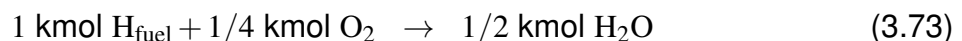
This then leads to

$$G_d = 9.10 \cdot C_f \cdot \frac{CO_{2,\max}}{CO_2} = \frac{C_f}{0.537 \cdot CO_2} \approx \frac{C_f - C_r}{0.536 \cdot (CO_2 + CO)}, \quad (3.72)$$

where 0.537 is only 0.18 % larger than the earlier value of 0.536.

### 3.6.2 Calculation of Specific Volume of Water Vapour in Flue Gas

The specific volume of water vapour in the flue gas (under standard conditions) determines how much volume of water vapour is produced per unit mass of burned fuel. Water vapour in flue gas comes from two sources: from moisture (bound water between wood cells) and from oxidation of hydrogen present in the fuel. The following chemical balance equations show the hydrogen oxidation into water vapour:



There is no nitrogen involved in the balance equations above, as it does not contribute to the overall volume of the water vapour in the flue gas, but is rather accounted for in the specific volume calculation of the dry flue gas.

It is clear that 1 kg of H in fuel produces  $(1/2 \cdot 18.02)/1.01 \text{ kg} (= 8.92 \approx 9 \text{ kg})$  of  $H_2O$  (water vapour) in the flue gas, hence the mass content of water vapour produced by the hydrogen in the fuel per mass unit of hydrogen is

$$Y_{H_2O, H_{\text{fuel}}} = \frac{1/2 \cdot 18.02}{1.01} = 8.92 \approx 9 \frac{\text{kg } H_2O}{\text{kg } H_{\text{fuel}}}. \quad (3.75)$$

Therefore, the mass content of flue gas water vapour per mass unit of fuel amounts to

$$Y_{H_2O, fuel} \left[ \frac{\text{kg } H_2O_{\text{reaction}}}{\text{kg fuel}} \right] = 9 \cdot H_f, \quad (3.76)$$

where  $H_f$  is the mass content of hydrogen in the fuel in (kg H)/(kg fuel).

When water vapour produced by evaporation of moisture in wood is added to the water vapour produced from the chemical reaction of hydrogen, one gets

$$Y_{H_2O} = 9H_f + W_f, \quad (3.77)$$

where  $W_f$  is the mass content of moisture (as fired basis) in wood in (kg moisture/kg fuel).

In order to calculate the specific volume of water vapour, the mass contents need to be multiplied by the water vapour specific volume (at standard conditions). The ideal gas law can give a good approximation for estimation of the water vapour specific volume:

$$v = V_m/M, \quad (3.78)$$

where  $V_m$  is the molar volume and is calculated as

$$V_m = \frac{R_u \cdot T}{p}. \quad (3.79)$$

Combining equations (3.78) and (3.79), the specific water vapour volume at standard conditions can be calculated:

$$v = \frac{R_u \cdot T}{p \cdot M} = \frac{8.31 \frac{\text{Pa} \cdot \text{m}^3}{\text{K} \cdot \text{mol}} \cdot 273.15 \text{K}}{101325 \text{Pa} \cdot 18.02 \frac{\text{kg}}{\text{kmol}}} = 1.244 \frac{\text{Nm}^3}{\text{kgH}_2\text{O}}. \quad (3.80)$$

Hence, the specific volume of water vapour (per mass unit of fuel) reads

$$G_{wv} = v \cdot Y_{H_2O} = 1.244 \cdot (9H_f + W_f) \quad (3.81)$$

and if  $H_f$  and  $W_f$  are expressed in mass %, rather than kg/kg, one gets the formula:

$$G_{wv} = v \cdot Y_{H_2O} = 1.244 \cdot \frac{9H_f + W_f}{100}. \quad (3.82)$$

The standard BS EN 16510-1 defines the formula for specific volume of wet flue gases  $G_w = G_d + G_{wv}$ :

$$G_w = \frac{C_{\text{daf}} - C_r}{0.536 \cdot (CO_2 + CO)} + 1.244 \cdot \frac{9H_f + W_f}{100}. \quad (3.83)$$

### 3.6.3 Final Formula for Flue Gas Mass Flow

By taking into account equations (3.44), (3.50) (3.51), (3.70) and (3.82), one can derive the following expression for calculation of the flue gas mass flow:

$$\Phi_g = \frac{\dot{m}_f \cdot 1.3 \cdot \left( \frac{C_f - C_r}{0.536 \cdot (CO + CO_2)} + 1.244 \cdot \frac{9H_f + W_f}{100} \right)}{3.6}, \quad (3.84)$$

which is defined in the BS EN 16510-1.

## 3.7 Thermal Heat Loss in Flue Gas

The first law of thermodynamics states

$$Q^* = C \cdot \Delta T, \quad (3.85)$$

where  $Q^*$  is heat in kJ,  $C$  is the heat capacity of an object<sup>5</sup> in kJ/K and  $\Delta T$  is the temperature difference between the systems or states, in K.

If the heat capacity per unit volume (at constant pressure) of a substance is known, one obtains:

$$Q^* = V \cdot C_p \cdot \Delta T, \quad (3.86)$$

where  $V$  is the volume of a substance in m<sup>3</sup> and  $C_p$  is its specific heat capacity (per unit volume) in kJ/(m<sup>3</sup> K).

If equation (3.86) is divided per unit mass of fuel it becomes:

$$Q = G \cdot C_p \cdot \Delta T, \quad (3.87)$$

where  $Q$  is the heat per unit mass of fuel in kJ/(kg fuel) and  $G$  is the specific volume of a substance, per unit mass of fuel, in m<sup>3</sup>/(kg fuel).

If the substance is wet flue gas (denoted with  $w$ ), which consists of dry flue gas (denoted with  $d$ ) and water vapour (denoted with  $wv$ ), equation (3.87) becomes

$$Q_w = Q_d + Q_{wv} = G_d \cdot C_{p,d} \cdot \Delta T + G_{wv} \cdot C_{p,wv} \cdot \Delta T = (G_d \cdot C_{p,d} + G_{wv} \cdot C_{p,wv}) \cdot \Delta T. \quad (3.88)$$

Since thermal heat loss refers to the heat not being extracted from the flue gases, i.e.

<sup>5</sup>It can be either solid or fluid; in this case a flue gas.

to the heat given to the atmosphere, from flue gas temperature to room temperature,  $\Delta T$  is calculated as

$$\Delta T = T_{\text{flue gas}} - T_{\text{room}}. \quad (3.89)$$

Hence, by taking into account equations (3.70), (3.82) and (3.89), equation (3.88) becomes

$$Q_a = (T_{fg} - T_a) \cdot \left( \frac{C_{p,fg}(C_f - C_r)}{0.536(CO + CO_2)} + C_{p,fgw} \cdot 1.244 \cdot \frac{9H_f + W_f}{100} \right), \quad (3.90)$$

which is the formula defined in BS EN 16510-1.

If thermal heat losses are to be expressed relative to the lower calorific value of the fuel, one gets:

$$q_a = \frac{Q_a}{H_{i,f}}, \quad (3.91)$$

or as a percentage

$$q_a = 100 \cdot \frac{Q_a}{H_{i,f}}, \quad (3.92)$$

as defined in BS EN 16510-1.

### 3.8 Chemical Heat Loss in Flue Gas

Chemical heat loss in the flue gas is modelled through the enthalpy of oxidation of carbon monoxide which has left the combustion process unburned. This can be shown through the following equation:

$$Q_{\text{chem}}^* [\text{kJ}] = \Delta H_{\text{CO,oxidation}} \left[ \frac{\text{kJ}}{\text{m}^3 \text{CO}} \right] \cdot V_{\text{CO}} [\text{m}^3 \text{CO}]. \quad (3.93)$$

When divided by a unit mass of fuel and taking into account that CO is present in the dry flue gases, equation (3.93) reads:

$$Q_{\text{chem}} \left[ \frac{\text{kJ}}{\text{kg fuel}} \right] = \Delta H_{\text{CO,oxidation}} \left[ \frac{\text{kJ}}{\text{Nm}^3 \text{CO}} \right] \cdot CO \left[ \frac{\text{Nm}^3 \text{CO}}{\text{Nm}^3 \text{dry flue gases}} \right] \cdot G_d \left[ \frac{\text{Nm}^3 \text{dry flue gases}}{\text{kg fuel}} \right]. \quad (3.94)$$

$\Delta H_{\text{CO,oxidation}}$  is enthalpy of CO oxidation reaction



$\Delta H_{\text{COoxid}}$  is used because it quantifies the loss of energy which is stored as potential chemical energy in CO.  $\Delta H_{\text{COoxid}}$  can be calculated as the difference between the enthalpies of formation of  $\text{CO}_2$  and CO [67]:

$$\Delta H_{\text{COoxid}} = \Delta H_{f,\text{CO}_2} - \Delta H_{f,\text{CO}} = -393.5 \frac{\text{kJ}}{\text{mol}} - \left( -110.5 \frac{\text{kJ}}{\text{mol}} \right) = -283 \frac{\text{kJ}}{\text{mol}} \quad (3.96)$$

If  $\Delta H_{\text{COoxid}}$  is to be expressed in  $\text{kJ}/\text{Nm}^3$ , one gets

$$\Delta H_{\text{COoxid}} = \frac{-283 \frac{\text{kJ}}{\text{mol}}}{M_{\text{CO}}} \cdot \rho_{\text{CO}} = \frac{-283 \frac{\text{kJ}}{\text{mol}}}{28.01 \frac{\text{g}}{\text{mol}}} \cdot 1.25 \frac{\text{kg}}{\text{Nm}^3} = -12629.4 \frac{\text{kJ}}{\text{Nm}^3} \quad (3.97)$$

The absolute value of the CO oxidation reaction is  $|\Delta H_{\text{COoxid}}| = 12629 \text{ kJ}/\text{Nm}^3$ , which is very close to the 12644 value defined in BS EN 16510-1 - the relative error is 0.1 % .

Hence, by combining  $|\Delta H_{\text{COoxid}}| \approx 12644 \text{ kJ}/\text{Nm}^3$ , and equations (3.94) and (3.70), one gets:

$$Q_b = Q_{\text{chem}} = 12644 \cdot CO \cdot \frac{C_f - C_r}{0.536(CO + CO_2)}, \quad (3.98)$$

and if  $CO$  is to be expressed in vol%, one gets:

$$Q_b = Q_{\text{chem}} = 12644 \cdot \frac{CO}{100} \cdot \frac{C_f - C_r}{0.536(CO + CO_2)}, \quad (3.99)$$

i.e. the formula as defined in BS EN 16510-1.

Analogously to relative thermal heat losses, relative chemical heat losses can be expressed as

$$q_b = 100 \cdot \frac{Q_b}{H_{i,f}}, \quad (3.100)$$

as defined in BS EN 16510-1.

Another potential chemical heat loss is the one due to unburned carbon in the char residue,  $q_r$ . In BS EN 16510-1 this loss is fixed to

$$q_r = 0.5\%. \quad (3.101)$$

### 3.9 Efficiency

The efficiency of a wood stove is defined as the proportion of useful exchanged heat to the overall heat (or internal energy) being produced by the wood combustion. Efficiency

(in %) can, therefore, be expressed as

$$\eta = 100 - (q_a + q_b + q_r), \quad (3.102)$$

as defined in BS EN 16510-1.

### 3.10 Heat Output of the Appliance

The heat output of the wood stove refers to the useful heat flow rate (in kW), which can be expressed through the efficiency  $\eta$  and overall heat output. The overall heat output is defined through the mass consumption rate of the fuel and its calorific value:

$$P_{\text{overall}} = \dot{m}_f H_{i,f}. \quad (3.103)$$

Therefore, the useful heat output is expressed as

$$P = \eta/100 \cdot \dot{m}_f H_{i,f}. \quad (3.104)$$

Since  $P$  is to be expressed in kW and  $\dot{m}_f$  is expressed in kg/h, the corrected formula reads

$$P = \frac{\eta \dot{m}_f H_{i,f}}{100 \cdot 3600}, \quad (3.105)$$

as defined in the BS EN 16510-1.

### 3.11 Conversion of Units of Pollutant EFs

In this section the unit conversion procedures for different pollutant emission factors will be given, since different literature sources and sources from technical specification reports use different units for pollutant emissions.

**Vol ppm pollutant to (mg pollutant)/(Nm<sup>3</sup> dry flue gas)**

Since

$$EF \left[ \frac{\text{mg pollutant}}{\text{Nm}_{dfg}^3} \right] = EF \left[ \frac{10^{-6} \cdot \text{kg pollutant}}{\text{Nm}_{dfg}^3} \right] \quad \text{and} \quad (3.106)$$

$$EF [\text{vol ppm}] = EF \left[ 10^{-6} \cdot \frac{\text{Nm}^3 \text{ pollutant}}{\text{Nm}_{dfg}^3} \right], \quad (3.107)$$

where  $EF$  is an emission factor of a pollutant and  $dfg$  denotes dry flue gases, one obtains

$$EF \left[ \frac{10^{-6} \cdot \text{kg pollutant}}{\text{Nm}_{dfg}^3} \right] = EF \left[ 10^{-6} \cdot \frac{\text{Nm}^3 \text{ pollutant}}{\text{Nm}_{dfg}^3} \right] \cdot \rho_{\text{pollutant}} \left[ \frac{\text{kg pollutant}}{\text{Nm}^3 \text{ pollutant}} \right] \quad \text{i.e.} \quad (3.108)$$

$$\cdot \rho_{\text{pollutant}} \left[ \frac{\text{kg pollutant}}{\text{Nm}^3 \text{ pollutant}} \right] \quad \text{i.e.} \quad (3.109)$$

$$EF \left[ \frac{\text{mg pollutant}}{\text{Nm}_{dfg}^3} \right] = EF [\text{vol ppm}] \cdot \rho_{\text{pollutant}} \left[ \frac{\text{kg pollutant}}{\text{Nm}^3 \text{ pollutant}} \right]. \quad (3.110)$$

It is clear that the conversion coefficient from vol ppm to mg/m<sup>3</sup> is the density value of the pollutant.

**(mg pollutant)/(Nm<sup>3</sup> dry flue gas @ 13 % O<sub>2</sub>) to (mg pollutant)/(MJ input energy)**

The conversion equation reads

$$EF \left[ \frac{\text{mg pollutant}}{\text{MJ input energy}} \right] = EF \left[ \frac{\text{mg pollutant}}{\text{Nm}_{dfg}^3 @ 13 \% \text{ O}_2} \right] \cdot \frac{G_{d,13\% \text{ O}_2} \left[ \frac{\text{Nm}_{dfg}^3 @ 13 \% \text{ O}_2}{\text{kg fuel}} \right]}{H_i \left[ \frac{\text{MJ input energy}}{\text{kg fuel}} \right]}, \quad (3.111)$$

where  $G_{d,13\% \text{ O}_2}$  is a specific volume of dry flue gases normalised to 13 % oxygen and  $H_i$  is the lower calorific value of fuel.  $G_{d,13\% \text{ O}_2}$  in the equation above (3.111) is calculated by using equation (3.70), as follows:

$$G_{d@13\% \text{ O}_2} = \frac{C_f - C_r}{0.536 \cdot CO_{2,13\% \text{ O}_2}} \approx \frac{43}{0.536 \cdot 7.8} = 10.28 \frac{\text{Nm}_{dfg}^3}{\text{kg fuel}} \quad (3.112)$$

$CO_{2@13\% \text{ O}_2}$  is set to 7.8 %, which follows from equations (3.15) and (3.16):

$$\lambda = \frac{CO_{2,\text{max}}}{CO_2} = \frac{21}{21 - O_2}, \quad (3.113)$$

so when  $O_2 = 13\%$ ,  $CO_2 = 7.8\%$ .

Taking into account the equation (3.112) and that  $H_i = 15.8$  MJ/kg as a representative calorific value of all wood (at cca 12 % moisture), one obtains an approximate conversion coefficient  $G_d/H_i = 0.65$  (m<sup>3</sup> dfg)/(kg fuel), and equation (3.111) the becomes

$$EF \left[ \frac{\text{mg pollutant}}{\text{MJ input energy}} \right] = EF \left[ \frac{\text{mg pollutant}}{\text{Nm}_{dfg}^3 @ 13 \% O_2} \right] \cdot 0.65 \frac{\text{Nm}_{dfg}^3 @ 13 \% O_2}{\text{kg fuel}}, \quad (3.114)$$

Obviously, the conversion coefficient depends on the wood composition, mostly on the carbon content in the wood, and on the calorific value of the wood. However, while calorific value per unit volume varies from species to species depending on their density, the calorific value per unit mass is similar for all wood species (15.5 - 16 MJ/kg lower heating value) [68].

## 3.12 Chapter Summary

In this chapter theoretical aspects of combustion were presented and formulae for calculation of important quantities that define a wood stove's performance, also specified in the EN 16510-1 standard, were derived. The following quantities and formulae were derived: i) the maximum possible volume fraction of carbon dioxide in flue gases  $CO_{2,max}$ , ii) a method for normalisation of a constituent's concentration to a defined oxygen content in flue gases (in this case being 13 vol%  $O_2$ ), iii) two different methods for averaging concentration values: one based on a charge based average (which is in accordance to BS EN 16510-1), and one for an instantaneous average (used for leakage assessment), iv) and v) formulae for calculation of normalised concentrations of OGC and PM, vi) a formula for the calculation of flue gas mass flow, vii) a formula for the calculation of thermal heat loss in flue gases, viii) a formula for the calculation of chemical heat loss in flue gases, ix) a formula for the calculation of thermal efficiency, x) a formula for the calculation of heat output of the appliance, and xi) two methods to convert units for pollutant emission factors.

In the next chapter the research methods to be used are presented, including specifications and requirements of the BS EN 16510-1 standard, deviations undertaken from the standardised procedure, specifications of testing equipment, explanation of statistical design of experiments methodology used in this work and, lastly, firewood specifications used during tests.



# Chapter 4

## Research Methodology

In the last chapter theoretical aspects of combustion and important equations were presented, while this chapter presents the research methods used in this study, including:

- Specifications of the BS EN 16510-1:2018 industrial standard, including undertaken deviations from the standardised procedure
- Specifications of the testing equipment used in the experiments of this study.
- A brief overview of the statistical design of experiments methodology,
- Specifications of firewood used during the testing.

### 4.1 BS EN 16510-1:2018 Standard Specifications and Ecodesign Requirements

In this section some details and specifications of EN 16510-1 that are of importance to this EngD dissertation will be given.

The standard BS EN 16510-1 applies to residential solid fuel burning appliances and it supersedes EN 13240:2001, EN 13229:2001, EN 12815:2001 and EN 12809:2001. The standard specifies requirements relating to the design, manufacture, construction, safety and performance of room heaters fired by solid fuel. It defines test methods for measuring carbon monoxide (CO), nitrogen oxides (NO<sub>x</sub>), total hydrocarbons (THC) and particulate matter (PM) emissions, but does not contain any limit values for these

emissions [63]. The limits are given by the Ecodesign directive [9], and for closed room sealed solid fuel appliances (stoves) these are given in Table 1.1.

The nominal heat output test consists of ignition batch, pretest batch(es) [63] and a minimum of 3 test batches (or test periods), each with a minimum duration of 40 minutes [69]. The results of 2 consecutive batches, plus one additional batch from the same burn period, are to be averaged and reported. It is to be noted that the usual procedure during certification tests in the Danish Technological Institute (DTI) [70] is averaging 3 consecutive batches, since the testing procedure is also in accordance with the DIN<sup>1</sup> standard.

Refuelling is permitted once one of the following two criteria is met:

1. Firewood mass at the end of the test period is less than 100 g more than the firewood mass at the end of the previous test period
2. CO<sub>2</sub> concentration is  $(4 \pm 0.5)$  vol%

Adjustment of air controls (if they exist) is permitted within 3 minutes of closing the appliance's door. The 3 minute period is also included as part of the test period duration. There were no air controls on gasification stoves tested in this study.

Gas sampling occurs in intervals of no longer than 30 s. The sampling interval used in this study was 5 s.

#### 4.1.1 Particulate Matter Sampling Procedure

Two possible particulate matter measurement methods are included in the standard:

1. Heated filter method and
2. Full flow dilution tunnel.

Here only the heated filter method will be explained as this method was used in the experiments in this study.

Particulate matter sampling starts no longer than 3 minutes after refuelling and lasts 30 minutes. The heated filter needs to be kept at a temperature between 70°C and

---

<sup>1</sup>German Institute for Standardisation; in German: Deutsches Institut für Normung

160°C. In the experiments conducted for this research the temperature of heated filter was kept at 160°C.

Filters are to be dried in an oven at 180 °C for at least 1 h and stored in a dessicator for at least 4 hours, weighed within 1 minute once they have been taken out of the dessicator, before and after sampling. The sampling volume flow rate is to be set to (0.5 - 0.6) m<sup>3</sup>/h. The flow rate is to be maintained by manual adjustment of the bypass valve on a vacuum pump every 5 min.

In this study the samples were not dried in the dessicator as one was not available at the time of the test. However, an identical testing procedure was kept for all conducted tests, therefore, test data from in-house prototype tests are fully comparable.

#### 4.1.2 Calculation Methods

In this section the formulae for calculation of different performance parameters defined by the standard BS EN 16510-1:2018 are presented. All formulae that were used in the calculations in this study are derived and/or presented in the previous chapter and cross-referenced here in Table 4.1.

Table 4.1: Formulae for calculation of stove performance parameters defined by the BS EN 16510-1:2018 standard. Formulae are derived and specified in the chapter 3.

| Quantity                   | Method  |
|----------------------------|---|
| Thermal heat loss          | Equation 3.90; $C_r = 1.4925 \cdot 10^{-5} \cdot H_{i,f}^*$ |
| Chemical heat loss         | Equation 3.99   |
| Heat loss in the residue   | $q_r = 0.5$ % of calculated efficiency**                    |
| Efficiency                 | Equation 3.102  |
| Heat output                | Equation 3.105  |
| Flue gas mass flow rate    | Equation 3.84   |
| $CO_{2,max}$               | Equations 3.13, 3.9, 3.3, 3.5 and 3.7                       |
| $CO$ @ 13% O <sub>2</sub>  | Equation 3.32   |
| $OGC$ @ 13% O <sub>2</sub> | Equations 3.36, 3.70 and 3.83                               |
| $PM$ @ 13% O <sub>2</sub>  | Equations 3.41, 3.42 and 3.43                               |

\* $H_{i,f}$  is lower calorific value of the test fuel \*\* if the test fuel are wood logs

### 4.1.3 Deviation from BS EN 16510-1 Procedure

The testing procedure according to BS EN 16510-1 was followed almost fully, with three exceptions:

1. In all test runs conducted for the statistically designed experiment, the sampling probe was located in the heat exchanger, near the secondary chamber outflow - instead of inside the flue stack, 1315<sup>2</sup> mm above the stove body. This was done due to unwanted flue stream dilution by air, as shown later in section 6.3.5 and in Figure 6.23. The stove in the optimum configuration was then tested with the correct sampling location according to the standard.
2.  $NO_x$  was not recorded, as the  $NO_x$  measuring module was not installed in the gas analyser.
3. After drying the used filters in the oven, they were not dried in the desiccator as it was not available for use. This change in the procedure might have an effect on the objectivity of results in comparison with other results (e.g. the ones obtained by the DTI), however, an identical procedure was followed for all experiments conducted in-house, hence comparison of results from in-house experiments are fully valid. One, however, has to take into account this limitation of results if replication would be attempted.

## 4.2 Testing Equipment Specifications

In this section the specifications of the testing equipment used for experiments on the developed stove prototype will be presented.

### *Gas Analyser*

The gas analyser for testing  $CO_2$ , CO, and OGC was ABB AO2020 [71], with modules

- Uras26 - for testing concentrations of  $CO_2$  and CO. The declared repeatability of measurement is  $\leq 0.5\%$  of span, whereas the detection limit is  $\leq 0.4\%$  of span [71]. For carbon monoxide, the lower span was set to 2000 ppm, whereas the higher span value was 3%.

---

<sup>2</sup>Formula for calculation of the distance between the stove body and the sampling probe from the BS EN 16510-1 [63] standard reads:  $h = 330 + 350 + 5d$  [mm], where  $d$  is the flue pipe diameter. With  $d = 5$  inches  $\approx 127$  mm,  $h \approx 1315$  mm

- Fidas24 - for testing the concentration of OGC. The declared repeatability of measurement is  $\leq 0.5\%$  of span, whereas the detection limit is  $\leq 1\%$  of span [71]. For OGC, span was set to 1500 mgC/Nm<sup>3</sup>.

The data logger was Keysight 34970A [72].

#### *Particulate Matter Testing Equipment*

Particulate matter sampling equipment was manufactured by Paul Gothe GmbH<sup>3</sup>. The used parts were following:

- Plane filter device 7.22-A [73],
- Glass fiber filters GF-PF-45 [74],
- Filter device heater 35.03-MK [75],
- Package with complete equipment for gas volume measurement 22.0K-1 [76],
- Absolute pressure measurement instrument HMG B [77], and
- Differential pressure measurement instrument HMG 03 [78].

The scale for weight measurement of the wood logs was Ohaus Defender 3000 [79].

The micro balance for weight measurement of filters for PM concentration measurement was Adoner 300 [80], with the resolution of 0.1 mg.

The setup of the testing equipment is schematically shown in Figure 4.1.

---

<sup>3</sup>Paul Gothe GmbH, Wittener Straße 82, D-44789 Bochum, Germany

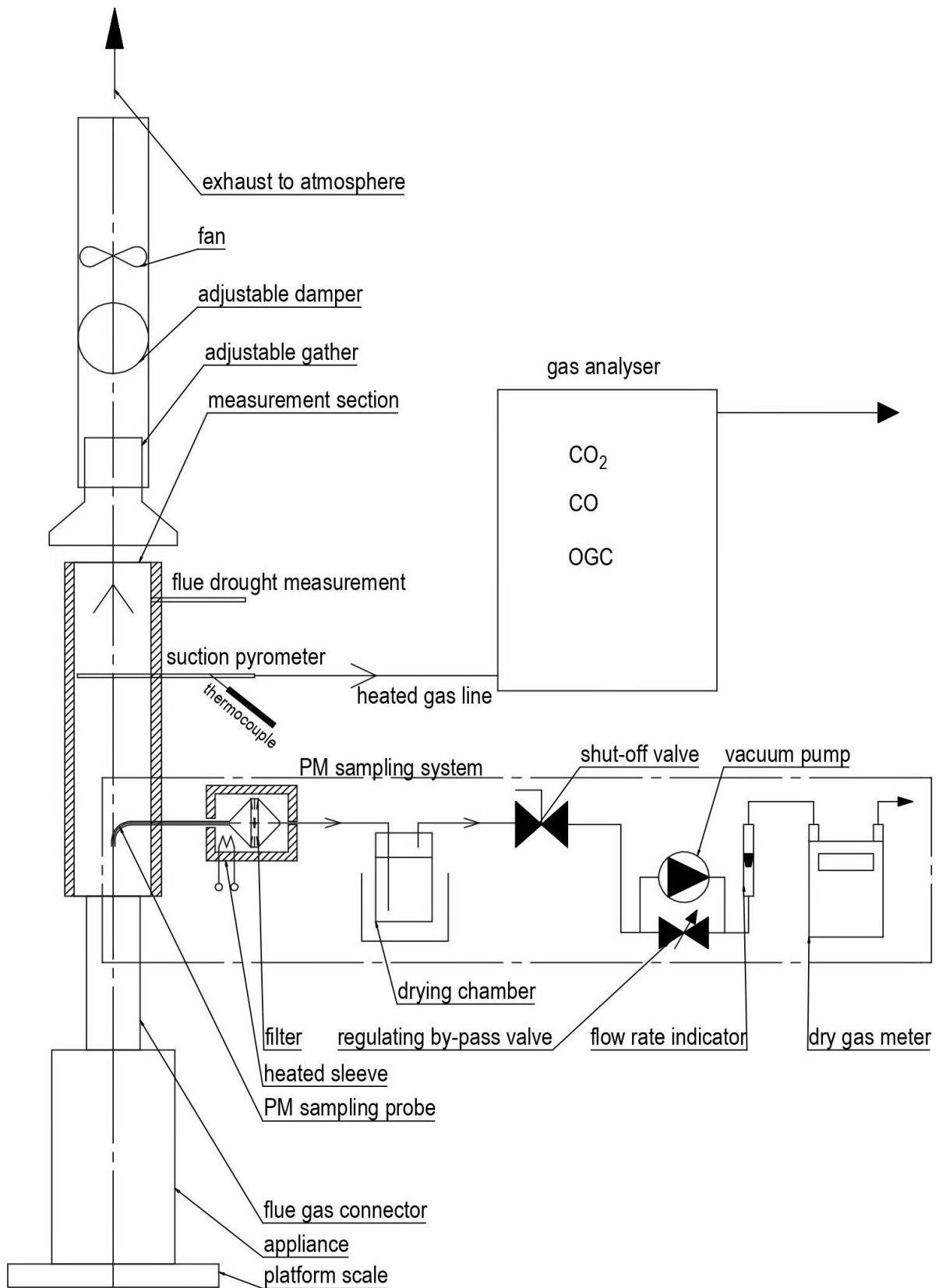


Figure 4.1: Schematic diagramme of test setup.

### 4.3 Statistical Design of Experiments

In this section a brief explanation of statistical design and analysis of experiments methodology is provided.

According to Montgomery [81], 'statistical design of experiments (DoE) refers to the process of planning the experiment so that appropriate data will be collected and analyzed by statistical methods, resulting in valid and objective conclusions'. Such a method was used to plan, conduct and analyze the experiments conducted for this study.

It is to be noted that DoE methods were generally not used in the reviewed literature related to biomass combustion, except for the work of Boman et al [32], where they used two factor, three level, central composite experimental design. The reason for not using this methodology could be the fact that university based researchers rarely aim to develop a new low emission residential wood burning appliance, or to experimentally optimise it, but rather to provide side-by-side comparison of some influential parameters (e.g. burning moist versus dry wood, or wood log versus pellet versus wood chip burning appliances, or characterisation of numerous gas species emissions (or PM size distribution) from particular appliance, etc.). Hence, in terms of DoE methodology, there is no equivalent study available for comparison.

DoE methods are often used if the research aim is to identify factors influencing the response variable<sup>4</sup> and/or to find the best combination of factor levels<sup>5</sup>, i.e. the combination of factor levels that give the optimum value for a response variable. If the number of tested factors is greater than one, the experimental design is called a *factorial experiment* or *factorial design*. Usually factors are tested across the same number of levels. If 3 factors are tested across 2 levels, the full factorial design is called  $2^3$  factorial design. It is called 'full' since all factor combinations are tested in  $2^3 = 8$  experimental runs. Full factorial designs and subsequent statistical analysis give effect estimates of all tested factors and of all possible factor interactions. For example, a full factorial design with factors A, B and C, provide 9 effect estimates: 3 of factors A, B and C, 3 of 2-factor interactions AB, AC and BC, and 1 of a 3-factor interaction ABC.

Since increasing the number of factors and levels results in a very rapid increase in the necessary runs, *fractional factorial* designs are used. In such designs only a fraction (e.g. 1/2, 1/4, 1/8, etc.) of all possible runs is conducted. However, this reduction of

<sup>4</sup>Response variables in this study are pollutant emission levels: *CO*, *PM* and *OGC*.

<sup>5</sup>Factor levels are values that factors take, e.g. factor 'Drilling speed' could be tested across two levels - 20 rpm and 10 rpm.

experimental runs comes at a cost; it results in the *aliasing* of effects. For example, in a one-half fraction of a 4-factor 2-level design with factors A, B, C and D, one 2-factor interaction AB is aliased with another 2-factor interaction CD, meaning that effects of these two 2-factor interactions are coupled into a single effect AB + CD and cannot be isolated. This type of fractional factorial design was conducted in this thesis and will be explained in more detail in section [5.3.2](#).

A method for statistical analysis of data obtained through factorial experiments is analysis of variance (ANOVA). For more details regarding the statistical design and analysis of experiments methodology the reader is referred to Montgomery [81].

## 4.4 Firewood

Supplied firewood used in the tests is labeled as mixed hardwood by the supplier. Its moisture content is cca 15%, however, it might vary between different crates of firewood. In the entire set of conducted experiments, the firewood from a single crate was used.

### 4.4.1 Test Firewood Humidity Control

Danish Technological Institute, and probably other certified laboratories in the EU and UK, use seasoned firewood for type testing. This is done in such way where an end few centimeters of every single log to be burned during testing is sawn off and weighed before and after drying in an oven, in order to determine the moisture level of firewood batch. However, during testing for this project, kiln dried wood was used, which contains greater moisture gradients within a single log, compared to seasoned wood. Hence, applying the same moisture testing procedure would result in much greater errors. Therefore, using firewood from a single crate as the only moisture control procedure was determined to be the only possible practical solution to minimise variation in results due to firewood moisture variation.

## 4.5 Chapter Summary

In this chapter the research methods used in this study were presented, including important specifications of the BS EN 16510-1 standard, specifications of the test-



ing equipment, an overview of the statistical design of experiments methodology and specifications of firewood used in testing. In the following chapter the design of different stove types and experimental setup are explained.

# Chapter 5

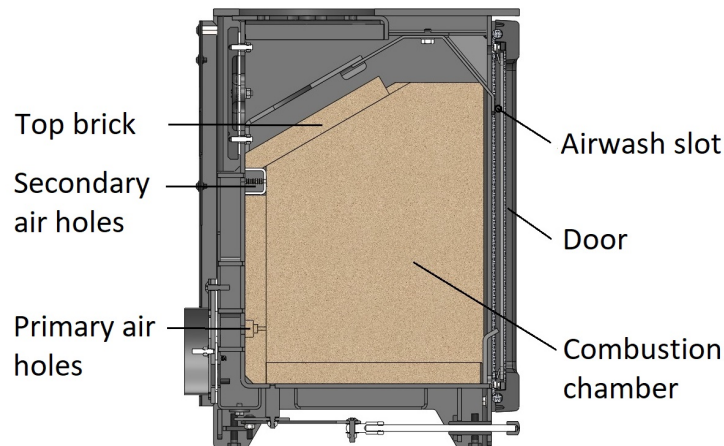
## Stove Design Development and Experimental Setup

The objective of the work in this chapter is to identify the factors in the stove design which impact its emissions and outline the experiments used to analyse the effect of varying these particular factors. This chapter covers the following topics:

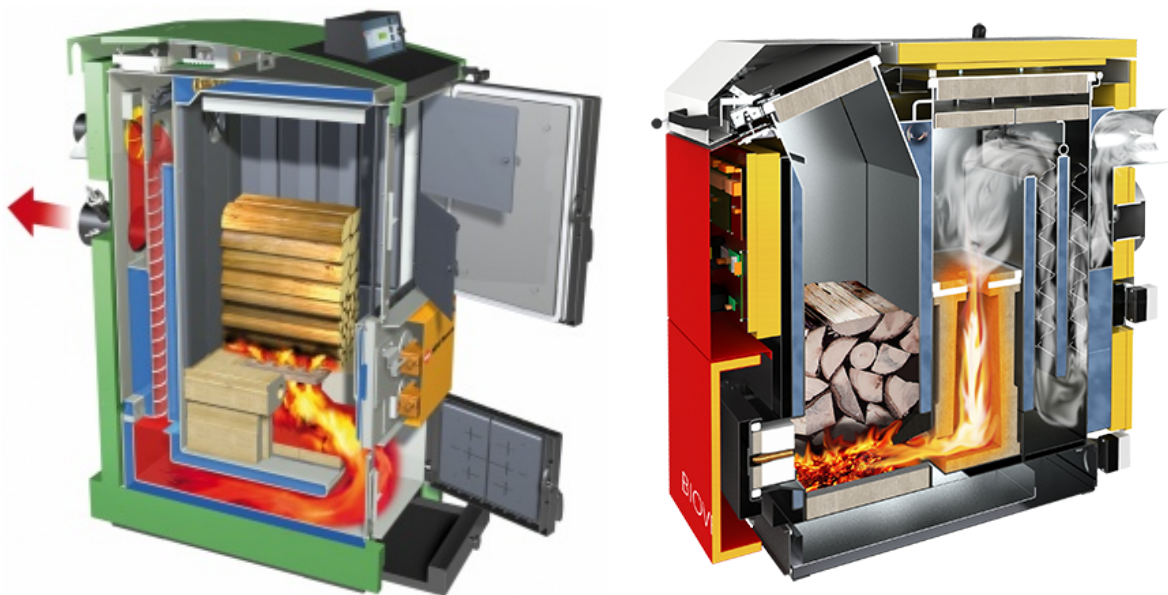
- An introduction to the two basic designs of residential wood log burning appliances: *conventional* (or up-draft) and *gasification* (or down-draft) stoves,
- An analysis of a sequence of five gasification stove prototypes developed during the initial stages of the project, leading to a base design for the new stove,
- Presentation of the experimental setup using the statistical design of experiments method, whereby four factors with two levels each are defined,
- An overview of seven conventional commercial stoves, manufactured by Hunter Stoves and tested by the DTI, each with different combustion chamber dimensions.

### 5.1 Basic Types of Residential Wood Burning Stoves

With regard to residential wood log burning appliances, there are two basic types: conventional (up-draft design), shown in Figure 5.1 (a), and gasification design, shown in Figure 5.1 (b) and (c).



(a) Central cross-section of a conventional (up-draft) burning appliance



(b) Down-draft gasification appliance. Source: [82]

(c) Side-draft gasification appliance. Source: [83]

Figure 5.1: Basic designs for residential wood log burning appliances.

Conventional appliances feature a combustion chamber with several air inflow locations (this is current state-of-the-art in wood stoves, as shown in Figure 5.1 (a)):

- *Primary air* - air inflow directly into the char and/or fuel bed<sup>1</sup>,
- *Secondary air* - air inflow above the fuel bed, oriented horizontally, and
- *Airwash air* (also called window purge air) - air inflow through a slot, oriented downwards, located along the top edge of the door glass area; the slot is usually 5 or more mm wide, and as long as the combustion chamber is wide. The purpose

<sup>1</sup>Char bed is a certain volume within the combustion chamber filled with char. This volume is adjacent to the base of the chamber. Analogously, fuel bed is a volume filled with firewood. Fuel bed is located above the char bed.

of airwash air is twofold: i) to ensure the soot is not deposited onto the inner glass surface at the beginning of a burn time when the glass is still cool, and ii) to partly contribute to the air inflow into the gaseous combustion area (i.e. the region above the fuel bed).

The terminology used for air inflow locations is common in the wood stove industry, but also might vary. In conventional wood burning appliances, all the fuel conversion processes take place in a single chamber: heating, drying and pyrolysis of wood, combustion of pyrolytic gases (syngas) and oxidation of char. Modern appliances usually feature a top plate, made out of either steel or vermiculite, which serves to prolong the residence time of the flame inside the combustion chamber.

Gasification appliances are characterised by two reaction zones, or chambers (*primary* and *secondary*), instead of one, with a connecting nozzle between the two chambers (as shown in Figure 5.2):

- In the *primary chamber* wood logs are placed onto the char bed created from previous fuel charges. In this chamber, heating, drying and pyrolysis of the wood, together with a portion of gaseous combustion (of the pyrolytic gases) and char oxidation occur.

Char oxidation and a portion of gaseous combustion occur due to the presence of air supplied through primary and airwash air holes. These two reaction processes are exothermic and supply the heat necessary for the endothermic processes, namely heating, drying and pyrolysis of the wood, as well as for any heat losses (through the primary chamber walls and through direct radiation through the door glass).

The fuel rich pyrolytic gases (or syngas) pass through the char bed down into the connecting nozzle, further increasing the syngas temperature. The overall downward oriented flow is generated by the pressure differential created by the chimney draft.

- Upon inflow of the hot syngas stream into the *nozzle*, the syngas mixes with the secondary air stream distributed on the nozzle walls. The two streams, partially mixed, leave the nozzle downwards into the secondary chamber.
- In the *secondary chamber* the major proportion of gaseous combustion takes place. Because the nozzle ensures good initial conditions for mixing, efficient mixing of fuel rich syngas with the secondary air stream can take place in a short period of time. Isolated from the wood and all the corresponding endothermic

processes, the secondary chamber can be thermally insulated and thus provide optimum conditions for gaseous combustion: i) appropriate volume and geometry which ensures sufficient residence time of gases, ii) good mixing as fuel and air stream meet in the confined nozzle zone, and iii) sufficiently high temperature due to a) thermal insulation of the secondary (or combustion) chamber walls and b) isolation from endothermic processes occurring in the primary chamber.

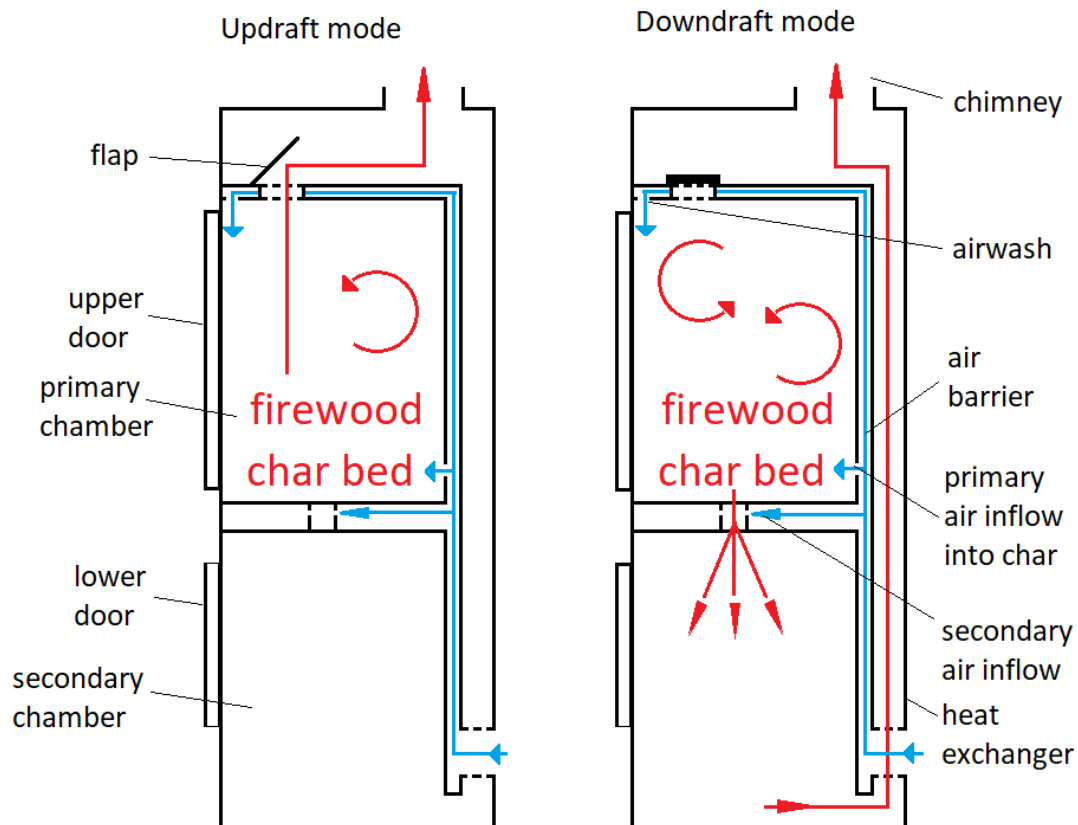


Figure 5.2: Side cross-section of a gasification stove concept; the left figure is showing the updraft mode of combustion, while the right one is showing the downdraft mode.

Upon leaving the secondary chamber, flue gases enter the heat exchanger. In case of a boiler, the heat is being exchanged with water, whereas in case of a wood stove, heat is being exchanged with room air through the outer steel walls. Once the flue gases reach the top of the appliance, they enter the flue system (i.e. the chimney). In case of fan-assisted appliances there is also a fan (usually of centrifugal type) at the exit of the heat exchanger.

In recent years, natural draft gasification appliances, or stoves, have been developed and marketed. In the case of natural draft driven wood burning appliances the draft, i.e. pressure difference, of cca 12 Pa<sup>2</sup> is created through the chimney effect. A list of such

<sup>2</sup>The draft could be between 10 and 20 Pa.

appliances present on the European market is shown in Table 2.4. Several examples of gasification wood stoves are shown in Figure 5.3.



Figure 5.3: Examples of commercially available natural draught down-flow domestic heating appliances.

### *Sealed flap*

One specific feature of natural draft gasification appliances is the presence of a *sealed flap*, i.e. sealed flue gas valve, at the exit of the primary chamber. When the flap is open the stove operates in the conventional (up-draft) mode, whereas when it is closed the stove operates in the gasification mode. The ability to run a natural draft gasification stove in the up-draft mode is of crucial importance for three major reasons:

1. *Creation of chimney draft* - The stove, the flue pipe and (thermally massive) chimney are cold at the beginning of the burn time, when the first firewood batch, with kindlings, is being ignited. Thus the draft created by the whole system is minimal. Hence the up-draft flue path, which has a lower pressure drop than the alternative, down-draft path, needs to be open in order to maximise the air inflow, which, consequently, accelerates the wood ignition process.

2. *Ability to ignite the syngas for the gasification mode of operation* - After the ignition firewood batch, one or two additional fuel charges are needed in the up-draft mode in order to create the char bed around the nozzle inlet. The presence of char around the nozzle inlet is important in order for *successful* syngas ignition in the secondary chamber when the flap is closed by the stove operator. This char is crucial for ensuring the syngas created in the primary chamber is at sufficiently high temperature, so that, when mixed with still cold secondary air (in the nozzle) in the still cold secondary chamber, it can be ignited.
3. *Avoiding smoke spillage into the room when the door is open* - During the most of the burn time (in gasification mode), when the wood is pyrolysing, the primary chamber is filled with fuel-rich syngas. Hence, when the door is open while the flap is closed, a lot of soot is created which then spills into the room. However, if the flap is open, e.g. for a minute before opening the door, much more flame in the primary chamber is created and any soot left could be extracted through the top flue exit.

The flap seal needs to be as tight as possible, because the pressure above the flap is lower than the pressure below (i.e. in the primary chamber) which presents an increased risk of leakage of pollutant rich syngas from the primary chamber. It will be shown in section 6.3.5 that minimisation of leakage through the flap is a design challenge that needs to be tackled and is a subject for further research.

As concluded in section 2.6, the gasification stove design is superior to the conventional one. Hence the stove prototype developed in this project will be of gasification type<sup>3</sup> and will be presented in the following section.

## 5.2 Gasification Stove Prototypes

A sequence of five stove prototypes (all of gasification type) have been designed, fabricated, assembled and tested. In the first three prototypes, the secondary chamber was built as a cyclone, i.e. as a cylinder with a tangential inflow of syngas-air mixture from the nozzle. The cyclonic secondary chamber was inspired by the combustion chamber design present in some gasification boiler models (e.g. [90, 65, 91]). The fourth and fifth prototypes had a rectangular geometry for the secondary chamber, and a centrally located nozzle, as featured in extant gasification wood stove designs (see Figure 5.3). It is to be noted that the development of a wood log burning stove has aesthetic

---

<sup>3</sup>Novel stove design development is one of the objectives of this study.



limitations that can be in conflict with design objectives related to performance. Since aesthetics plays a crucial role for any wood stove, it was decided that both chambers need to have a window (i.e. glass area) in order for the user to be able see the combustion processes in both chambers - as is the case with gasification stoves already present on the market, see Figure 5.3.

All three prototypes with cyclonic secondary combustion chamber featured an inherent flaw: the secondary glass failed within the five to ten burn cycles. This has occurred because the entire flow of high temperature burning gas stream hit the secondary glass surface. Since it is a mineral glass, made for high temperature environment, it did not break, however, it became opaque over time (e.g. 10 burning cycles). Due to this unsatisfactory outcome for all three prototypes, such design was not considered for further testing and optimisation within this project.

The two gasification stove prototypes did not feature the issue with failed secondary glass, while very low pollutant emission regimes were achievable.

Hence, the three prototypes with cyclonic secondary chamber and one prototype with rectangular geometry were precursors to the fifth prototype, which was then fully tested, according to the BS EN 16510-1 standard, through the statistical design of experiments methodology.

In the following sections the summary of features and observations of each of the prototypes is given. The reader should note that testing of these early prototypes has not been structured or systematised, as the objective of these tests was to explore the possible design space of gasification stoves, which includes tens of different parameters. Hence, the evidence and observations summarised in the following sections are of an anecdotal nature. All precursor prototypes are shown in Figure 5.4, as side cross-sections.



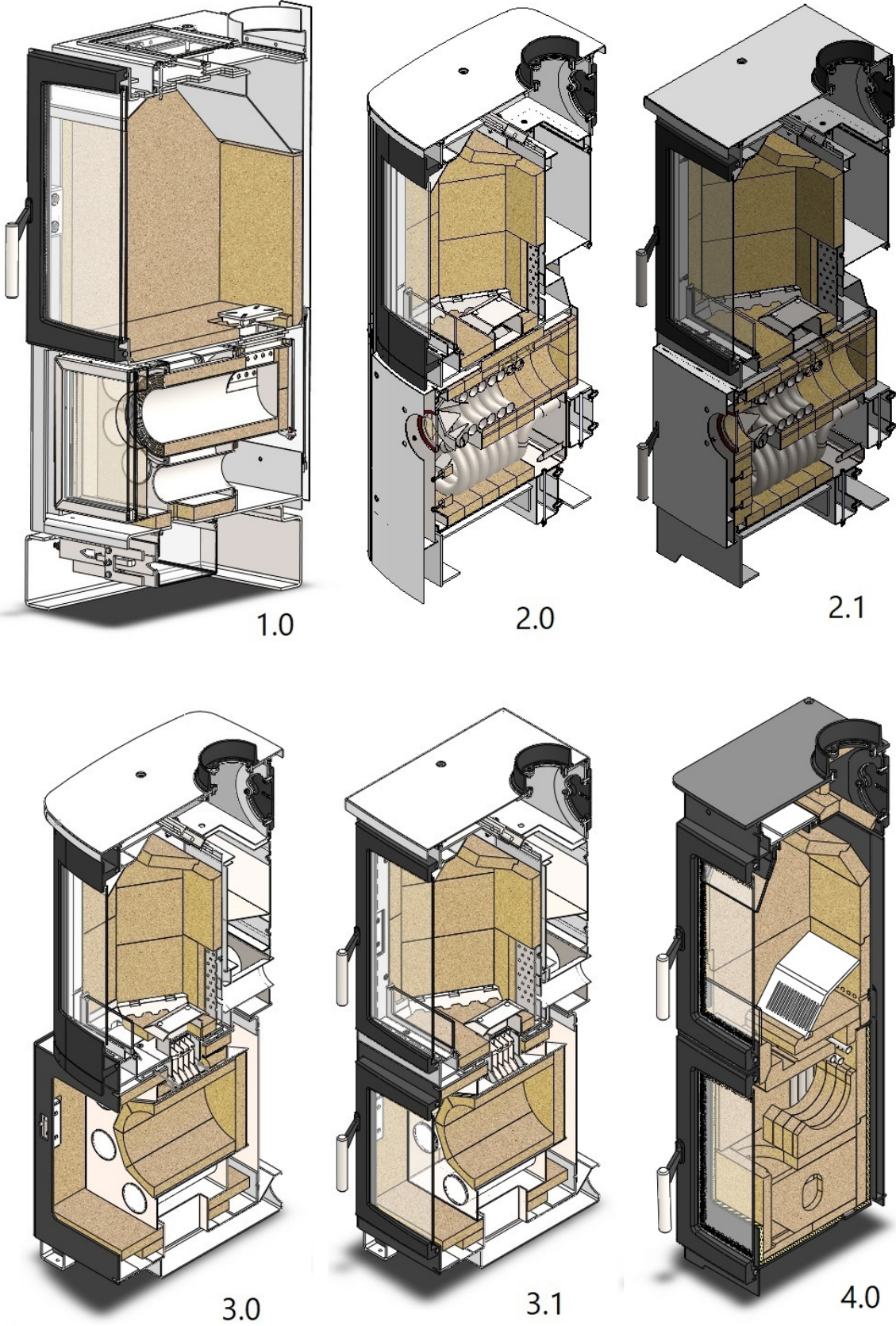


Figure 5.4: All prototypes.

### 5.2.1 First prototype - 1.0

The first prototype featured a large volume and large base area primary combustion chamber, a 100 mm diameter tubular secondary chamber with tangential flame entrainment and a combustion air recuperator, whose function was to exchange heat between the hot flue gases and cool air supply for the nozzle. The objective of such gasification stove design was to enable flameless combustion mode in the secondary chamber, as explained in a third EngD portfolio submission [92]. The stove featured high heat output (cca 20 kW) and highly uneven rates between pyrolysis and char consumption - which resulted in staged mode of firewood decomposition: high rate of pyrolysis in the first part of the charge cycle, and relatively lower rate of char consumption in the second half. During the pyrolytic stage, the secondary chamber temperature was above 1100 °C, sometimes above 1200 °C. The temperature of the combustion air, preheated by the recuperator and to be entered into the nozzle, was between 600 °C and 700 °C (in the long-term steady-state).

The stove suffered from many qualitative issues, most of which are explained in section 6.3.1, namely: primary chamber sooting, leakage of fuel rich pyrolytic gases into the flue way, secondary flame ignition issues, frequent blow-back issues, secondary chamber glass failure, failure of steel components exposed to high temperatures, inadequate primary chamber air entrainment locations, high pyrolysis rate, excessive heat output, etc.

The gaseous PIC emissions reached very low levels<sup>4</sup> very sporadically, probably during less than 1% of overall burn time. The gaseous PIC emissions were mostly observed to be high (e.g. CO over 2000 ppm), however, during these short lasting intervals, the gaseous PICs dropped to very low levels, after which they returned to more stable and much higher values. This observation confirmed the possibility of reaching very low PIC levels within such designed gasification stove, which led to the decision to design and produce the second prototype.

During the initial stage of secondary combustion (cca at least 1 hour after the secondary flame ignition) the stove always performed at elevated PIC emission levels. Only after the temperature of the secondary chamber rose above 900 °C the low PIC emission regime was enabled. The hypothesis for such dependence of PIC emission levels on the secondary chamber temperature is the fact that there is great interaction between secondary chamber walls and the gases coming from the nozzle due to the tangential jet orientation, as shown in Figure 5.4. Hence, when the walls are still

---

<sup>4</sup>OGC below 10 mg/Nm<sup>3</sup> and CO below 50 ppm

cool, they also cool the gases to below the ignition temperature, thus making the flame unstable.

During most of the burn time the stove operated in a low air excess ratio regime, which made high secondary chamber temperatures possible. Very low PIC emission regime was observed at oxygen levels between 1.5% and 2.5%, which means that air excess ratio range was 1.08 to 1.14, according to equations (3.17) and (3.18). Such low air excess ratio regime providing conditions for low minimum PIC emission levels was unique to this prototype, in comparison to all other prototypes. Other prototypes at such low air excess ratios performed at highly elevated PIC emission levels. For comparison, the final (fifth) prototype performed optimally at air excess ratio range of 1.5 to 3.

### **5.2.2 Second prototype(s) - 2.0 and 2.1**

Considering all issues observed during tests of the first prototype, many design changes were implemented in the second prototype: smaller primary chamber volume, distributed locations for air entrainment into the primary chamber, attempt to improve recuperator efficiency, re-scaling the secondary chamber (similar volume, different dimensions), and axially orienting the nozzle to the back of the secondary combustion chamber (while retaining the tangential component) to maximise recirculation.

Heat output was reduced to 7 or 8 kW (in 2.0 prototype version), primary chamber soot-ing was also reduced (however still inadequate), secondary flame ignition was still not stable, secondary door glass was transparent for more charge cycles, but still failed after a certain time, and low PIC levels regime was observed for incrementally longer time intervals and for almost every charge cycle. Temperature of preheated combustion air for secondary flame was not measured due to the specific geometry of the recuperator (which was a coiled stainless steel tube); the adequate placement of a thermocouple within the coil cavity was not possible. Secondary chamber temperatures were lower than in the first prototype (900 to 1100 °C) due to leaner air-fuel mixture.

Another version (2.1) was also built and tested. It had the same features as 2.0 version, but larger primary chamber, as the objective of the company was to test the possibility of larger heat output for boiler applications. Qualitatively similar features were observed as in 2.0 version, but at a slightly higher heat output (10 to 12 kW).

### 5.2.3 Third prototype - 3.0 and 3.1

Third prototype stage (stoves 3.0 and 3.1) went one step further with secondary chamber size, as can be seen from Figure 5.4. The primary chambers were reused from earlier two prototypes (2.0 and 2.1). Recuperator was not longer tubular, but of analogous geometry to the one in 1.0 prototype - due to fabrication issues and costs related to the coiling procedure.

Primary chamber still suffered from sooting and, in relation to the nozzle cover and nozzle tube geometry, inability to create stable secondary flame. However, once the conditions enabling stable secondary flame were reached, low PIC emission regime was observed for longer periods of time. This achievement was attributed to larger secondary chamber volume, which led to the design decision to prioritise secondary chamber volume in a future prototype.

### 5.2.4 Fourth Prototype

This prototype was made fully modular; both the primary and secondary chambers provided rectangular shell, without welded steel plate as a boundary between the two chambers. Vermiculite brick was used as interface between the two chambers in order to enable internal geometry flexibility. Such design development approach enabled geometry changes within days, rather than months, as it was with earlier prototypes. Apart from saving time, such development approach was also very economical in comparison to earlier approach where every design iteration required an entirely new stove prototype.

The geometry of a 4.0 stove, as shown in Figure 5.4, featured very unstable secondary flame ignition, so was soon internally redesigned numerous times, by using vermiculite bricks of different geometry, into a design similar to marketed gasification stoves, as the ones shown in Figure 5.3. The specific features of the final design, other than those provided in this document, cannot be disclosed due to confidentiality reasons.

## 5.3 Experimental Setup

### 5.3.1 Experiment Planning

During the pilot experimentation on the final (fifth) gasification stove prototype (referred to just as the gasification stove in what follows), four factors were identified as candidates for having significant effects on the stove's performance: 1) the char bed surface area<sup>5</sup>, 2) the nozzle inlet geometry, 3) the glass area of the secondary chamber door and 4) the outlet geometry of the secondary chamber. Hence, Stove E was designed modularly so that certain parts are interchangeable between experiments, while the rest of the system remains identical. It was decided that these four factors should be tested further in a statistically designed experiment. Hence, two levels (i.e. factor values) were assigned to each factor. The tested factors and their levels are presented in Table 5.1 and Figures 5.5 and 5.6. All 4 factors are treated as categorical.

Table 5.1: Identified factors and their levels to be tested in a factorial experiment. Nozzle inlet geometry is depicted in more detail in Figure 5.5. Secondary chamber outlet geometry is depicted in more detail in Figure 5.6.

| Factor description                        | Factor enumeration | Levels              |                     |
|---|--------------------|---------------------|---------------------|
|   |                    | High (+)            | Low (-)             |
| Char bed surface area                     | A                  | 472 cm <sup>2</sup> | 337 cm <sup>2</sup> |
| Nozzle inlet geometry                     | B                  | Flat cover          | Tubular cover       |
| Glass area of the secondary chamber door* | C                  | 400 cm <sup>2</sup> | 60 cm <sup>2</sup>  |
| Secondary chamber outlet geometry         | D                  | Holes               | Slots               |

\*any other secondary chamber surface that is not glazed is insulated with ceramic wool and vermiculite bricks

The objective of this designed experiment was to conduct screening of factors, rather than optimisation. Factor screening is needed here because it is not yet known whether

<sup>5</sup>Char bed surface area is defined as surface area of base of primary chamber, i.e. in the level of char bed.



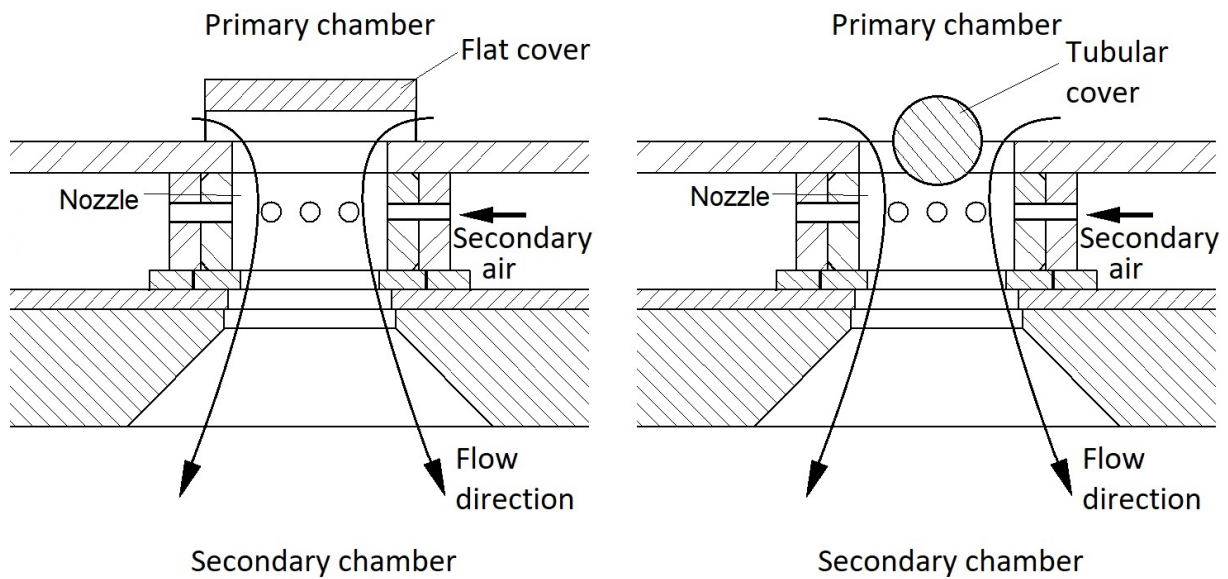


Figure 5.5: Two types of nozzle inlet covers - factor C. Left: Flat cover (high level); Right: Tubular cover (low level).

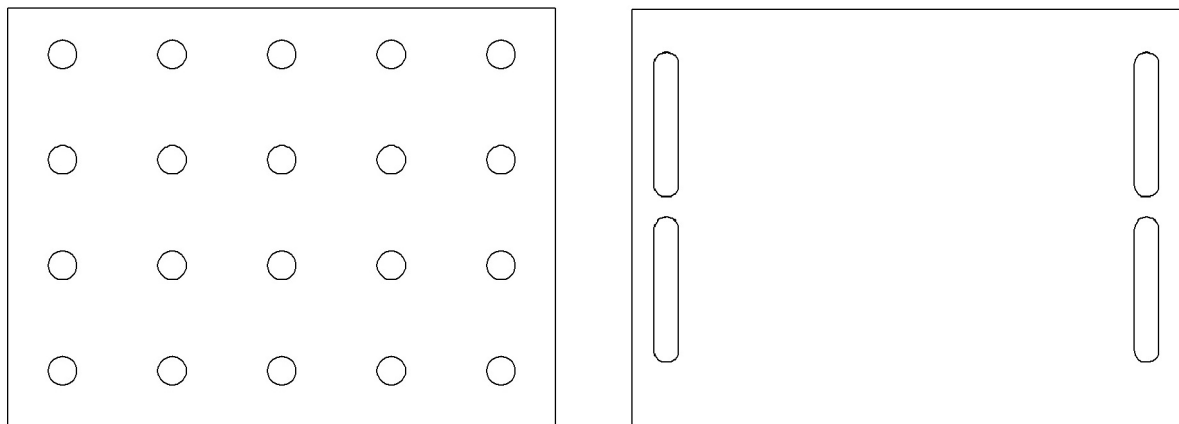


Figure 5.6: Two types of secondary chamber outlet geometries - factor D. Left: 20 equidistant holes (high level); Right: 4 lateral slots (low level).

all involved factors play significant role for stove's performance. Once the significant factors have been identified through the screening experimentation, optimisation experiments can be conducted. This last step was not a part of this project.

### 5.3.2 Factorial Experiment

Four factors with corresponding levels are defined in Section 5.3.1. As such, it is possible to run a full factorial experiment, where all factors and their interactions would be tested. Four factors at two levels each yield  $2^4 = 16$  different design configurations.

Since in this case it is not necessary to fully resolve all effects, but rather to evaluate the most important factors, one half fraction of the full factorial analysis was tested, i.e. 8 runs. Therefore, a one-half fraction of  $2^4$  design was run with the defining relation  $I = ABCD$ <sup>6</sup>, i.e.  $2_{IV}^{4-1}$ , where IV denotes resolution IV design.

The alias structure of this design ( $2_{IV}^{4-1}$ ) is

$$\begin{aligned} [A] &\rightarrow A + BCD \\ [B] &\rightarrow B + ACD \\ [C] &\rightarrow C + ABD \\ [D] &\rightarrow D + ABC \\ [AB] &\rightarrow AB + CD \\ [AC] &\rightarrow AC + BD \\ [AD] &\rightarrow AD + BC. \end{aligned}$$

From this it can be seen that in this experimental design (and any other resolution IV design) the estimates of the main factor effects are not aliased with any 2-factor interaction, but only 3-factor (or more) interactions. Only estimates of 2-factor interaction effects are aliased with other 2-factor interaction effects. The fact that the main factor effects are aliased only with 3-factor interactions is beneficial as it is possible to deduce strong conclusions about the main factor effect estimates.

The experimental design with fully randomised run order is shown in Table 5.2.

#### *Experimental unit*

One day of testing was chosen as an experimental unit, rather than one firewood batch. This was to ensure independence and to avoid auto-correlation of results.

## 5.4 Comparison of Several Conventional Stove Models

Independently from the gasification stove development and optimisation project, experimental results from several conventional stove models were analysed and compared. The stove models were produced by Hunter Stoves and the testing was conducted according to EN 13240 and EN 16510-1 standards in the Danish Technological Institute (DTI) during 2019. All seven stoves have almost identical topology, but different com-

<sup>6</sup>Defining relation  $I = ABCD$  is chosen because it gives highest possible design resolution.

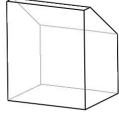
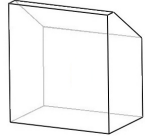
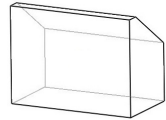
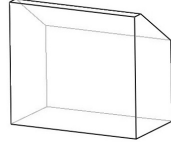
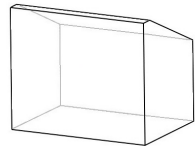
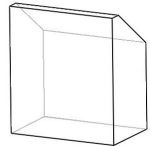
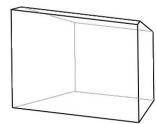
Table 5.2: Experimental design table. High level: +, Low level: -.

| Run | Run order | A | B | C | D=ABC |
|-----|-----------|---|---|---|-------|
| 1   | 5         | - | - | - | -     |
| 2   | 3         | + | - | - | +     |
| 3   | 8         | - | + | - | +     |
| 4   | 1         | + | + | - | -     |
| 5   | 6         | - | - | + | +     |
| 6   | 2         | + | - | + | -     |
| 7   | 7         | - | + | + | -     |
| 8   | 4         | + | + | + | +     |

bustion chamber dimensions. All the stoves have the distribution of air inflow (primary, secondary and airwash) as shown in Figure 5.1 (a). Representative combustion chamber dimensions, top plate material and a visual representation of combustion chamber sizes and shapes are given in Table 5.3.



Table 5.3: List of the seven conventional stoves with corresponding combustion chamber dimensions, volumes and top plate material.

| Stove | Top brick material | Rear height [mm] | Front height [mm] | Mean width [mm] | Depth [mm] | Volume [L] | Visual comparison   |
|-------|--------------------|------------------|-------------------|-----------------|------------|------------|---|
| a     | Vermiculite        | 228              | 381               | 324             | 265        | 26.1       |    |
| b     | Vermiculite        | 305              | 456               | 414             | 272        | 42.8       |   |
| c     | Vermiculite        | 224              | 375               | 499             | 272        | 40.6       |  |
| d     | Vermiculite        | 310              | 467               | 524             | 288        | 58.6       |  |
| e     | Vermiculite        | 311              | 467               | 558             | 393        | 85.3       |  |
| f     | Vermiculite        | 334              | 490               | 430             | 267        | 47.3       |  |
| g     | Steel              | 263              | 376               | 429.5           | 315        | 43.2       |  |

# Chapter 6

## Results

In this chapter the experimental data and the statistical analysis are presented and interpreted. The chapter consists of the following sections:

1. First, the comparison of *CO* and *THC* data between conventional and gasification stove models is presented.
2. Then the data from the conventional stove tests is presented, and useful findings and observations derived.
3. The the most important distinct qualitative features of gasification stoves are identified and explained.
4. The time evolution of *CO* levels is presented, where events impacting the PIC levels are identified.
5. The statistical analyses of the experimental data is then presented.
6. Then the leakage of air and pollutants into the flue way is assessed.
7. Lastly, the results obtained through BS EN 16510-1 (without deviations) of an optimal stove configuration are presented.

### **6.1 Emission Data Overview - Conventional versus Gasification Stoves Comparison**

In this section the PIC emission data from conventional and gasification stove designs are compared. It is to be noted that in all cases, the normalised values of *CO*, *THC* and

$PM$  (@ 13%  $O_2$ ) are calculated by using equation (3.32), i.e. by using the averaged  $CO_2$  volume fraction ( $CO_{2,avg}$ ) of the corresponding firewood batch. The alternative option for the normalisation calculation is equation (3.20), where instead of  $CO_{2,avg}$  the instantaneous  $CO_2$  value would be used. The latter calculation method was used for assessing leakage from the gasification stove (presented in section 6.3.5) where  $CO_2$  and the instantaneous normalised  $CO$  values were the only available objective metrics.

In Figure 6.1 the normalised  $CO$  versus the corresponding  $CO_2$  values for all sampled data of both the conventional (blue colour) and gasification (red colour) stove designs are plotted. The graph contains data for all seven conventional and all eight gasification stove variants. Due to the higher sampling frequency for the gasification stove tests as against the conventional stoves (5 s vs 30 s sampling period) the gasification data was sparsed in order to plot a similar number of data points, that is, 8297 and 9027, respectively. In the plot (a) the  $CO$  axis is logarithmically scaled due to the large  $CO$  range. For both gasification and conventional stove test data the same qualitative trend can be observed - a 'U' shaped curve: higher  $CO$  values at low and high  $CO_2$  and low  $CO$  at intermediate  $CO_2$ . This observation corresponds to the three phases of combustion, as mentioned in the literature review in section 2.3.1. Local  $CO$  minima occur at different  $CO_2$ , when conventional and gasification designs are compared. A very obvious difference between conventional and gasification  $CO$  values is the fact that a large fraction of all gasification  $CO$  data is at least one order of magnitude lower than that in the conventional design (5 - 100 ppm versus 100 - 1000 ppm). Plot (b), which has both axes linearly scaled, shows  $CO$  data for higher values of  $CO_2$ , i.e. for lower values of air excess ratio. It can be seen from the plot (b) that the gasification stove variants that were tested exhibit higher sensitivity to decreased oxygen levels than some conventional stoves, due to steeper  $CO$  ascent. As will be explained later, rapid  $CO$  ascent past cca  $CO_2 = 15\%$  in the gasification design probably occurs due to nozzle related limitations on effective mixing. In both plots the Ecodesign limit of  $CO = 1200$  ppm is plotted as a dotted line for comparison.

A similar U shaped trend can be observed on the  $THC - CO_2$  scatter plot, as presented in Figure 6.2. Also, a difference of more than one order of magnitude in the local minimum 'plateau' can be observed between conventional and gasification designs: 1 - 10  $mg/Nm^3$  versus 10 - 30  $mg/Nm^3$ , respectively. The Ecodesign limit of  $THC = 120$   $mg/Nm^3$  is plotted as a dotted line.

In the author's opinion the assessment of any PIC levels versus  $CO_2$  (or alternatively  $O_2$ , or air excess ratio values) is very beneficial for evaluation of PIC levels of any stove, as such graphs account for the stoichiometry, i.e. they give information on the optimum  $CO_2$  range to yield minimum PIC levels. Such analyses where the instantaneous stoi-

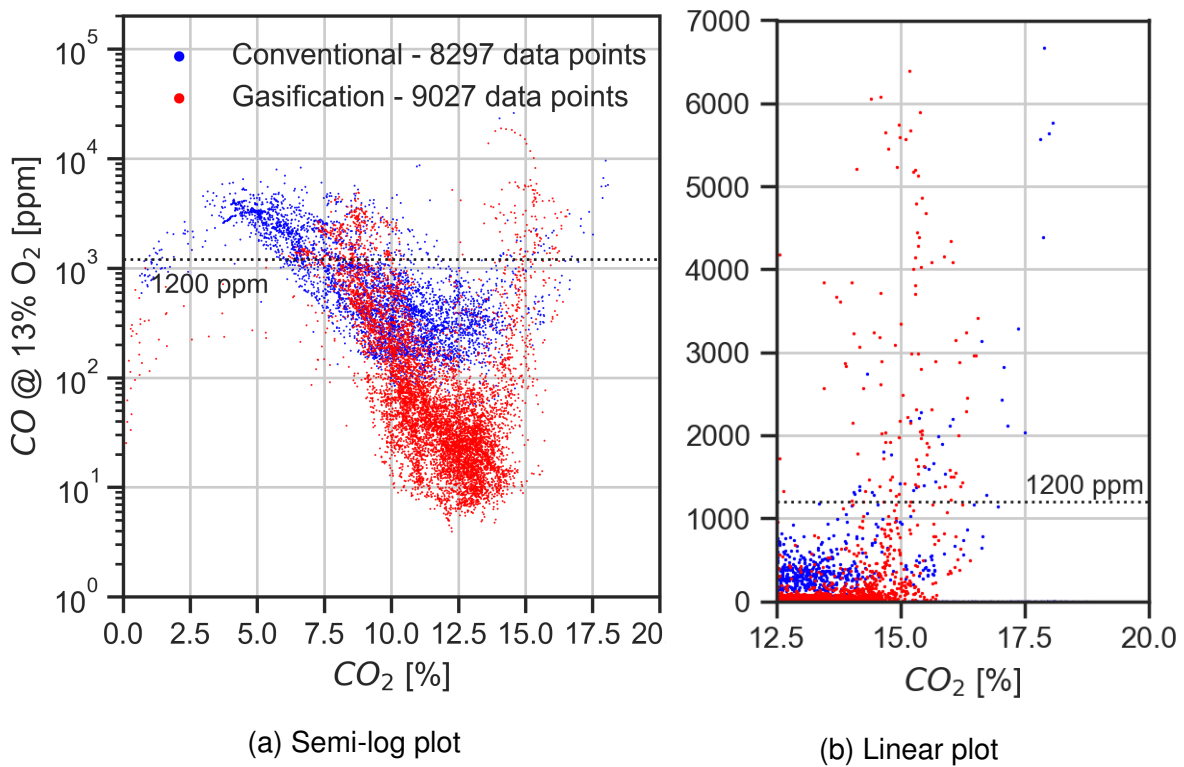


Figure 6.1: Comparison of normalised  $CO$  and  $CO_2$  values between the conventional and gasification stove designs.

chemistry is accounted for are rarely found in the literature<sup>1</sup>.

In Figure 6.3 the scatter plot of  $THC$  versus  $CO$  values is presented, with both Ecode-sign limits included. It can be seen that the correlation is not linear, when the instantaneous values are compared. On the other hand, when charge averaged values are correlated, a linear model fits the data well, as shown in Figure 6.4.

In Figure 6.4  $THC$  and  $CO$  values are also presented, not instantaneous ones but averaged for every firewood batch. In both cases a linear model can be used to describe the trend. The plotted linear regression lines are calculated using a standard least squares method, as with all other cases presented later. It can be observed that the two models have different slopes; in the gasification stove design the increase in averaged  $THC$  is less sensitive to the increase in averaged  $CO$  than in the conventional one. The linear models of conventional and gasification stove designs are defined through the following formulae, respectively:

$$THC_{conv} = -15.42 + 0.107 \cdot CO_{conv} \quad (6.1)$$

$$THC_{gasif} = 1.77 + 0.022 \cdot CO_{gasif}. \quad (6.2)$$

<sup>1</sup>An example of such analysis is the work of Nussbaumer [93] in Figure 5

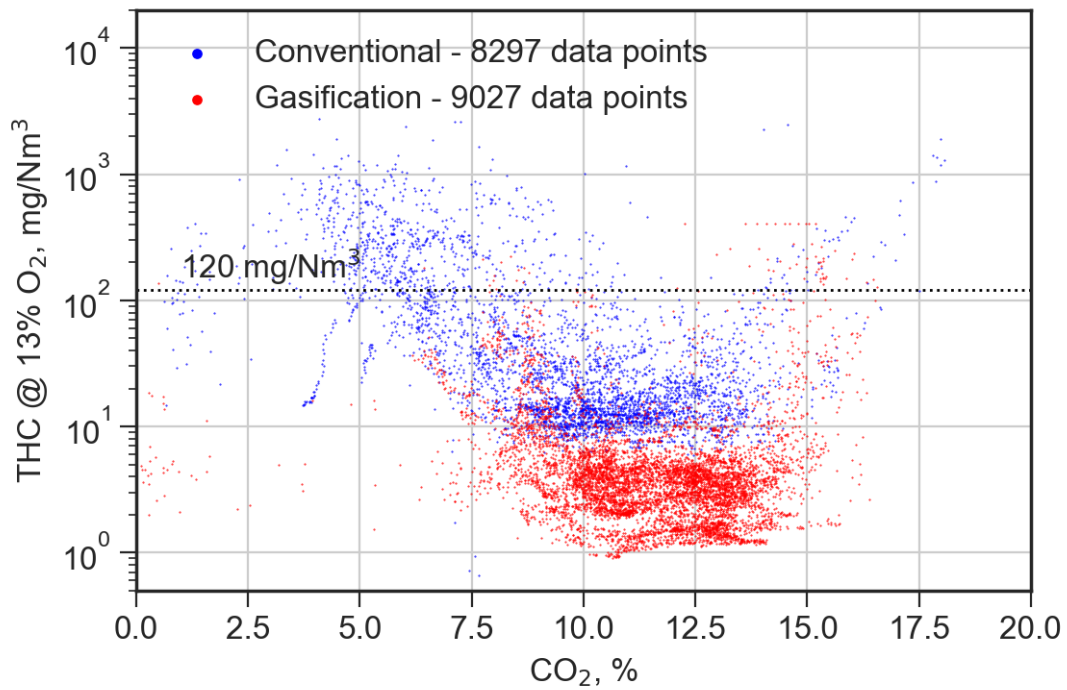


Figure 6.2: Comparison of normalised *THC* and *CO<sub>2</sub>* values between the conventional and gasification stove designs; semi-log plot.

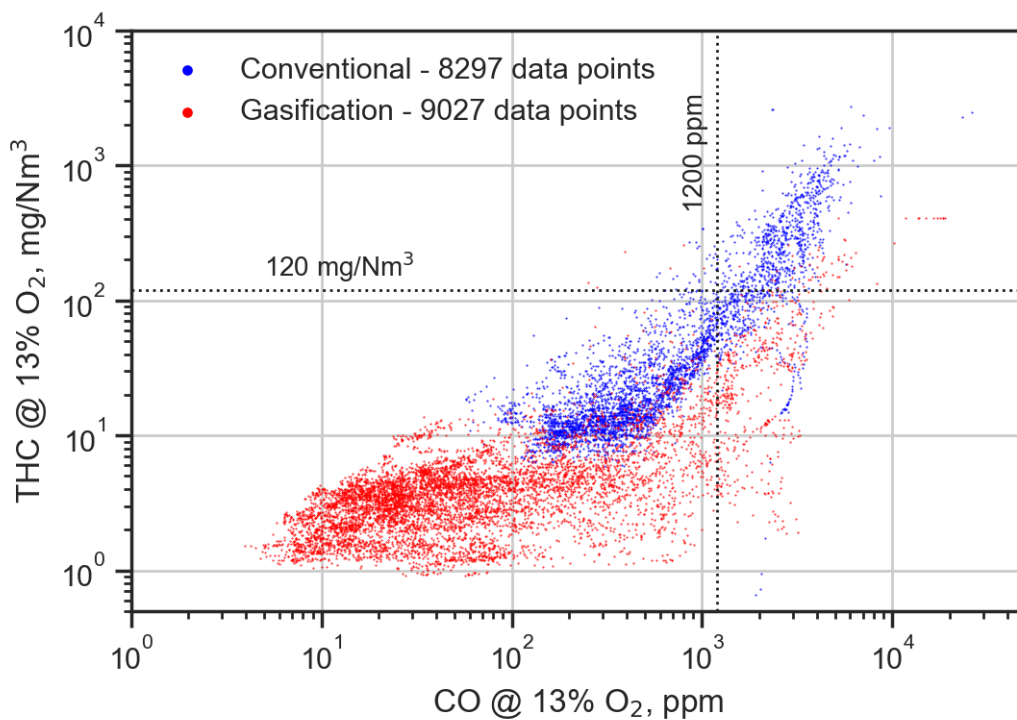


Figure 6.3: Comparison of normalised *THC* and normalised *CO* values between the conventional and gasification stove designs; log-log plot.

It is to be noted that while the two linear models above are appropriate for the data range they fit, they are not global. For example in the very low emission range, both

models should have an intercept of 0, due to the fact that when there is no  $CO$  emission,  $THC$  also needs to be 0. It can also be observed that the linear regression line for conventional stove designs passes very close to the intersection of the two Ecodesign limits.

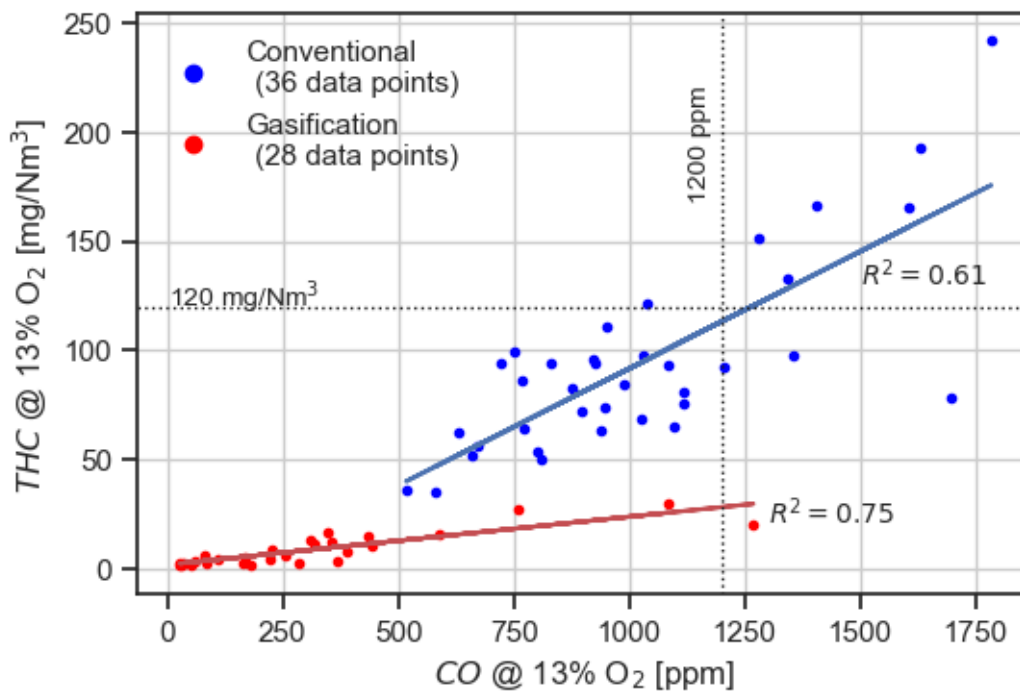


Figure 6.4: Comparison of  $THC_{avg}$  and  $CO_{avg}$  values between the conventional and gasification stove designs; plotted data are averaged values for every firewood batch. Dotted lines show Ecodesign limits for  $CO$  and  $THC$ .

Hence, from the comparison of both the instantaneous and charge averaged PIC data of all tested conventional and gasification models, the following observations can be made:

- The minimum achievable  $CO$  and  $THC$  levels are considerably lower (at least one order of magnitude) in gasification than in conventional stove models.
- Charge averaged  $THC$  is less sensitive to the increase of charge averaged  $CO$  levels in gasification than in conventional stove models, due to the different slopes of the regression lines.
- At a certain upper limit of  $CO_2$ , the nozzle in gasification models reaches its effective mixing limit and  $CO$  increases very rapidly (more so than in the case of conventional models). This limit for the tested gasification stoves is around  $CO_2 = 15\%$ .

- A 'U' shaped curve for both the *CO* and *THC* versus *CO*<sub>2</sub> levels can be observed for both the conventional and gasification stove variants.
- Local minima of *CO* and *THC* versus *CO*<sub>2</sub> are different between gasification and conventional stoves.

In the next section the test results of conventional stoves will be presented, as well as some useful observations and analyses.

## 6.2 Conventional Stoves' Test Results

Seven conventional stove models were tested during 2018 in DTI<sup>2</sup>, Denmark, for the purpose of their certification. All models feature almost identical combustion chamber topology, that is, the primary air, secondary air and airwash holes are located at the same relative locations. All feature flat window and vermiculite base, walls and top cover<sup>3</sup>. Stove features that are different and fully measurable are the combustion chamber dimensions.

In the first section the gaseous PIC EFs, that is *CO* and *THC*, whereas in the following section the *PM* emissions are analysed, and useful data presented.

### 6.2.1 Gaseous PIC Emissions of Tested Conventional Stoves

In Figure 6.5 the normalised values of *CO* and *THC* are plotted against *CO*<sub>2</sub> values for each of the seven stove models (from a to g). The presented data is organised in such a way that *CO* and *THC* data between every whole number of *CO*<sub>2</sub> is averaged and assigned to the middle *CO*<sub>2</sub> value. For example, all *CO* data between 13 and 14 % *CO*<sub>2</sub> is averaged and assigned to 13.5 % *CO*<sub>2</sub>. Such grouping was done in order to make the comparison of the different stove models possible on the graph.

For the high values of *CO*<sub>2</sub> (e.g. over 14 %) in both graphs two distinct paths can be recognised: that of stoves a and f, and that of stoves c and g. *CO*<sub>2</sub> values for other stoves never reached values above 14 %. Stoves a and f emit lower *CO* and *THC* than stoves c and g at high *CO*<sub>2</sub> levels, e.g. 15.5 %. The same stoves are also paired at low *CO*<sub>2</sub> (e.g. below 7 %), which is especially visible in *THC* – *CO*<sub>2</sub> graph. At low *CO*<sub>2</sub> values stove b is joined with a and f group, whereas stoves d and e are joined with c and g group. At low *CO*<sub>2</sub> the emission values are flipped: stoves a, b and f emit more *CO* and *THC* than stoves c, d, e and g.

One metric can be identified that distinguishes the two groups of stoves, which is the *h/A* ratio (which can be called the 'slimness'), where *h* is the mean height of the stove's combustion chamber in mm and *A* is the surface area of the base of the stove's combustion chamber in dm<sup>2</sup>. *h/A* for every stove is shown in Table 6.1. It is clear that in the a, b and f group, *h/A* is in the range 33.8 to 35.9 mm/dm<sup>2</sup>, whereas for the other group it is in the range 17.7 to 25.7 mm/dm<sup>2</sup>. Hence, for higher *h/A* values, the *CO*<sub>2</sub>-*CO* and

<sup>2</sup>Danish Technological Institute

<sup>3</sup>In term of top cover material one exception is stove g, where it is made out of steel, not vermiculite.



$CO_2$ - $THC$  'U' - shaped curves are shifted to the right, towards the high  $CO_2$  end.

Table 6.1:  $h/A$  ratio values for every conventional stove model.

| Stove                       | a    | b    | c    | d    | e    | f    | g    |
|-----------------------------|------|------|------|------|------|------|------|
| $h/A$ [mm/dm <sup>2</sup> ] | 35.5 | 33.8 | 22.1 | 25.7 | 17.7 | 35.9 | 23.6 |

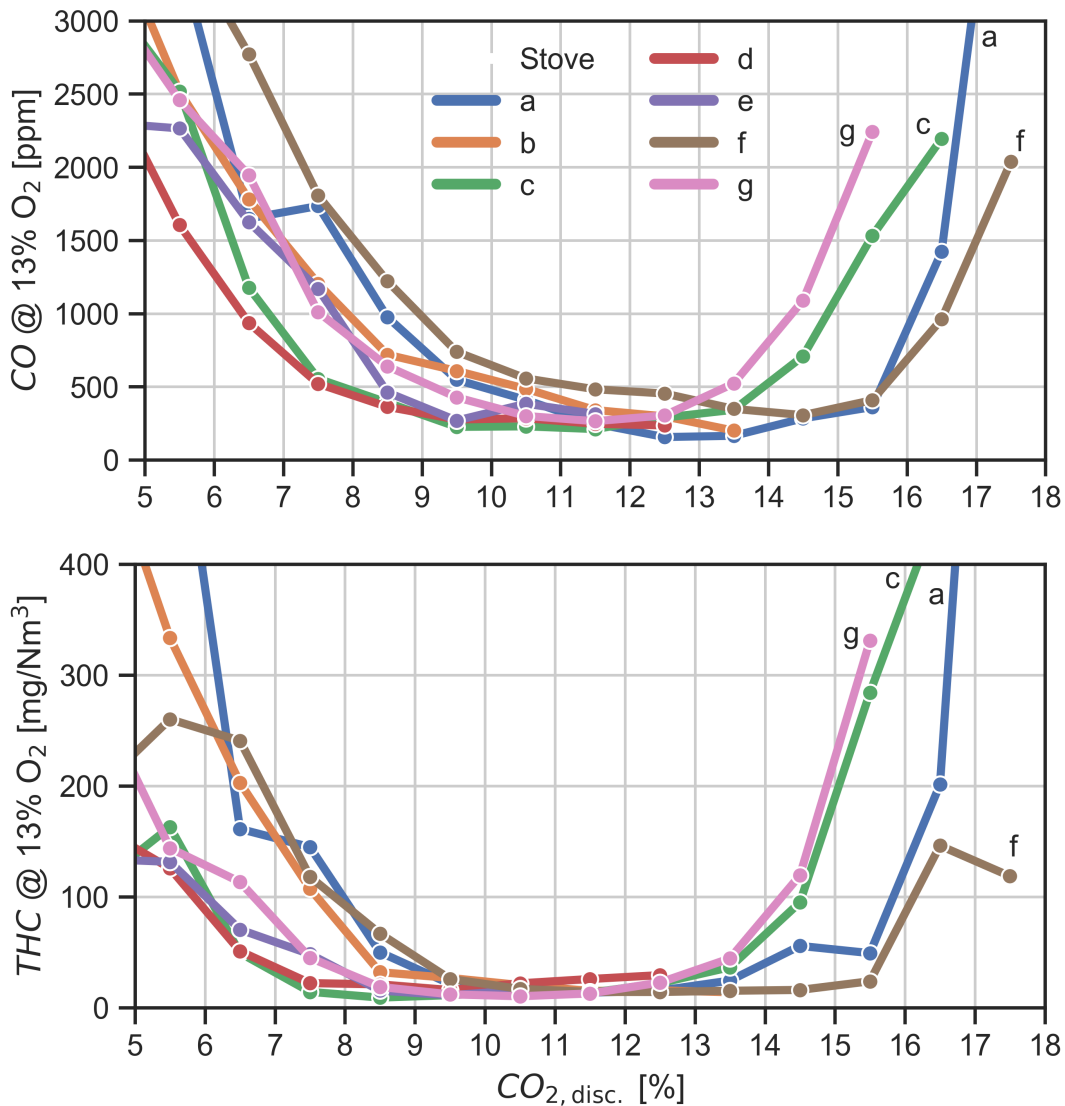


Figure 6.5: Normalised  $CO$  and  $THC$  versus  $CO_2$  for 7 conventional stove models.

### 6.2.2 Particulate Matter Emission from Conventional Stoves

Analogously to the elevated  $CO$  and  $THC$  levels at high  $CO_2$ ,  $PM$  also follows a similar trend. As shown in Figure 6.6,  $PM$  levels are correlated to the maximum observed  $CO_2$  value ( $CO_{2,max}$ ) for a given charge. In the figure the linear regression lines are plotted

for stoves a<sup>4</sup>, c, f and g with the aim of showing the difference in the *PM* emission trend for these four stove models - the same ones already identified in the previous section (6.2.1). The trend in the other stoves is not as clear since for none of them did the  $CO_{2,max}$  go above 14%. The two groups of stoves separated by *CO* and *THC* emission levels, identified in the previous section, are also clearly separated when considering the *PM* emissions. Therefore the same  $h/A$  metric identifies both trends.

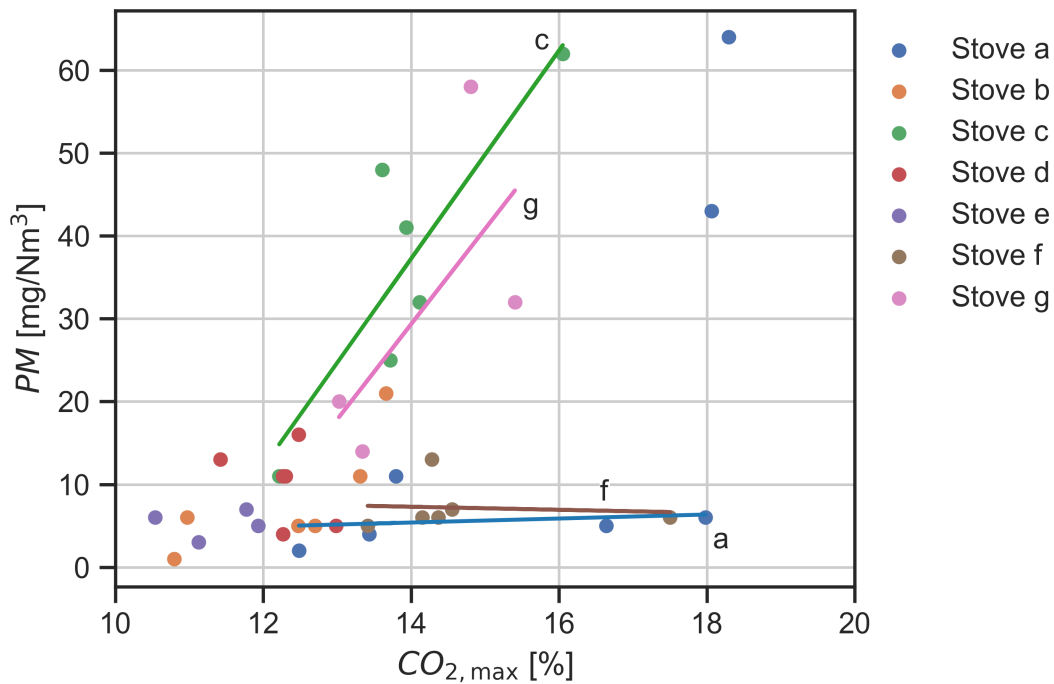


Figure 6.6: Scatter plot of *PM* versus  $CO_{2,max}$  values, with corresponding linear regression lines.

From the analysis of the graphs on Figures 6.6, 6.5 and 6.7 four conclusions can be drawn:

- In low  $h/A$  ratio stoves, *PM*, *CO* and *THC* levels are more sensitive to the oxygen deficient regime than for higher  $h/A$  ratio stoves.
- For lower  $CO_{2,max}$  values (i.e.  $10\% < CO_{2,max} < 12\%$ ), *PM* emission levels are similar for all stove models. When  $CO_{2,max}$  passes 12%, differences in combustion chamber geometries and the relative positions of the air inlets begin to play an increasingly important effect on the *PM* levels. Hence, according to this analysis, any of the tested stove variants could achieve very low *PM* levels (i.e. below 10 mg/Nm<sup>3</sup>) if conditions of  $CO_{2,max} < 12\%$  could be fulfilled for all tested charges.

<sup>4</sup>The two data points for stove a where  $CO_2 > 18\%$  are not included in the regression, as beyond  $CO_2 = 18\%$  the relation becomes highly non-linear.

- Low  $h/A$  ratio stoves feature a  $CO-CO_2$  and  $THC-CO_2$  'U'-shaped relation that is shifted to the lower  $CO_2$  end, compared to the corresponding relations for the higher  $h/A$  ratio stoves.
- Stoves with larger combustion chambers usually feature lower  $CO_{2,max}$  values.

The last statement is explored in more detail in the following section.

### 6.2.3 Influence of Combustion Chamber Volume on $CO_{2,max}$

The fact that some stoves feature higher  $CO_{2,max}$  values than others can be partly explained by their corresponding combustion chamber volume. However another parameter influencing the  $CO_{2,max}$  is probably the air inflow rate during the initial 3 minute period, which depends solely on the operator of the stove. Figure 6.7 shows a scatter plot of  $CO_{2,max}$  values versus the corresponding combustion chamber volume for each stove, identified by the letter. It is clear that smaller stoves feature higher  $CO_{2,max}$  value for an average charge cycle, and vice versa. Therefore, due to comparatively large combustion chamber volumes, stoves b, d and e feature lower  $CO_{2,max}$  values (< 14%) and, thus, lower  $PM$  values. Hence their trend is not as clear on the graph in Figure 6.6.

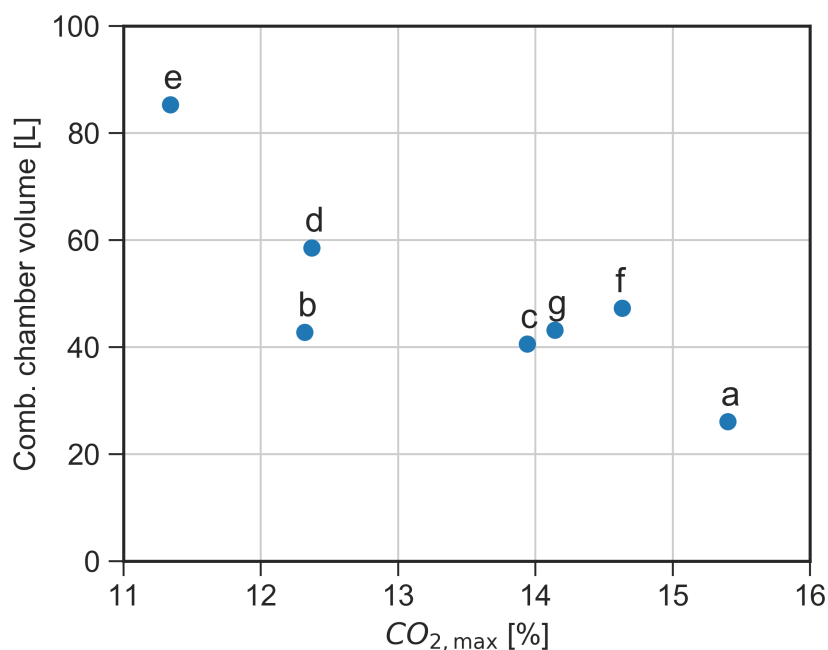


Figure 6.7: Scatter plot of  $CO_{2,max}$  (averaged across all charges) versus combustion chamber volume for every conventional stove model.

With the aim of answering the question as to why larger stoves feature lower  $CO_{2,max}$

values, the following analysis is presented. BS EN 13240 and BS EN 16510-1 standards allow that during the initial 3 minutes of a charge cycle the air controls can be adjusted. This is usually done on every conventional stove during certification tests. During the initial 3 minutes the air controls are generally kept more open than during the remaining period of a charge cycle. This is done with aim of the fire being ignited around all firewood surfaces. Otherwise, wood logs would pyrolyse without necessarily igniting the full stream of pyrolytic gases, which would result in smoldering and excessively high PIC levels. Just before the initial 3 minutes pass, the air inflow is reduced by adjusting the air controls to an optimum position<sup>5</sup>. It was found that different air inflow rates determine different characteristic  $CO_2$ - $CO$  and  $CO_2$ - $THC$  'U' curves. Hence, after reducing the air inflow rate just before the 3 minute time mark, the  $CO_2$ -PIC relation moves from one 'U' curve to another. The new 'U' curve usually starts from low PIC levels. However, during the following several minutes  $CO_2$  rises to its maximum value (and therefore, possibly, to a maximum PIC value), and then monotonously diminishes to a minimum value at the end of a charge cycle when refuelling occurs. In larger volume stoves the aforementioned  $CO_2$  increase after closing the air controls usually lasts a comparatively shorter timer and, thus, rises to comparatively lower  $CO_{2,max}$  and PIC levels than in smaller volume stoves. Such behaviour is evident from the two graphs in Figure 6.8. The red line shows the data for stove e, the one featuring the biggest combustion chamber volume, whereas the blue line shows the data for stove a, which is the one with the smallest combustion chamber volume. Dashed lines denote the initial 3 minute period of a charge cycle - that is, 6 data points<sup>6</sup>. For both stoves only the data for a single charge cycle is plotted. In both graphs the dotted black horizontal lines show the corresponding Ecodesign limits, whereas black circles and crosses show the start and end of the corresponding charge cycle, respectively. From the graphs it is evident that, after diminishing the air inflow rate, both PIC levels and  $CO_2$  (which represents the pyrolysis rate), reach greater values in a smaller stove a. In case of a bigger stove e, PIC levels do not grow beyond the plateau of minimum  $CO$  and  $THC$ . The fact that the smaller volume stoves feature greater elevations of PIC and  $CO_2$  levels during the initial 5 to 10 minutes can be explained as follows.

<sup>5</sup>The optimum position of air controls for a specific stove with a specific size and number of wood logs is determined through an iterative process.

<sup>6</sup>6 data points with measurement period of 30 s correspond to the 3 minute time interval.

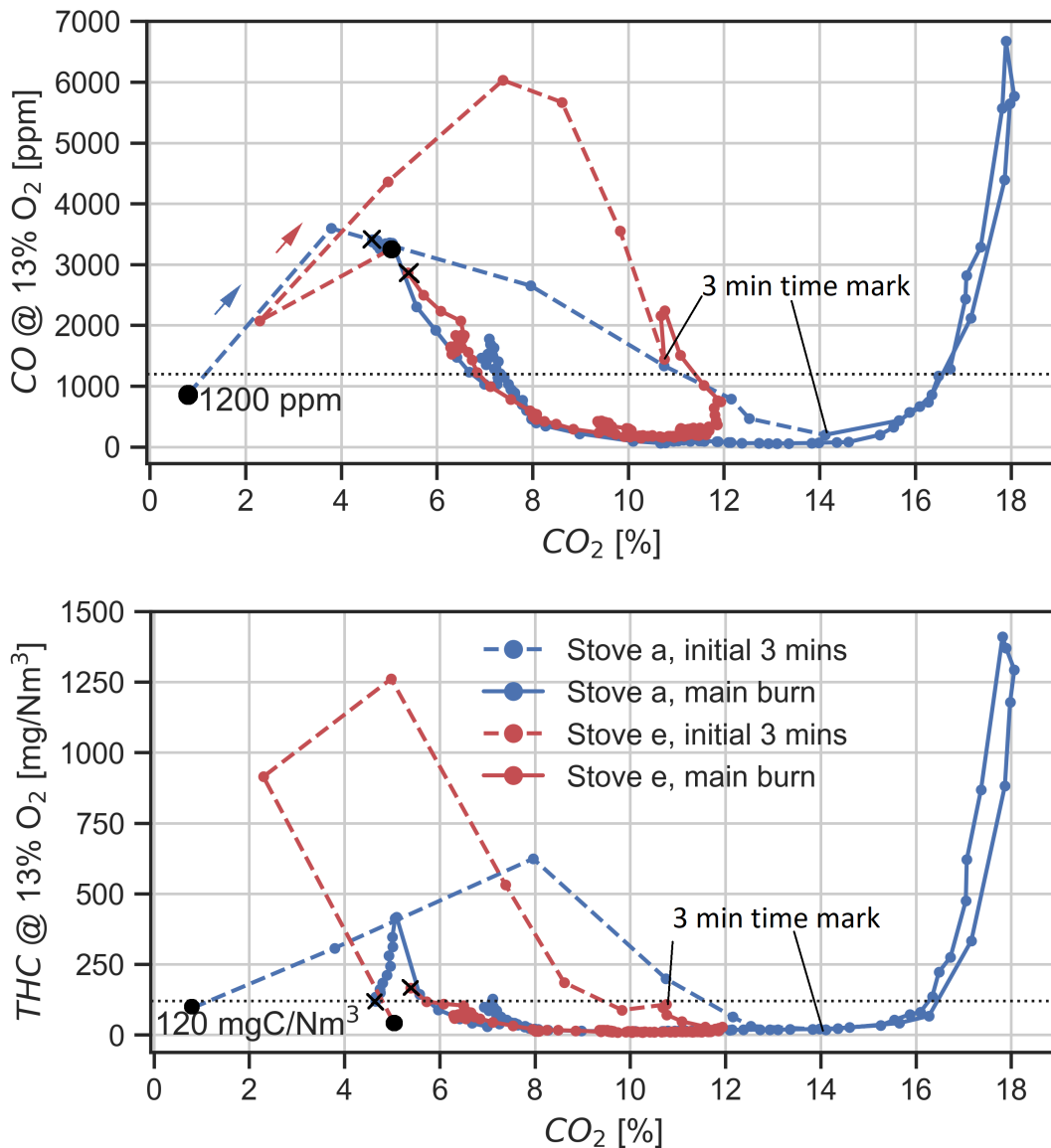


Figure 6.8:  $CO_2$  versus normalised  $CO$  and  $THC$  values for stoves a (smallest one) and e (biggest one). Black circles denote the start of a charge cycle (first data point), whereas black crosses denote the end of a charge cycle (last data point). The dotted black horizontal lines show the corresponding Ecodesign limits.

In smaller volume stoves combustion of pyrolytic gases occurs closer to the firewood than in larger volume stoves, where flames are being stretched. Moreover, smaller volume stoves feature a smaller glass area (less flame radiation transmission) than larger stoves (more flame radiation transmission). Therefore, there is probably higher intensity flame radiation onto the firewood in the case of smaller volume stoves. Higher radiation heat influx causes a higher rate of pyrolysis, which then supplies more combustible gases for further increased flame radiation. Such a feedback loop causes more pyrolysis during this initial PIC 'spike' which, under the conditions of constant air inflow, causes the air excess ratio to diminish, thus elevating the  $CO_2$  and  $PIC$  levels.

In the following section the test results and analyses for the gasification stove prototype are presented.

## 6.3 Gasification Stoves' Test Results

In this section the qualitative and quantitative results from the testing of the gasification stove models are given. The section contains:

- An explanation of significant features of gasification stoves, which are distinct from conventional ones.
- Averaged *CO*, *THC* and *PM* emission results for every stove variant.
- An analysis of the time evolution of the *CO* and *CO<sub>2</sub>* emission data
- Statistical analysis of the designed experiment using the DoE method
- Evaluations of air and PIC leakage effects from the reaction area into the flue stream, and
- Presentation of test results according to BS EN 16510-1 of an optimal stove configuration.

### 6.3.1 Significant Features of a Wood Gasification Stove

In this section observed qualitative features of a gasification stove that are distinct from a conventional one will be presented.

The observed features that are explained in following sections are:

- Primary chamber sooting
- Blow-back
- Channel creation in the char bed
- Secondary flame ignition stability
- Flap seal leakage
- Missed weld leakage

### 6.3.1.1 Primary Chamber Sooting

Since the majority of the conversion of chemical into thermal energy occurs in the secondary chamber, the gas phase in the primary chamber features, on average (both spatial and temporal), fuel rich conditions. As glass on the primary chamber door is a comparatively cool surface area, soot can be formed on its surface. Since glass is intended to be transparent to the user, glass sooting is considered as an unfavourable feature of a stove.

It was noticed that sooting can be minimised if a certain portion of the gaseous combustion (that is, the flame) is continuously kept in the primary chamber, above both the char and firewood bed. Further explanation of this, together with opinions and solution proposals are given later in the discussion (section 7).

### 6.3.1.2 Blow-back

It was noticed that in some cases flame "blow-back" occurs in the primary chamber. This is a small explosion of combustible syngas in the primary chamber, with an observed pressure increase from 2 to 15 or 20 Pa, occurring intermittently - e.g. every 30 s to a minute. Blow-back needs to be avoided due to its unfavourable consequences:

- Blow-back can push smoke into the room through either the air supply system, imperfect seals on the doors or through the threads on the fasteners.
- High rate of soot formation on the glass surface, and
- Secondary flame blow-out.

Blow-back has almost the same causes as primary chamber sooting. It was observed that blow-backs usually occur when there is no continuous flame in the primary chamber, during the second half of a charge period.

### 6.3.1.3 Secondary Flame Ignition Stability

Before the stove operation can be switched into downdraft mode, enough char needs to be created for successful secondary flame ignition. Moreover, the chimney draft needs to be established to enable downdraft gas motion. Hence, during the initial updraft mode a few firewood batches need to be burned before the stove system is ready to



switch the mode of operation from updraft to downdraft. For this change to occur, the secondary flame needs to be ignited. However, based on, mostly, the nozzle geometry, the successful ignition can take significantly different amounts of time, counting from the ignition of the first batch. It was observed that sometimes it takes 15 minutes, whereas sometimes the secondary flame does not ignite even after 45 minutes. For example, a nozzle inlet with a tubular cover (level -1 of factor B) enabled a much more stable and faster secondary ignition than the flat cover (level +1 of factor B).

Further explanation is provided later in the discussion section.

#### 6.3.1.4 Channel Creation in Char Bed

During wood combustion in a gasification stove, channels are created in the char bed. These were observed to be connections (containing no char) between the zone above the char and firewood bed, and the nozzle inlet. The creation of channels corresponded with elevated *CO* and *THC* emission levels and were identified as one of two major contributors to elevated *CO* and *THC* levels (the other one being the oxygen deficient combustion regime at the beginning of some charges). Channels are created because a portion of char is still not decomposed into smaller pieces and thus provides structural support for the rest of the char and burning firewood above it. Creation of char bed channels is described in the following paragraph.

Just before refuelling the stove with firewood, the remaining char bed is usually packed by the operator poking the bigger pieces of char into smaller pieces and by levelling the char bed. Hence, channels almost never occur during the first half of a charge cycle as the char bed is very packed. Channels are usually created at different times during the second period of a charge cycle, or potentially even beyond the next refuelling time - that is, sometimes an entire charge cycle passes without any channeling effects - which is the objective.

The presence of channels corresponds to lowered  $CO_2$  and elevated PIC levels. Such behaviour was in accordance with the  $CO_2$ -*CO* and  $CO_2$ -*THC* 'U'-shaped curves, shown in Figures 6.1 and 6.2.

The presence of channels also corresponds to a lowered char decomposition rate (which will be explained later in discussion section 7), which results in lowered radiation, and thus lowered pyrolysis rates of the firewood. Since the air openings are fixed, the air excess ratio rises<sup>7</sup>, which results in decreased flame temperatures and

---

<sup>7</sup>which was evident from decreased  $CO_2$  levels in flue gas stream.

elevated PIC levels.

Once a channel is created, it can collapse, that is, char pieces supporting the firewood above decompose enough to break, thus filling the channels with char and overall packing the char and firewood beds. Also, a collapse can occur when the channel is still narrow or after, when channels become very wide - which is definitely the worse case. It was observed that if wetter or bigger firewood is used, channel collapse events occur with significant delay.

### **6.3.1.5 Flap Seal Leakage**

As explained earlier, the gas phase in the primary chamber can be very fuel rich. This means that it contains a large fraction of combustible gases, which, if present in the flue stream, represent a significant source of pollution. Hence, any leakage into the flue stream, however small, can massively affect the *CO* and *THC* levels in the flue gases (which otherwise contain very low pollutant concentrations). This is the case because there is considerable static pressure difference between the primary chamber and the flue way - circa 9-10 Pa higher in the primary chamber.

In the current design, leakage was minimised by using  $\varnothing 15$  mm sealing ceramic fibre rope around the flap, compressed through a specially developed mechanism for this purpose. However, a portion of leakage was still present, as shown and explained later in section [6.3.5](#).

Minimisation of flap leakage is a problem to be further optimised through a new, potentially more innovative design of a flap mechanism and/or of a combustion system itself, in some other project.

### **6.3.1.6 Leakage through a Missed Weld**

If the primary chamber is isolated from the flue way by a single steel plate, and hence by a single weld layer, any missed spot during the welding process can cause a prohibitive amount of flue gas contamination. This leakage occurs according to the same physical mechanism as explained in section [6.3.1.5](#) above. In the tested stove this issue has been mostly solved by placing a continuous air supply cavity between the primary chamber and the flue way, as shown in Figure [5.2](#). That way pressure differentials occurring in the stove system ensure that potential leakage occurs either from the air supply cavity into the primary chamber and/or into the flue way, thus resulting in

negligible flue gas dilution by air - which is not a pollutant, in contrast to potentially leaked PIC.

### 6.3.2 Gasification Stove Experimental Design Table and Results

Testing results for averaged  $CO$ ,  $THC$  and  $PM$  data for every gasification stove configuration are presented in Table 6.2. Results from three data sets are shown: original, first filtered set (where  $CO_2 < 15\%$ ) and second filtered set (where the batch time is greater than 15 minutes). The reason for producing filtered data sets, besides the original (unfiltered) one, is that it was observed that there are two main contributions to the elevated PIC levels, which are independent. Filtered data sets were constructed with the aim of isolating those PIC sources and to gain a more clear understanding of the data. The data filtering and analysis are explained later in the section covering the statistical analysis 6.3.4.

Table 6.2: Experimental results from three data sets: 1, 3 and 4, with corresponding experimental design configurations. All response variables are normalised to 13 %  $O_2$ . Units for  $CO$ ,  $THC$  and  $PM$  are vol ppm,  $mgC/Nm^3$  and  $mg/Nm^3$ , respectively.

| Run | Design configuration | Response variables         |            |            |  |            |  |            |
|-----|----------------------|----------------------------|------------|------------|--|------------|--|------------|
|     |                      | Original data - data set 1 |            |            | Filtered data ( $CO_2 < 15\%$ ) - data set 3 |            | Filtered data (time > 15 min) - data set 4 |            |
|     |                      | $CO^*$                     | $THC^{**}$ | $PM^{***}$ | $CO^*$                                       | $THC^{**}$ | $CO^*$                                     | $THC^{**}$ |
| 1   | ----                 | 117.7                      | 6.31       | 9.25       | 44.1   | 3.28       | 43.1                                       | 2.75       |
| 2   | +--+                 | 133.5                      | 5.04       | 8.92       | 133.5  | 5.04       | 152.7                                      | 5.29       |
| 3   | -++-                 | 157.8                      | 2.08       | 5.62       | 157.3  | 2.08       | 192.0                                      | 1.99       |
| 4   | ++--                 | 375.4                      | 11.43      | 6.87       | 361.1  | 11.22      | 452.6                                      | 12.51      |
| 5   | --++                 | 140.7                      | 2.41       | 6.93       | 123.9  | 2.04       | 135.9                                      | 1.79       |
| 6   | +--+                 | 317.4                      | 9.05       | 10.48      | 267.5  | 7.91       | 295.1                                      | 6.63       |
| 7   | -++-                 | 593.2                      | 18.44      | 12.06      | 222.6  | 8.16       | 143.0                                      | 4.05       |
| 8   | ++++                 | 466.7                      | 10.35      | 10.84      | 466.4  | 10.35      | 585.3                                      | 11.97      |

\* calculated according to equation (3.32)

\*\* calculated according to equation (3.36)

\*\*\* calculated according to equation (3.43)

### 6.3.3 Time evolution of $CO_2$ and $CO$

In this section the time evolution of normalised  $CO$  and merged values of  $(CO_2 + CO)$  are presented for all eight gasification stove variations, i.e. eight experimental runs. The data is presented in Figures 6.9 to 6.12. In every graph a timeline (dotted line) is given to provide information for refuelling times (where the number denotes the firewood batch number) and for recorded significant events in the fuel bed that affected emission values<sup>8</sup>. Due to the fact that  $THC$  and  $CO$  levels are correlated, as shown in Figure 6.3, only the time evolution of  $CO$  was presented. The two merged values  $(CO_2 + CO)$  are plotted as they give a good estimation of oxygen levels - the higher the value of  $(CO_2 + CO)$ , the lower the concentration of  $O_2$ . Hence, in some cases, when  $(CO_2 + CO)$  rises above 15 % (always at the beginning of the charge period), a spike in  $CO$  can be observed, which is an indication of poor combustion conditions. In these cases the syngas and secondary air stream mixing effectiveness is no longer sufficient, hence more  $CO$  is being emitted from the secondary chamber. On the other hand elevated  $CO$  emissions also occur in the second half of some charge periods (e.g. run 2, batch 1; run 3, batch 1; run 4, all batches; etc.).

<sup>8</sup>There are other significant events noticeable on the graphs, but have not been recorded.

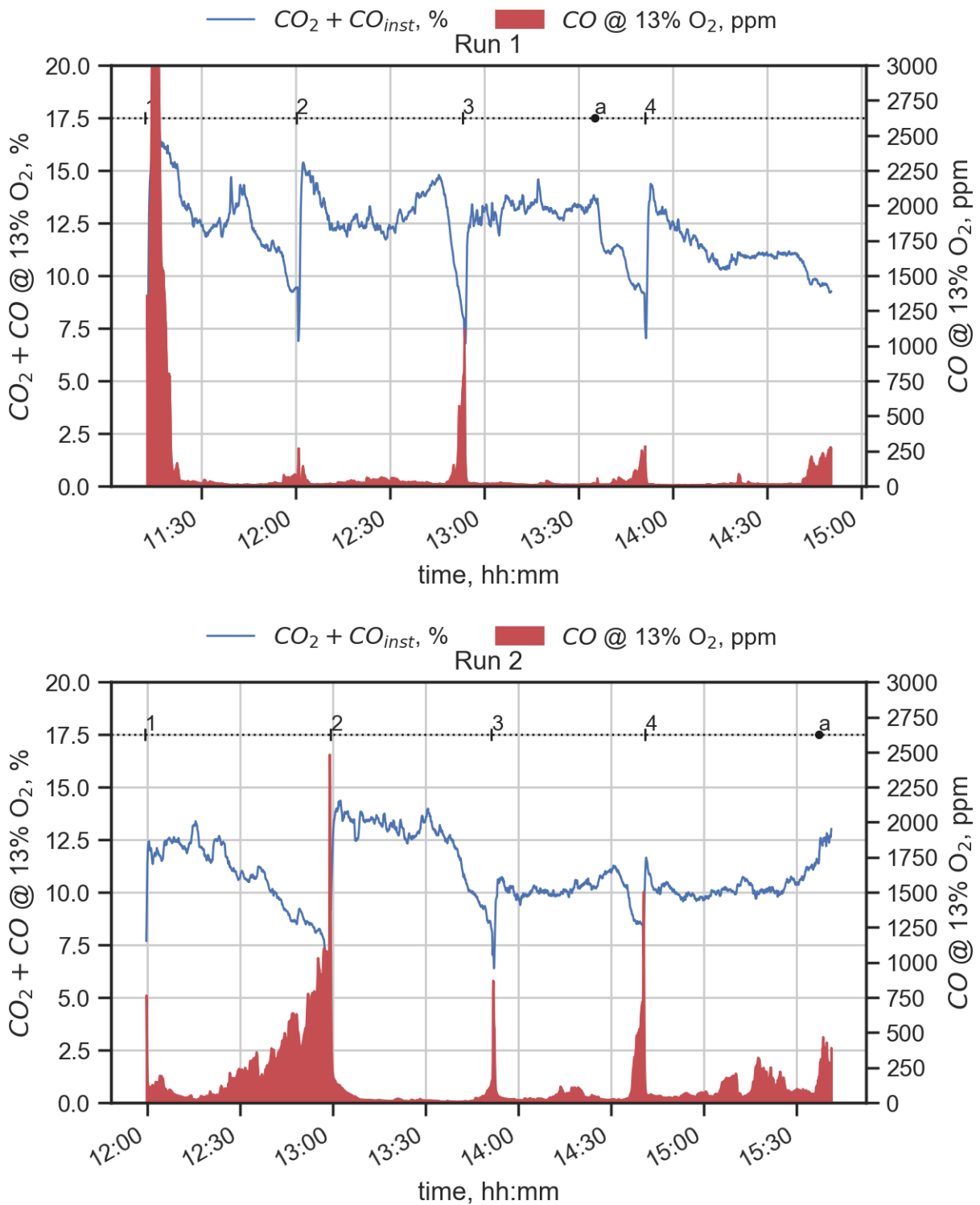


Figure 6.9: Original CO vs time data. Runs 1 and 2.

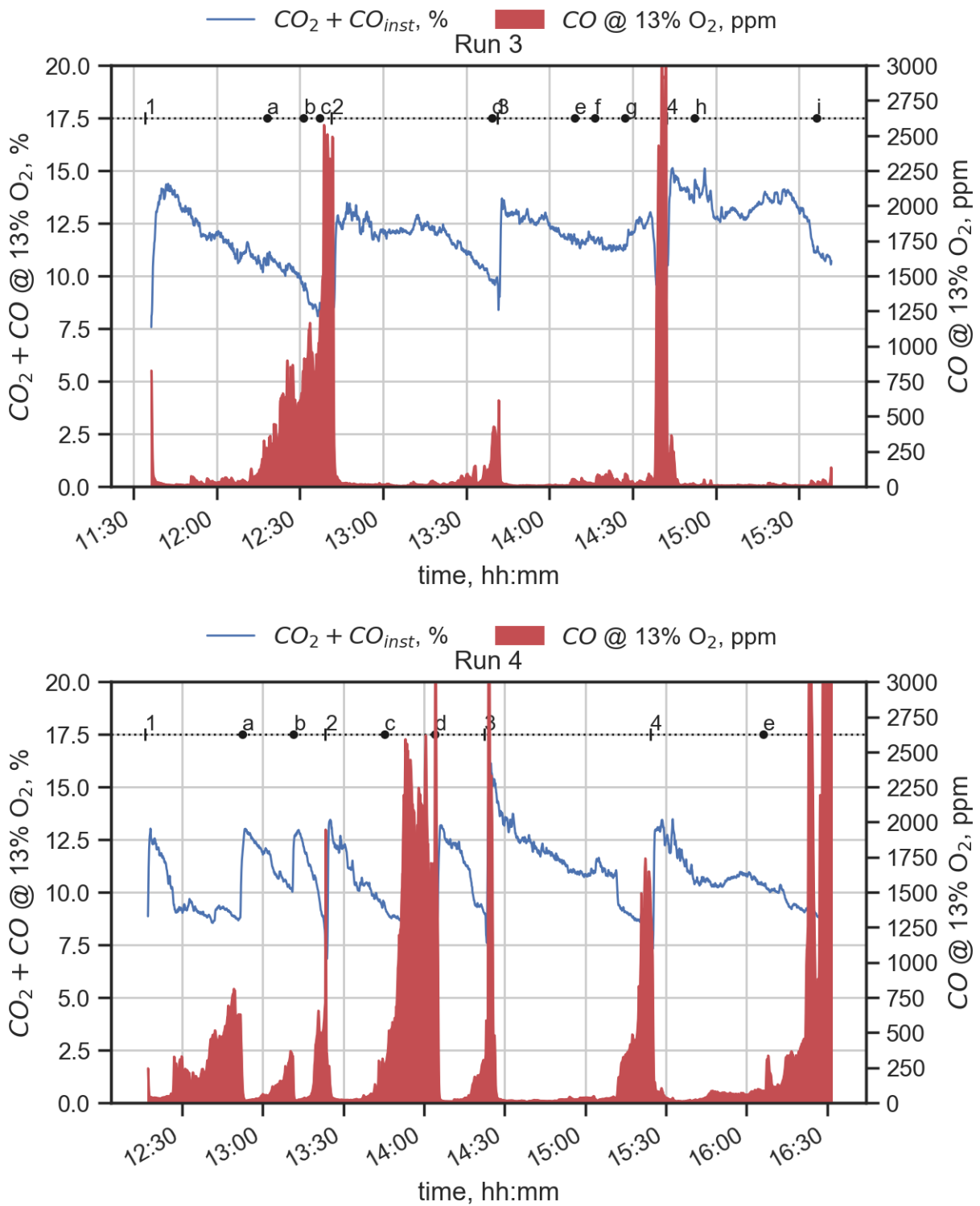


Figure 6.10: Original CO vs time data. Runs 3 and 4.

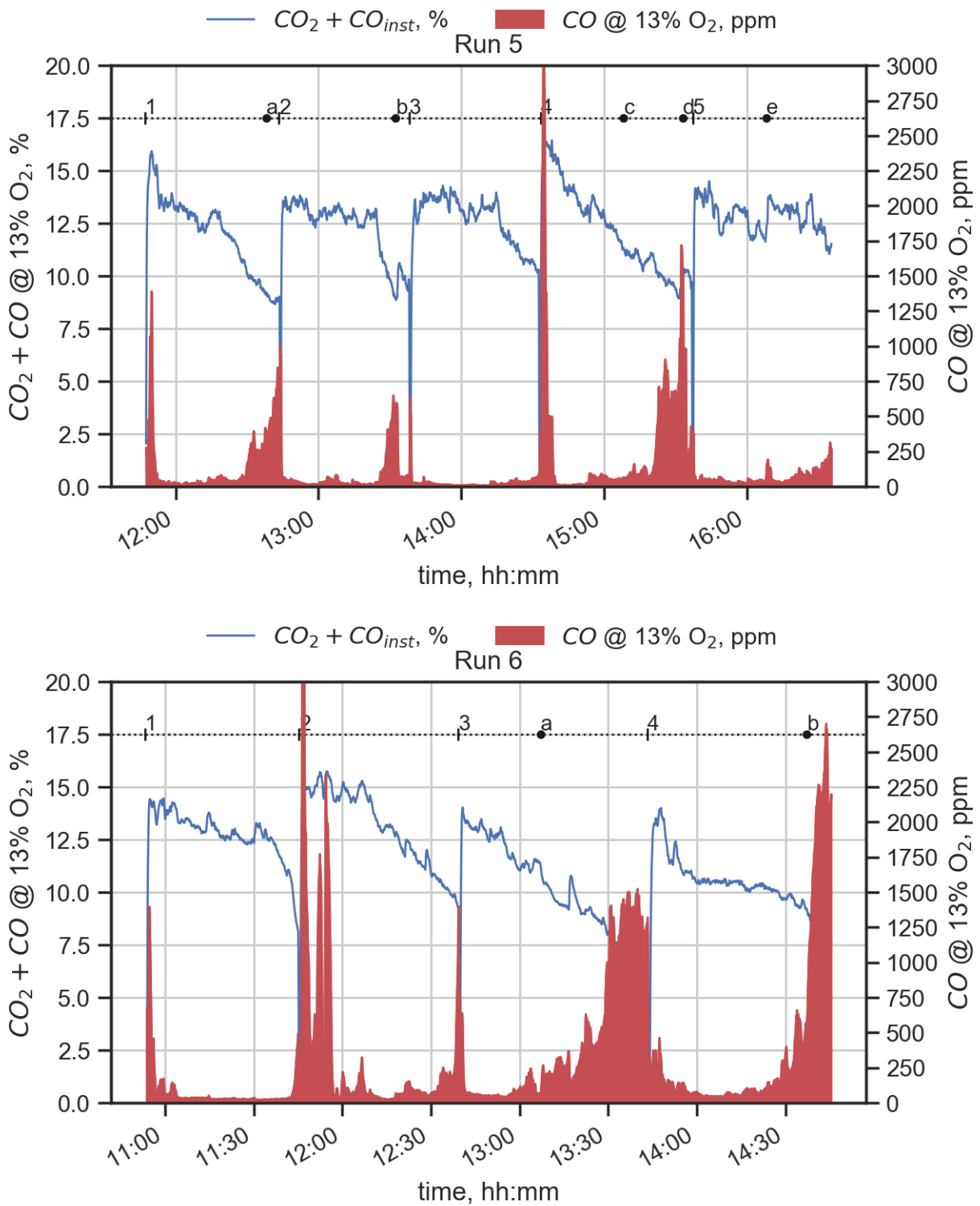


Figure 6.11: Original CO vs time data. Runs 5 and 6.



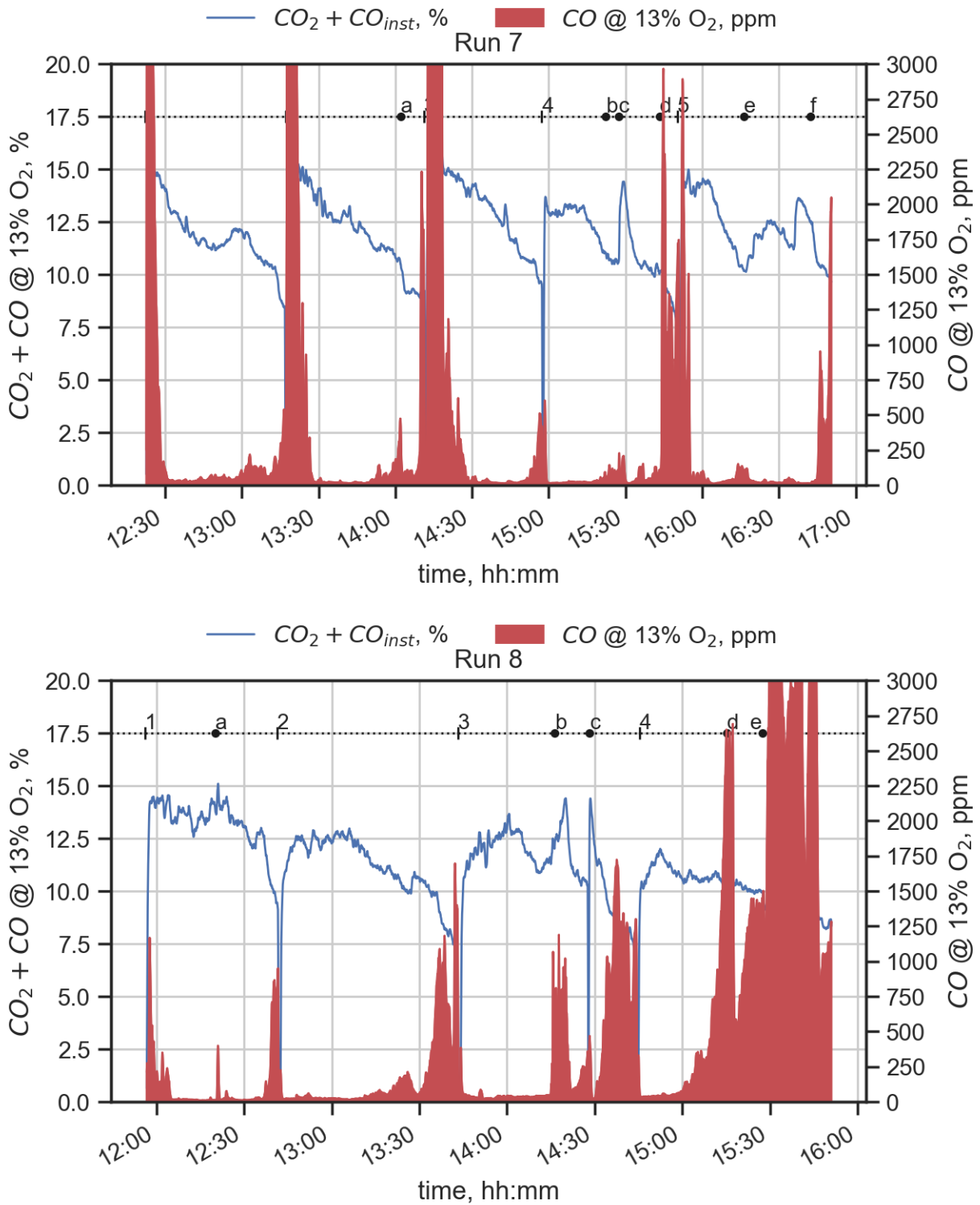


Figure 6.12: Original CO vs time data. Runs 7 and 8.

As can be seen from Figures 6.1 and 6.2, low  $CO_2$  values always yield elevated  $CO$  and  $THC$  values for both conventional and gasification stoves. However, while the end of any charge period in conventional stoves always features low  $CO_2$  and, thus, high  $CO$  and  $THC$ , this is not always the case with gasification stoves. The evidence for low  $CO$  levels at the end of some charge periods can be observed on graphs in Figures 6.9 to 6.12:

- All batches in run 1
- Batches 2, 3 and 4 in run 2
- Batches 2 and 4 in run 3
- Batches 2, 3 and 5 in run 5
- Batches 1 and 2 in run 6
- Batch 3 in run 7
- Batch 1 in run 8

On the other hand low  $CO_2$  and high  $CO$  levels during the second half of a charge period can be clearly observed in following cases;

- Batch 1 of run 2
- Batch 1 of run 3
- Batch 2 of run 4
- Batch 3 of run 6
- Batch 4 of run 7
- Batches 3 and 4 of run 8.

The increased levels of  $CO$  during the middle and end of some more polluting charge periods were always related to the channels created in the char bed. An example of such channels can clearly be seen on the photograph in Figure 6.16c. Channels were observed to be the char-free connection between the zone above the char bed and the nozzle inlet. They are created because a portion of char is still not decomposed into smaller pieces and thus provides structural support for the rest of the char and burning firewood above it. However, those channels can collapse due to ongoing char

decomposition, which was also recorded. In the following paragraph the events, such as channel creation and channel collapse, or blow-back events, that have occurred in the eight experimental runs, will be listed.

- *Run 1, event a* - low magnitude blow-backs occurring ( $\Delta p \approx 2 - 3$  Pa)
- *Run 2, event a* - blow-backs occurring
- *Run 3, event a* - channel created beneath the front log, photo in Figure 6.13a
- *Run 3, event b* - blow-backs occurring
- *Run 3, event c* - channel created beneath the front log, photo in Figure 6.13b
- *Run 3, event d* - channel created, Figure 6.13c
- *Run 3, event e* - low magnitude blow-backs occurring ( $\Delta p \approx 2$  Pa)
- *Run 3, event f* - channel created, front log supported by the remaining char piece, Figure 6.13d
- *Run 3, event i* - channel created, but covered with decomposing logs - no  $CO$  elevation, Figure 6.13e
- *Run 4, event a* - collapse of fuel bed
- *Run 4, event b* - collapse of fuel bed
- *Run 4, event c* - channel is being created
- *Run 4, event d* - collapse of created channel
- *Run 4, event e* - channel in creation
- *Run 5, event a* - channel created on the right back side, Figure 6.14a
- *Run 5, event b* - collapse of logs,  $CO$  falls, whereas  $CO_2$  rises
- *Run 5, event c* - channel between logs created, Figure 6.14b
- *Run 5, event d* - fuel bed collapse
- *Run 5, event e* - fuel bed collapse
- *Run 6, event a* - channel in creation
- *Run 6, event b* - created channels

- *Run 7, event a* - smaller collapse of fuel bed, Figures [6.16a](#) and [6.16b](#) show the fuel bed state before and after collapse, respectively
- *Run 7, event b* - channel is created in the front, Figure [6.16c](#)
- *Run 7, event c* - collapse of top log, however, upon covering of front channel, back one is created, Figure [6.16d](#)
- *Run 7, event d* - channel is created
- *Run 7, event e* - covered channel created, front log supported by two pieces of char, Figure [6.16e](#)
- *Run 7, event f* - covered channel created, response in  $CO_2$  and  $CO$  not clearly visible due to good coverage, Figure [6.16f](#)
- *Run 8, event a* -  $CO_2$  reaching 15 %, which is a limit for effective mixing for this particular stove variant: sensitive response in  $CO$  is clearly visible
- *Run 8, event b* - blow-backs occurring
- *Run 8, event c* - unscheduled door opening, hence the  $CO_2$  dip
- *Run 8, event d* - channel is created, soon to be collapsed
- *Run 8, event e* - large channel created between the two logs, Figure [6.15a](#)

From the correlation of documented events in the primary chamber and the response in  $CO$  emissions, it is clear that presence of char bed channels very strongly correlates to elevated  $CO$  levels.



(a) Run 3, event a - channel in the front



(b) Run 3, event c - channels in the front



(c) Run 3, event d - collapsed logs



(d) Run 3, event f - channel in the front



(e) Run 3, event i - covered channels

Figure 6.13: Photographs of influencing events in a primary chamber in run 3.





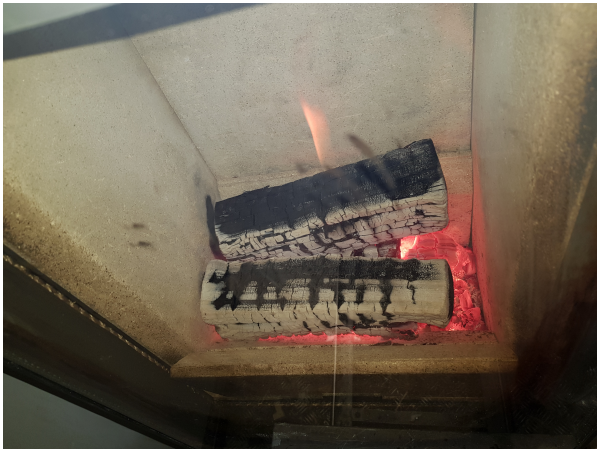
(a) Run 5, event a - channel at the back right      (b) Run 5, event c - channel between logs

Figure 6.14: Photographs of influencing events in a primary chamber in run 5.



(a) Run 8, event e - channel between logs

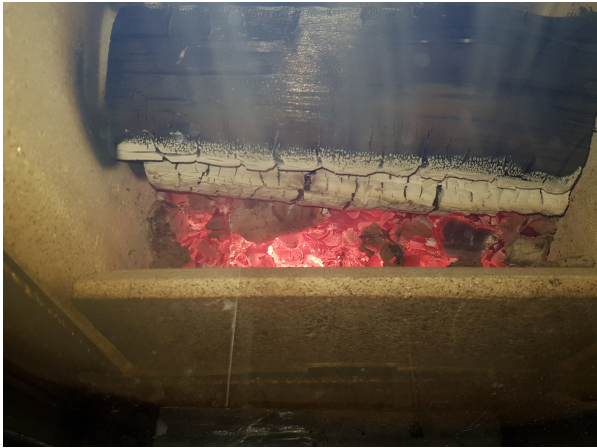
Figure 6.15: Photograph of an influencing event in a primary chamber in run 8.



(a) Run 7, event a - before collapse



(b) Run 7, event a - after collapse



(c) Run 7, event b - channel in the front



(d) Run 7, event c - collapsed log, channel at the back



(e) Run 7, event e - channel in the front



(f) Run 7, event f - covered channel

Figure 6.16: Photographs of influencing events in a primary chamber in run 7.



It was noticed that the char bed channel creation phenomenon was mainly present in the case of the bigger char bed surface area ( $472 \text{ cm}^2$ ), as against the smaller one ( $337 \text{ cm}^2$ ). The comparison is best seen in the two graphs in Figure 6.17.

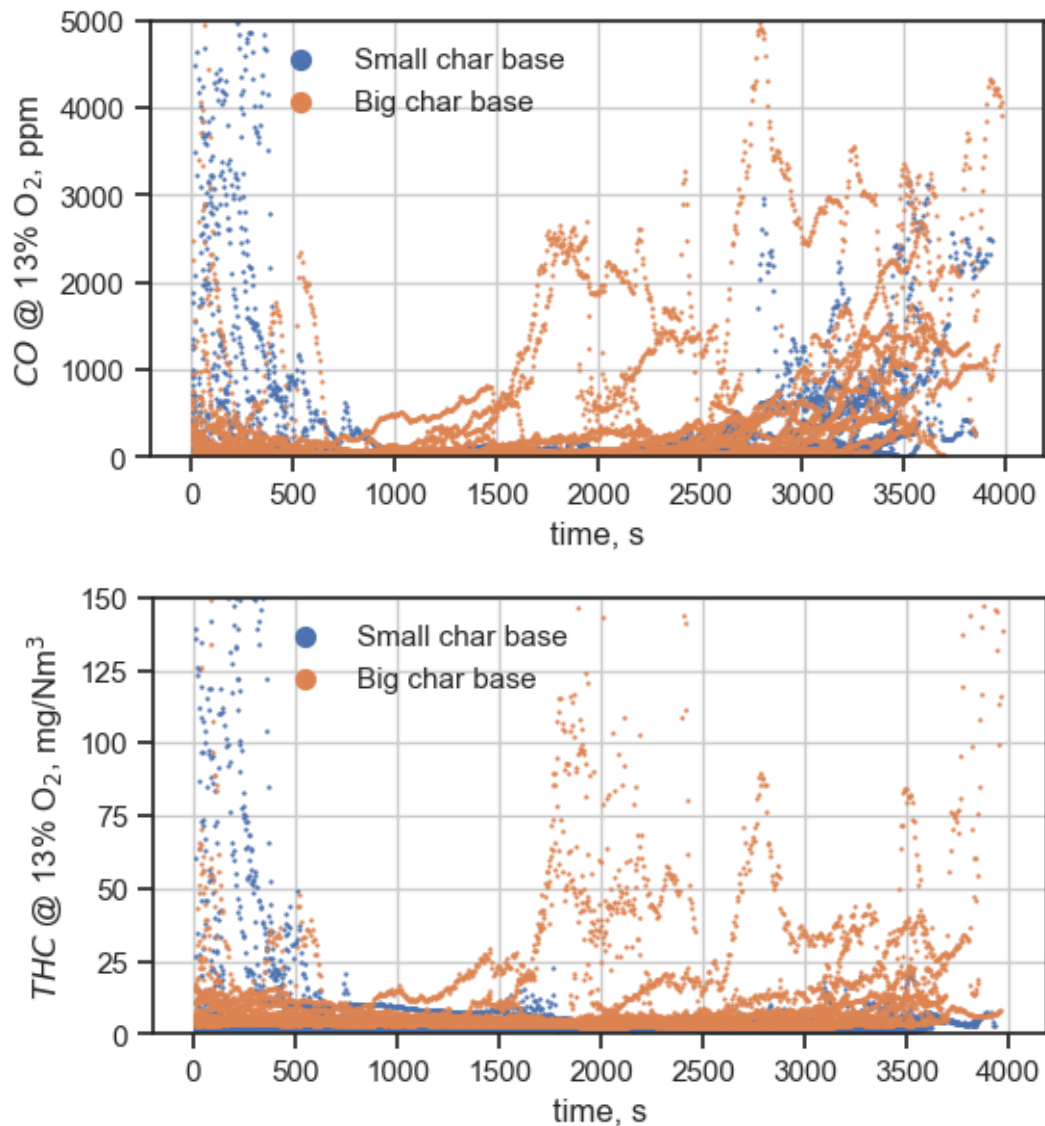


Figure 6.17: Comparison of time evolution of *CO* and *THC* between stove configurations with smaller and bigger char base areas.

The top graph shows the *CO* versus time in seconds for every batch of every run, whereas the bottom one shows the *THC* levels. The fact that stove versions with the greater char base area are more susceptible to char bed channel creation than the ones with smaller area is evident due to elevated *CO* and *THC* levels in the middle and end of the corresponding charge periods. While smaller char base area stove versions feature some *CO* increase in the last 10 to 15 minutes of a charge period, an equivalent increase in *THC* is not visible. On the other hand, elevated *CO* and *THC* at the beginning of a charge period is much more frequent in smaller char base area



stove variants. Hence, it is evident that there are two independent competing sources of elevated  $CO$  and  $THC$  for different stove variants:

1. At the beginning of a charge period for stove designs with the small char base area. This probably occurs due to ineffective mixing of syngas and secondary air, as well as due to elevated  $CO_2$  levels (i.e. decreased oxygen levels).
2. During the middle and the end of a charge period for designs with the big char base area. This occurs due to channels being created in the char bed.

The fact that two independent sources of elevated PIC emissions have been identified is taken into account in statistical analyses of the results.  $CO$ ,  $THC$  and  $PM$  analyses were conducted on four different data sets, the last three corresponding to different sources of elevated PIC levels. The statistical process and results are presented in following section.

### 6.3.4 Statistical Analysis

Overall, four sets of data were analysed statistically:

- *Data 1* - Original, unfiltered data, where both PIC sources are accounted for - *stoichiometry and char bed channeling effects*.
- *Data 2* - Data within the first 15 minutes of every charge of every experimental run (accounting for close to the first 1/4 of a charge period) - to account only for stoichiometry related sources of elevated PICs.
- *Data 3* - Data after the initial 15 minutes (cca 45 to 50 minutes, accounting for close to 3/4 of a charge period) - to account for all other sources of elevated PICs, including char bed channelling effects.
- *Data 4* - Data where there are no parts with  $CO_2$  levels above 15 % - to account for all data where oxygen deficiency does not play a crucial role. This data set is analogous to the 3rd one, i.e. it aims to account for the same sources of elevated PICs.

The detailed statistical results are presented in Appendix [A](#) through the following:

- Tables of factor effect estimates, regression coefficients and percent contributions<sup>9</sup> based on the full model (accounting for all factors and two factor interactions)<sup>10</sup>,
- ANOVA tables accounting only for significant factors,
- Summary tables of reduced regression models, including model  $R^2$  and adjusted  $R^2$ ,  $F$ -value and mean of response,
- reduced model equations - it is to be noted that all independent variables present in all presented model equations can take values either 1 or -1 (high and low level) as the variables are treated as categorical, not quantitative - and
- Graphs showing adequacy of proposed models:
  - standard normal probability plots of residuals and
  - plots of residuals versus predicted values.

As for every charge cycle only a single data point for PM emission is available, so  $PM$  is analysed only for the original data set. Hence, the analysed response variables were  $CO_{orig}$ ,  $THC_{orig}$  and  $PM_{orig}$  from the original data set,  $CO_{data2}$  and  $THC_{data2}$  from the 2nd data set,  $CO_{data3}$  and  $THC_{data3}$  from the 3rd data set, and  $CO_{data4}$  and  $THC_{data4}$  from the 4th data set.

5% was taken as a significance limit.

Analysis of  $THC$  in the original data set, and  $CO$  and  $THC$  for data set 2 (the initial 15 minutes of a charge cycle) have not produced any significant models. The statistical data for adjusted  $R^2$  and model p-values for the other 6 analyses are summarised in Figure 6.18 and plotted against each other in Figure 6.19. The adjusted  $R^2$  and model p-values correlate in such a way that the higher the adjusted  $R^2$  the lower the model p-value. Therefore, the fitness of derived regression models and their significance can be sorted from highest to lowest:

1.  $THC_{data3}$
2.  $CO_{data4}$
3.  $PM_{orig}$

<sup>9</sup>Percent contribution is calculated as the fraction between a magnitude of regression coefficient and the sum of all regression coefficients' magnitudes.

<sup>10</sup>The factors (and interactions) that were included in presented ANOVA tables are marked in bold text.

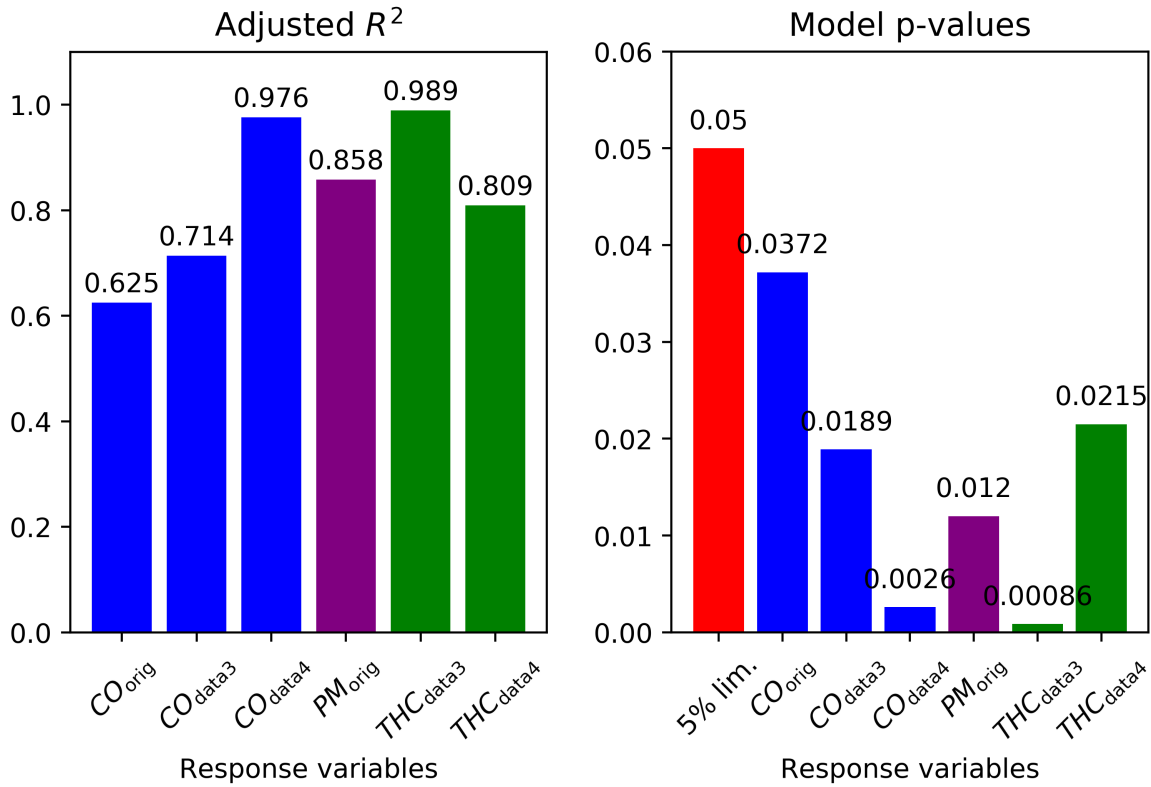


Figure 6.18: Adjusted  $R^2$  and model p-values for PIC data from 3 data sets: original (unfiltered), data3 (the one without initial 15 minutes) and data4 (the one with  $CO_2 < 15\%$ ). Red bar on the right chart shows the significance limit of 5%.

4.  $CO_{data3}$  and  $THC_{data4}$

5.  $CO_{orig}$

Hence, from Figures 6.18 and 6.19 it can be seen that the two best fitting and most significant models are the ones for  $THC_{data3}$  and  $CO_{data4}$ . These are from the data sets which both aim to capture parts of the charge periods without potential initial oxygen deficiency which elevates PIC levels. For comparison, regression analyses of  $CO_{data3}$  and  $THC_{data4}$  also yield significant models, however with lower adjusted  $R^2$  and higher p-values.

Regression models for  $CO_{data4}$  ( $R_{adj}^2 = 0.976$ ,  $p = 0.0026$ ) and  $THC_{data3}$  ( $R_{adj}^2 = 0.989$ ,  $p = 0.00086$ ) are shown through model equations:

$$\widehat{THC}_{data3} = 5.87 + 3.23 \cdot A + 1.76 \cdot B - 0.61 \cdot D + 1.38 \cdot AB \quad (6.3)$$

$$\widehat{CO}_{data4} = 222 + 85 \cdot A + 80 \cdot B + 48 \cdot C + 27 \cdot AB \quad (6.4)$$

From both equations - (6.3) and (6.4) - one can notice the following:

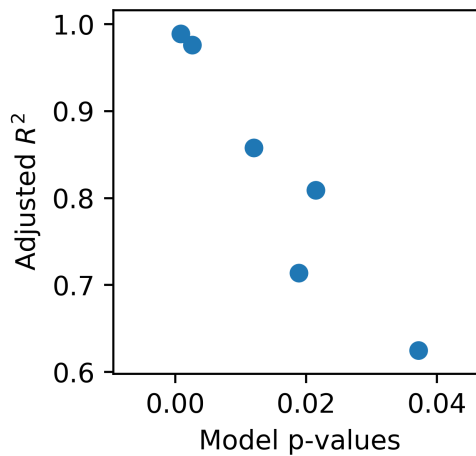


Figure 6.19: Scatter plot of model p-values versus adjusted  $R^2$  values.

- The two sources of variation of response value with greatest coefficients are factors A (char bed surface area) and B (nozzle inlet type).
- A:B factor interaction is also present - with higher influence in case of  $THC_{data3}$  model (eq. (6.3)).
- All coefficients are positive - with exception of the coefficient of factor D (secondary chamber outflow type) in equation (6.3). However, its magnitude is quite lower than that of factors A or B, and its p-value higher (0.032 versus  $<0.001$ , 0.002 and 0.003, see section A.3.2 in Appendix A).

It can be seen in sections A.3.1 and A.4.2 in Appendix A that regression analyses of alternative response variables  $CO_{data3}$  ( $R_{adj}^2 = 0.714$ ,  $p = 0.0189$ ) and  $THC_{data4}$  ( $R_{adj}^2 = 0.809$ ,  $p = 0.0215$ ) also produce models with significant coefficients for factors A and B, however without A:B interaction, with equations:

$$\widehat{THC}_{data4} = 6.26 + 2.37 \cdot A + 1.69 \cdot B \quad (6.5)$$

$$\widehat{CO}_{data3} = 250 + 121 \cdot A + 93 \cdot B \quad (6.6)$$

The adequacy of a linear regression model is evaluated through checking whether the errors are normally distributed around zero and whether they have constant variance. This is checked via standard normal probability plots of residuals (Figures A.1, A.3, A.5, A.7, A.9, A.11) and plots residuals versus predicted values (Figures A.2, A.4, A.6, A.8, A.10 and A.12). The three cases with both the normality and constant variance assumptions satisfied are  $CO_{data4}$ ,  $THC_{data3}$  and  $PM_{orig}$ . This is evident from the good fit to a straight line in the normal probability plots of residuals (Figures A.3, A.7 and A.9),

and due to the lack of apparent structure in plots of residuals versus predicted values (Figures A.4, A.8 and A.10).

There is a level of uncertainty in the estimated A:B factor interaction effect (or coefficient) due to its alias with the C:D factor interaction. However, since the char bed channeling effect was identified as causing elevated *CO* and *THC* levels, it is more reasonable to give higher credence to the interaction of factors that are much more related to the behaviour of the char bed (that is A:B interaction) than that located in the secondary chamber (that is, C:D interaction).

#### *Results from the original data set*

Out of  $CO_{orig}$ ,  $THC_{orig}$  and  $PM_{orig}$ , the PM analysis produced the best fitting and highest significance model, and will be explained in the following section. Analysis of  $CO_{orig}$  produced less fitting and less significant models ( $R_{adj}^2 = 0.625$ ,  $p = 0.0372$ ):

$$CO_{orig} = 287 + 110 \cdot B - 92 \cdot C, \quad (6.7)$$

where the coefficient of factor C is not within the significance limit ( $p = 0.065$ ). Furthermore, analysis of  $THC_{orig}$  did not produce any significant model either.

The inferiority of the analyses of gases (CO and THC) from the original data set compared to those from the filtered data sets probably occurs due to the fact that both the sources (which are independent) of elevated emission values are accounted for by the original data set.

#### *Particulate Matter*

Another significant model is that of particulate matter from the original data set -  $PM_{orig}$  ( $R_{adj}^2 = 0.858$ ,  $p = 0.012$ ):

$$\widehat{PM}_{orig} = 8.87 + 1.20 \cdot C - 0.079 \cdot D + 1.40 \cdot AD \quad (6.8)$$

Coefficients of factor C and interaction A:D are significant (p-values of 0.016 and 0.009, respectively), whereas the coefficient of factor D is on the significance limit ( $p = 0.056$ ). This model contains different sources of response value variation than the two models above (equations (6.3) and (6.4)). A:D interaction is aliased with B:C interaction. Since factor C has a larger coefficient and lower p-value than factor D, it is reasonable to give greater weight to the B:C interaction. Another fact that supports the importance of B:C interaction is that factors B (nozzle geometry) and C (secondary glass surface area) are both related to the secondary chamber. For comparison, factors A and D are

related to different chambers (i.e. factor A is related to primary, whereas factor D to secondary combustion chamber). From the standpoint of the effect heredity principle<sup>11</sup> in both options (A:D and B:C interactions) there is the case of weak heredity.

Another way to find the optimal solution regarding the *PM* emission is through correlating it to either

- the maximum value of  $CO_2$  for a corresponding charge,  $CO_{2,max}$  - as in the case with conventional stove design, shown in Figure 6.6, or
- to the other two PIC variables (*CO* and *THC*).

Figures 6.20, 6.21 and 6.22 show the relation between *PM* on the y-axis, and  $CO_{2,max}$ , *CO* and *THC* on the x-axis, respectively. Every data point corresponds to a value that is averaged and normalised to 13%  $O_2$  for the corresponding firewood charge, during the 30 min period when *PM* is being sampled.

Considering all data in Figure 6.20 there is almost no correlation. The only clear trend can be observed in the case of run 1, where higher  $CO_{2,max}$  yields higher *PM* levels. Therefore, based on the obtained experimental data,  $CO_{2,max}$  is not a good regressor, while it is in the case with conventional stove design, as presented in Figure 6.6. However, when using charge averaged *CO* and *THC* as regressors, as shown in Figures 6.21 and 6.22, one obtains  $R^2$  values of 0.29 and 0.37, respectively, after adequate data transformation. In each figure plot (a) shows data for each run, plot (b) transformed<sup>12</sup> data with a linear regression line, and plot (c) the plot of errors versus regressor variable showing no structure to the plotted data. Hence, the variable accounting for most of *PM* variation is averaged *THC* values which still accounts for only 37% of overall variation - and the other 2/3 must occur due to unknown source(s).

Particulate matter can also be compared based on its colour on the filter. Different colours correspond to the different chemical composition of sampled particulates, i.e. the darker the filter, the more unburned carbon it contains, and vice versa: the lighter the colour is, the more inorganics (fly ash) the sampled particles contain. However, chemical analysis was not an objective in this project, neither is it part of the BS EN 16510-1 testing procedure, hence it was not conducted. Nevertheless, comparison based on colour is possible. It can be seen from Table 6.3<sup>13</sup> that several filters are

<sup>11</sup> If a two factor interaction is significant and only one of its main effects is significant then this is called *weak heredity* (less common), whereas if both main effects are significant then it is called *strong heredity* (more common)

<sup>12</sup> log-log and sqrt-sqrt transformations for *CO* versus *PM* and *THC* versus *PM*, respectively.

<sup>13</sup> It is to be noted that *PM* has not been sampled for batches 2 to 4 in run 2, due to *PM* sampling equipment issues.

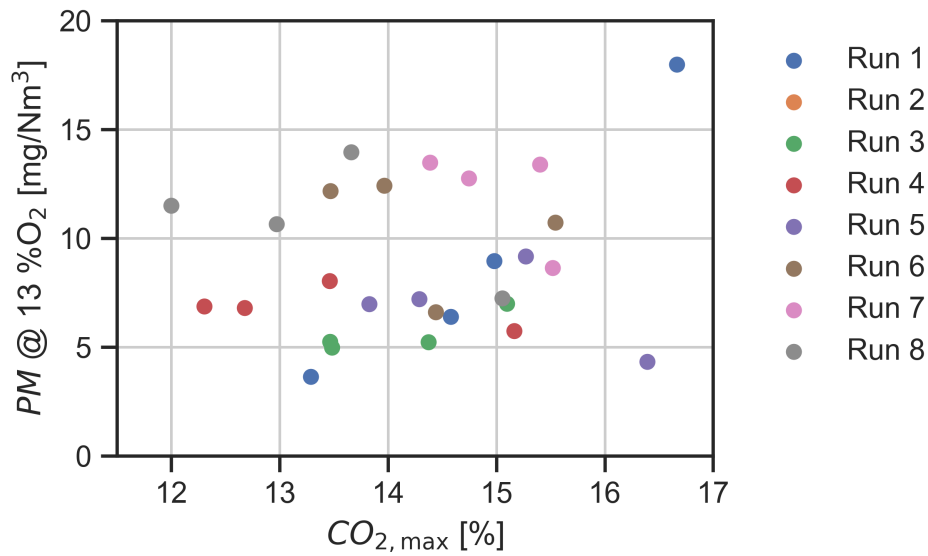
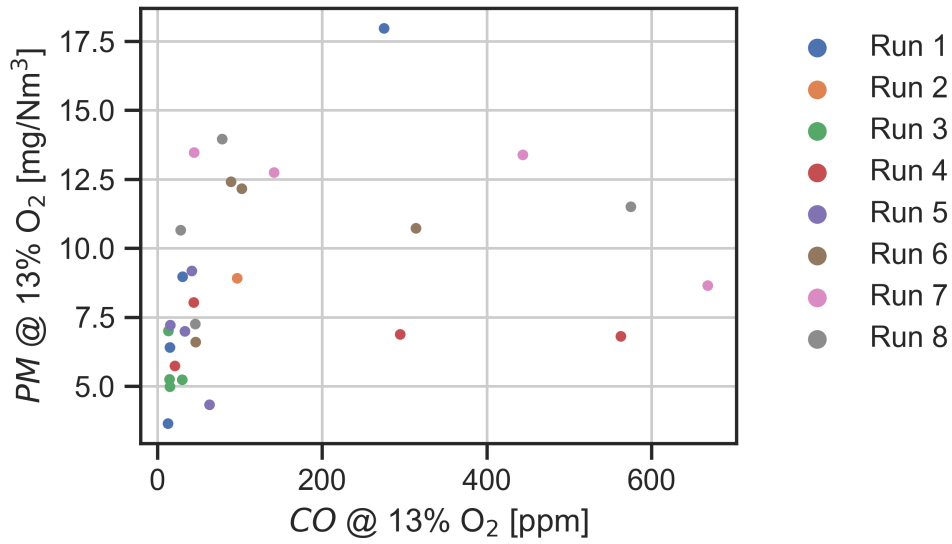
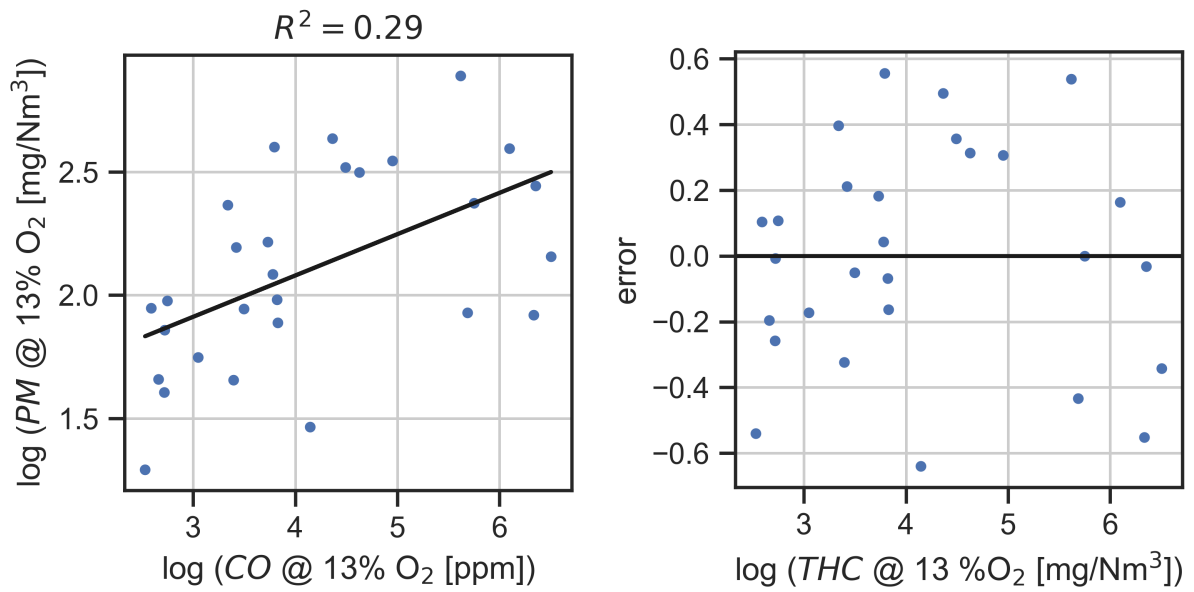


Figure 6.20: Scatter plot of  $PM$  versus  $CO_{2,max}$  during particulate matter sampling period of 30 minutes.

considerably darker than others, i.e. the ones belonging to following batches: batch 1 from run 1, batches 1 and 4 from run 5, batches 1 and 2 from run 6, batches 1, 2 and 3 from run 7 and batch 1 from run 8. It can be noticed from the graphs in Figures 6.9 to 6.12 that in all the identified batches a high  $CO$  emitting regime occurred during the initial 5-10 minute period, i.e. when oxygen was deficient. Hence, the chemical composition of the particulate matter obviously depends on whether the oxygen deficient regime has occurred or not.



(a) *CO* versus *PM* scatter plot

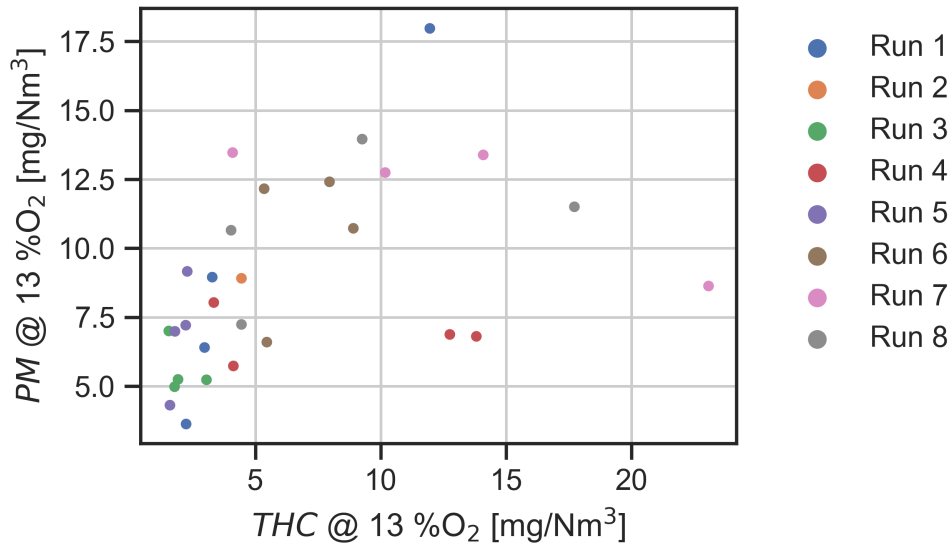


(b) Linear regression with log-log transformation

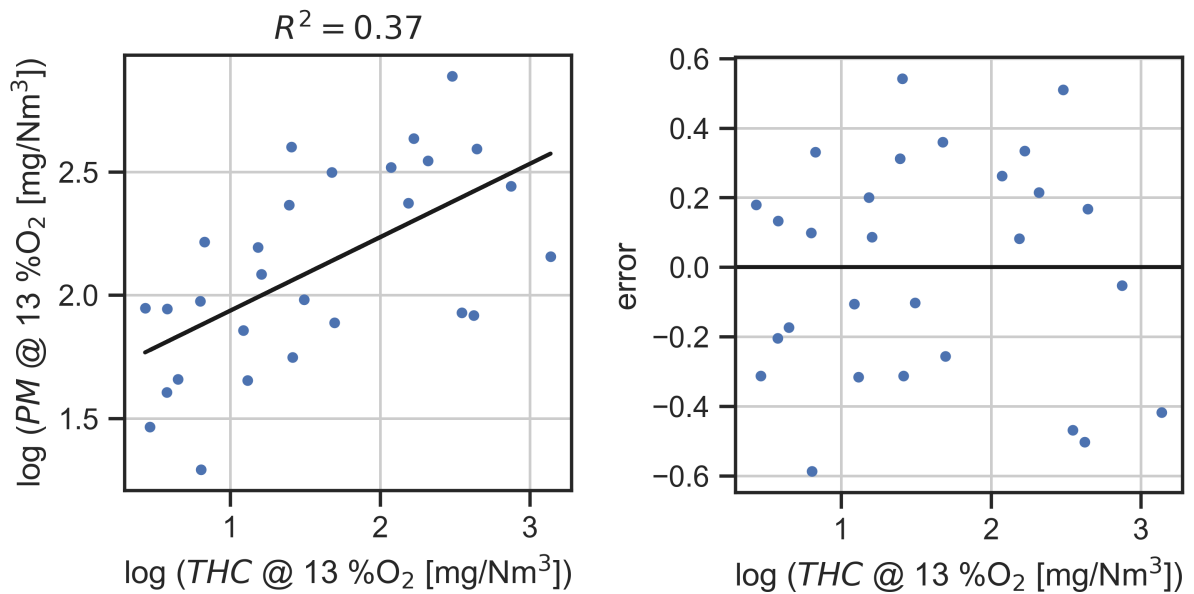
(c) Plot of errors

Figure 6.21: Charge averaged values of *CO* versus *PM*.





(a) *THC* versus *PM* scatter plot

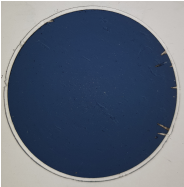
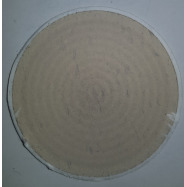
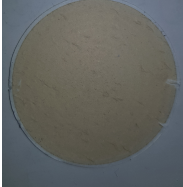
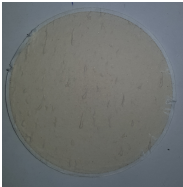
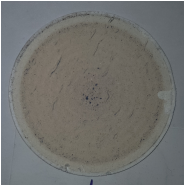
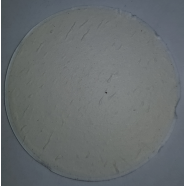
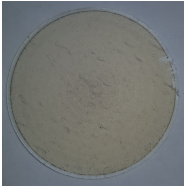
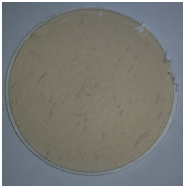
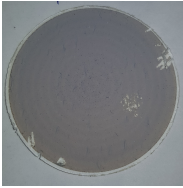
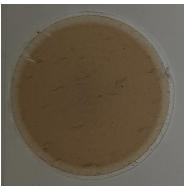
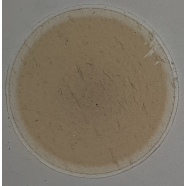
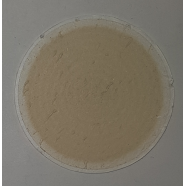
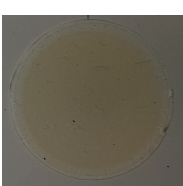
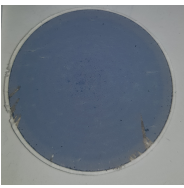
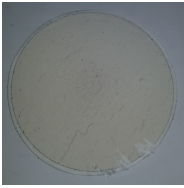
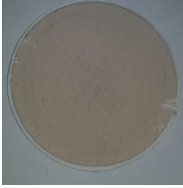
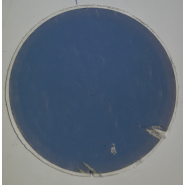
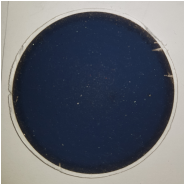
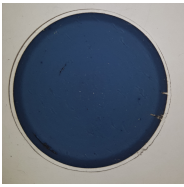
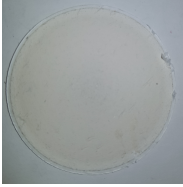
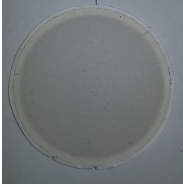
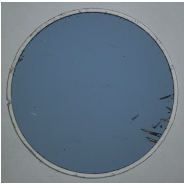
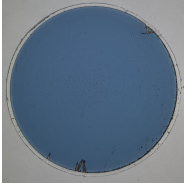
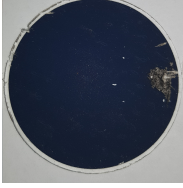

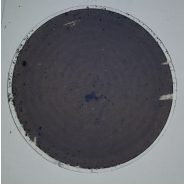
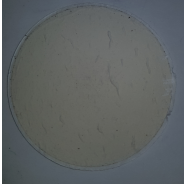
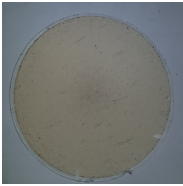
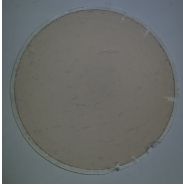


(b) Linear regression with log-log transformation

(c) Plot of errors

Figure 6.22: Charge averaged values of *THC* versus *PM*.

Table 6.3: Photographs of all particulate matter sampling filters.

|       | Batch 1   | Batch 2   | Batch 3  | Batch 4   |
|-------|---|---|--|---|
| Run 1 |    |    |    |    |
| Run 2 |    |   |  |   |
| Run 3 |    |    |    |    |
| Run 4 |  |  |  |  |
| Run 5 |  |  |  |  |
| Run 6 |  |  |  |  |
| Run 7 |  |  |  |  |
| Run 8 |  |  |  |  |

From the statistical analysis presented above it is reasonable to divide the conclusions into two parts, each addressing one of the two pollution regimes: *low air excess ratio* and *char channeling* regimes.

#### 6.3.4.1 Low Air Excess Ratio Regime ( $CO_2 > 15\%$ )

Despite the fact that neither of the two analyses ( $CO_{data2}$  or  $THC_{data2}$ ) produced significant models that account for proximate tested factors, the ultimate cause of elevated PIC emissions is well known, both theoretically and experimentally. Namely the *stoichiometry*, i.e. the fuel - air mixture has entered the regime of low air excess ratio, below the effective mixing limit. Fundamentally, three features of a combustion system can be addressed: i) *mixing quality*, ii) *combustion temperature* and iii) *residence time of gases at sufficiently high temperature*. The available design space has been explored regarding

- *temperature* - high limit of combustion temperature through level -1 of factor C<sup>14</sup>, and
- *residence time* - through a secondary combustion chamber volume fixed at the maximum practical size.

This leaves *mixing quality* to be optimised. The following potential solutions are proposed:

- *Increase the flow rate of secondary air stream* - With a secondary air flow rate increase, the average air excess ratio will be higher (and average  $CO_2$  lower) - that way the expected maximum value  $CO_{2,max}$  will also be lower. However, this change might have a consequent impact during the last third of a charge period, when the air excess ratio would be even higher. High dilution of a flame with air leads to lowered flame temperatures and increased  $CO$  and  $THC$  emissions.
- *Nozzle redesign to provide better initial conditions for mixing* - Another solution is to increase the effectiveness of mixing in order to move the mixing limit from  $CO_2 = 15\%$  to e.g. 18 %. This could be done by redesigning the nozzle to provide better initial conditions for mixing (the majority of which occurs in the secondary chamber). For example, the aspect ratio (length / width) of the nozzle can be

---

<sup>14</sup>Level -1 of factor C corresponds to fully insulated secondary combustion chamber, with minimum glass area.

reduced from 4.3 to closer to 1. This way the mixing of the syngas and secondary air streams is less sensitive to the conditions upstream of the syngas stream, i.e. whether, or by how much, the holes at the nozzle inlet are blocked by the nearby char. Other options include the installation of a diffuser, or a mixing tube with a backward-facing step, at the exit of the nozzle.

#### 6.3.4.2 Inferences regarding the char bed channeling effects

Taking into account the presented statistical results regarding data sets 3 and 4, i.e. the ones without an initial high pollution regime, accounting mostly for char bed channeling effects, one can infer the following:

- Factors A (char bed surface area) and B (nozzle inlet geometry) play the most important roles, due to their high coefficient values and low p-values
- In data set 3, in the *THC* model, A:B interaction is significant and influential.
- In data set 4, in the *CO* model, factor C (secondary glass area) plays a significant role, but is not as influential (the coefficient is half as great as for factors A and B).

Hence, it is reasonable to include only factors A and B in a future optimisation experimental design, possibly with 3 levels, through e.g. a *response surface method*. Factor B (nozzle inlet geometry, or cover) however will in such case have to be redesigned as any 3 (or more) level factor needs to be a quantitative variable, not categorical.

#### 6.3.4.3 Inferences regarding the *PM* emission

In the original data set, in the *PM* model, the significant effects are those of factor C (the secondary glass area, where a smaller area gives less *PM*) and of, most probably, B:C factor interaction. If *PM* emission is correlated with the charge averaged *THC* values, taken from the 30 min sampling period of *PM*, averaged *THC* values account for 37% of *PM* variation (as presented in Figure 6.22).

A very good correspondence between filter colours (shown in Table 6.3) and initial *CO* 'spike' in a charge cycle (evident from Figures 6.9 to 6.12) indicate elevated carbonaceous *PM* emission during the oxygen deficient regime.

### 6.3.5 Assessment of Leakage into the Flue Way

It was noticed that if the flue gas is being sampled in the flue stack (according to EN 16510-1) versus in the heat exchanger, close to the secondary chamber outlet, the instantaneous  $CO_2$  and  $CO$  results differ. It is to be assumed that  $THC$  also differs, however this has not been tested for the purposes of leakage assessment. The sampling stream located at the position defined by EN 16510-1 will be referred to as the 'EN' stream, whereas the sampling stream located in the heat exchanger will be referred to as the 'undiluted' stream, as between the two sampling points dilution occurs.

Three conclusions can be derived from the differing  $CO_2$  and  $CO$  values:

1. If there is a large discrepancy in the instantaneous  $CO_2$  values<sup>15</sup>, there is obviously a leakage of air into the flue way. This leakage could occur either through a missed weld, leaking connection between the stove and flue stack, or elsewhere. In the case of the tested gasification stove, it is unknown where the leakage occurs, which will need to be addressed later in the development process.
2. If there is a discrepancy in the instantaneous normalised  $CO$  values, where  $CO$  at EN sampling point is higher, this implies leakage, or contamination, from a fuel rich area, i.e. the primary chamber.
3. If the normalised  $CO$  (calculated according to equation (3.29)) is greater at the undiluted sampling point, this implies that the combustion reactions are extending into the heat exchanger area, past the undiluted sampling location.

In order to objectively and accurately compare the  $CO$  values under the conditions of flue gas dilution by any leaked air stream, these need to be normalised to a reference oxygen content, 13% in this case. Moreover, a formula containing instantaneous  $CO_2$  values (equation (3.29)) needs to be used, rather than charge averaged  $CO_2$  (equation (3.31)), as defined in BS EN 16510-1.

In Figure 6.23 a 3.5 hour time evolution of EN and undiluted  $CO_2$  values is presented. It is clear that through the entire period the EN sampling stream has considerably lower values of  $CO_2$  than the undiluted one (by around a third lower), thus implying stream dilution by air. From the entire sampling time the two periods, each without a door opening event, are shown on the graph and were isolated for more detailed evaluation.

---

<sup>15</sup>e.g. more than 1 or 2% higher  $CO_2$  at the undiluted point than at EN one. Lower  $CO_2$  values imply dilution of the flue gas stream with air.

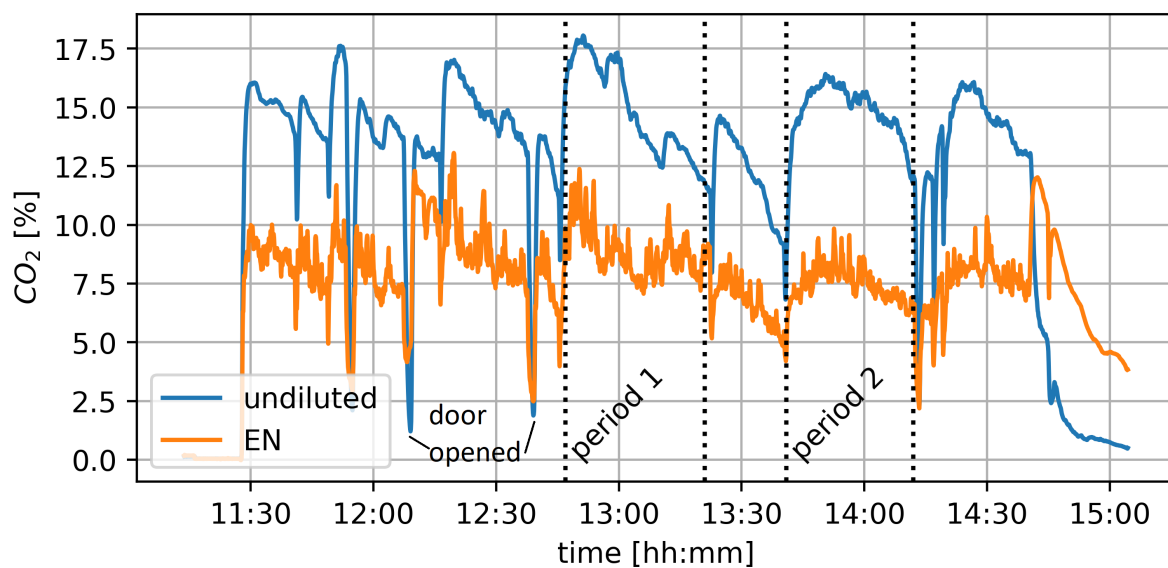


Figure 6.23: Time evolution of  $CO_2$  values at EN and undiluted sampling points during a 3.5 hour burn time.

Analysis of each period is presented on Figures 6.24 and 6.25, respectively. Each figure contains graphs showing time evolution of the secondary combustion chamber temperature,  $CO_2$  values, normalised  $CO$  values at both the EN and undiluted sampling point, and the difference between  $CO$  values at both sampling points,  $\Delta CO$ . From both figures it can be observed that EN and undiluted sampling points both contain regimes where  $CO$  levels are higher than at the other location. If  $CO$  levels are higher than circa 50 ppm the  $CO$  levels at undiluted sampling point are higher and, vice versa, if  $CO$  levels are lower than 50 ppm,  $CO$  is higher at EN sampling location.

This observation can also be presented on an undiluted  $CO$  versus  $\Delta CO$  scatter plot, as shown in Figure 6.26, which contains data from both periods. At  $CO_{undiluted} < 50$  ppm,  $CO$  at the EN sampling point is higher than at the undiluted point by up to 20 ppm. In the case of more elevated  $CO$  levels, i.e. when  $CO_{undiluted} > 50$  ppm, the undiluted sampling stream contains linearly more  $CO$  compared to the EN sampling stream.

Hence, it could be concluded that there is probably a constant leakage through the flap seal, contributing to up to 20 ppm of  $CO$  increase in flue gas. On the other hand, at elevated  $CO$  levels at the secondary combustion chamber exit, when average temperature is sufficiently high for reactions to occur, the oxidation of  $CO$  (and other PICs) continues into the heat exchanger, past the undiluted sampling point, thus further lowering the registered  $CO$  levels.

With the leakage occurring of both the PIC and air into the flue stream, it will be shown in the next section that overall  $CO$  and  $THC$  levels, sampled according to EN 16510-1,

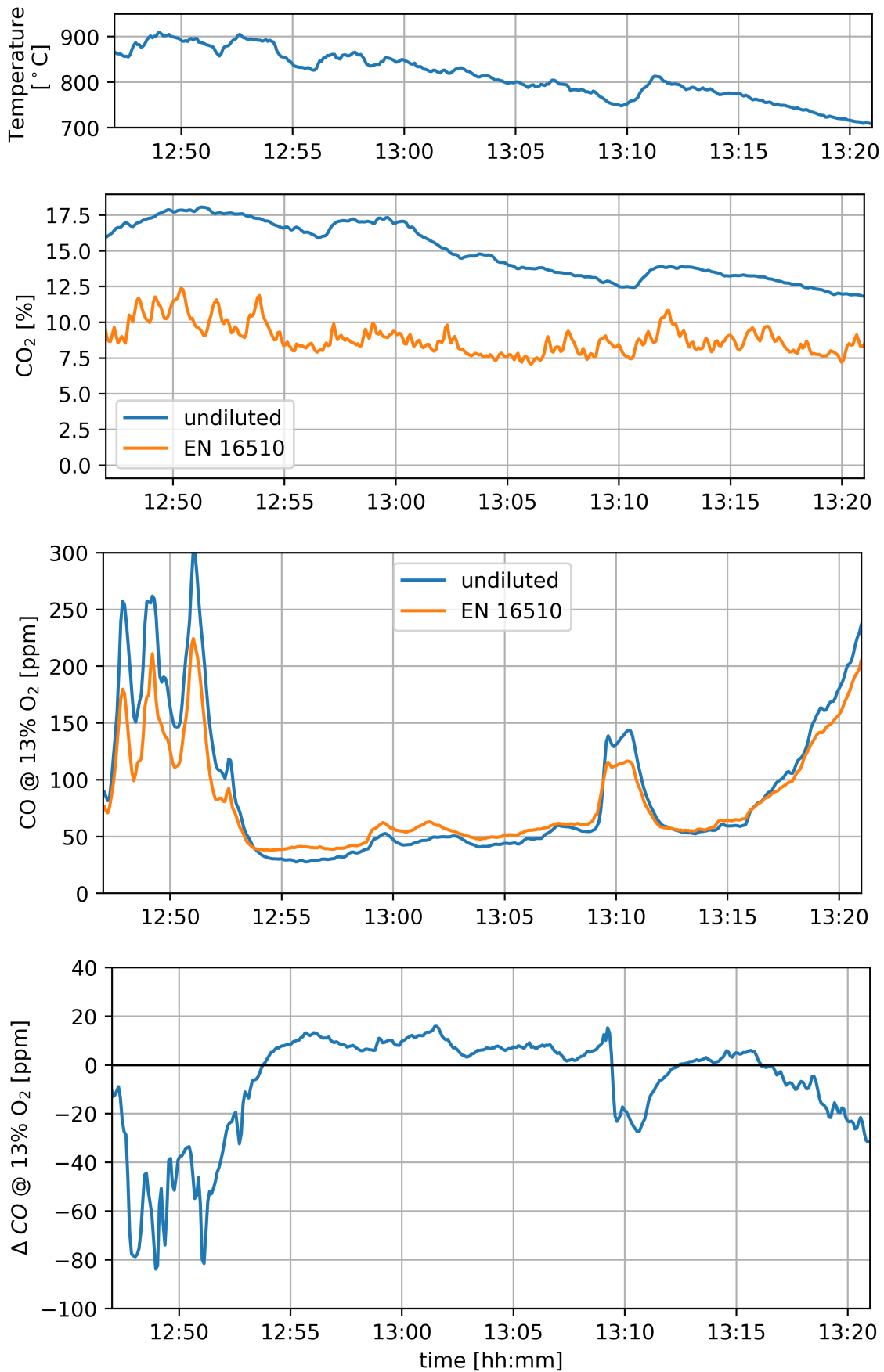


Figure 6.24: Period 1. Temperature,  $CO_2$ ,  $CO$  and  $\Delta CO$  versus time for both EN and undiluted sampling streams.



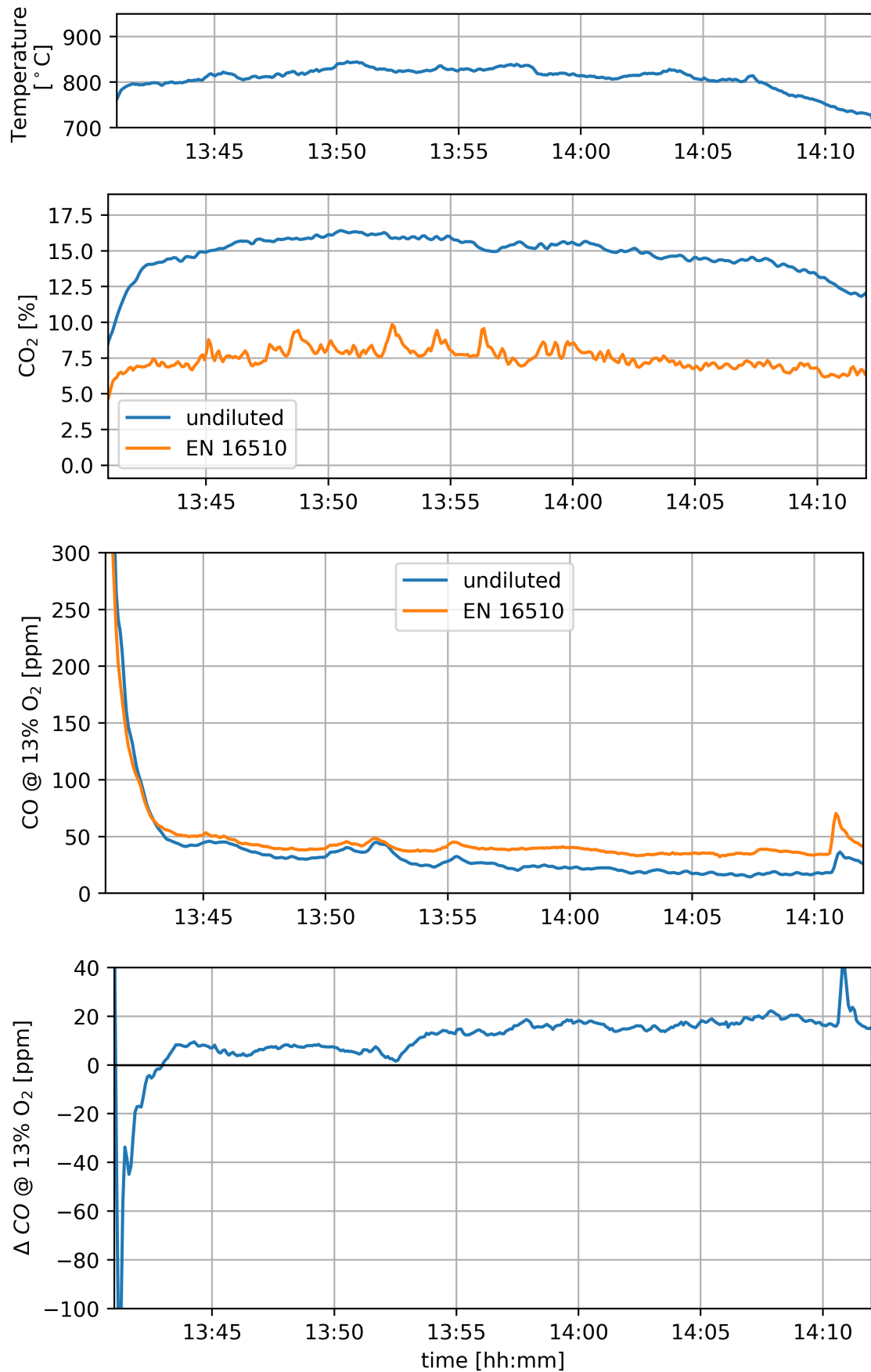


Figure 6.25: Period 2. Temperature, CO<sub>2</sub>, CO and ΔCO versus time for both EN and undiluted sampling streams.



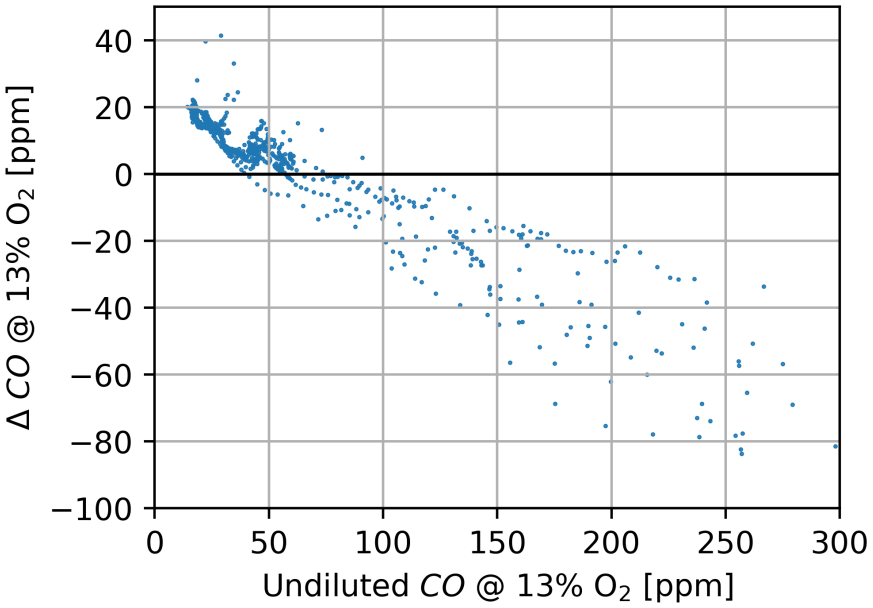


Figure 6.26: Scatter plot of undiluted CO versus ΔCO for both periods.

are not prohibitively affected.

### 6.3.6 EN 16510-1 Test Results of Optimal Stove Configuration

The stove design configuration with minimum average *CO* and *THC* emissions is the one from run 1 (configuration - - - -), i.e. with the following factor levels: small char bed surface area, tubular nozzle inlet, small secondary glass area and slotted secondary brick. The averages of *CO*, *THC* and *PM*, when accounting for 4 charges, are 117.7 ppm, 6.31 mg/Nm<sup>3</sup> and 9.25 mg/Nm<sup>3</sup>, respectively. However, according to the EN 16510-1 standard, only three consecutive charges are to be taken into account. In this case, when the last 3 charges are accounted for (as this combination gives the lowest values), emission levels become

- *CO* = 41 ppm
- *THC* = 2.80 mg/Nm<sup>3</sup>
- *PM* = 10.02 mg/Nm<sup>3</sup>

When the same configuration is tested using the flue gas sampling point located as defined by the BS EN 16510-1 standard, the results presented in Table 6.4 are obtained. In this experimental run particulate matter was not sampled due to the unavailability of the equipment, however, all the results of *PM* emission levels already presented were done according to EN 16510-1 (with the necessary adjustments, as explained in section 4.1.3). The average of the last three charges is given in the bottom row of Table 6.4. These emission values are final and comparable to the emission values of other stoves on the market that are tested according to either EN 13240 or EN 16510-1 standard.

Table 6.4: Performance data of the - - - - stove configuration, tested according to BS EN 16510-1. The data is presented for all charges, and for the average of the last three charges.

| Charge       | <i>CO</i> * [ppm] | <i>THC</i> * [mg/Nm <sup>3</sup> ] | <i>CO</i> <sub>2</sub> [%] | Efficiency [%] | Heat output [kW] |
|--------------|-------------------|------------------------------------|----------------------------|----------------|------------------|
| 1            | 218.2             | 20.46                              | 6.24                       | 91.7           | 6.67             |
| 2            | 136.3             | 8.69                               | 7.72                       | 93.1           | 9.36             |
| 3            | 16.1              | 4.2                                | 7.15                       | 92.5           | 6.82             |
| 4            | 32.7              | 6.00                               | 6.73                       | 92.0           | 6.51             |
| 5            | 59.7              | 3.55                               | 6.18                       | 91.6           | 5.83             |
| <b>3,4,5</b> | <b>36.1</b>       | <b>4.58</b>                        | <b>6.68</b>                | <b>92.0</b>    | <b>6.38</b>      |

\* each @ 13 % O<sub>2</sub>

# Chapter 7

## Discussion

The aim of this thesis was to minimise pollutant emissions from domestic wood log burning stoves via experimental methods. The goal was to surpass the EU 'Ecodesign' requirements, and, if possible, to surpass the emission levels of stoves already present on the market. The proximate objectives towards achieving the aim, with corresponding outcomes, are listed as follows:

### **1. Literature review of the scientific and industrial state-of-the-art in wood stove technology**

- The literature review gave an overview of pollutant gases and particulates being emitted from the wood combustion process.
- Furthermore, parameters that affect pollutant emission levels were identified in the scientific articles, and reviewed: biomass fuel species, fuel moisture, phase of wood combustion, type of appliance, combustion chamber heat load and user influence. Since the only parameters related to the design of a wood stove are appliance type and combustion chamber heat load, these were mostly addressed in the design development of the stove prototype. Fuel species seem to have the lowest effect on pollutant emissions, if compared to other factors. Fuel moisture is an important parameter, however, already limited by BS EN 16510-1 to a range of 12% to 20% moisture. The wood combustion phase was identified as an influencing parameter by both the reviewed literature and the experiments conducted for this project.
- Primary and secondary measures for reducing pollutant emissions were reviewed. Since only primary measures fall within the scope of this project, potential secondary measures have not been considered for implementation in a stove. One primary measure, or design parameter, was recognised by

Johansson et al [28], Obernberger et al [29] and Brunner et al [20] as very significant in reducing pollutant emissions of a wood log burning device: a gasification design of a wood burning appliance.

- Superiority of gasification (down-draft) over conventional (up-draft) design is also confirmed when comparing emission data from commercially available conventional stoves, gasification stoves and gasification boilers (see Figure 7.2 and Tables 2.3, 2.4 and 2.5). It is evident that those gasification boilers that were reviewed are superior to other categories in terms of *CO* and *THC* emission levels, and thermal efficiency. The reviewed gasification stoves were next in performance, while DTI tested conventional and market representative conventional stoves come last, with comparable performance values. Due to the evidence presented of the superiority of a gasification over a conventional wood log burning appliance design, it was decided to design and construct a gasification type stove prototype with integrated modular design elements that would enable optimisation of the stove's performance possible through interchange of different modular elements.

## **2. Identify and explain the industrial standard for stove construction, calculations and testing; derive and define adequate formulae for analysis; identify and explain necessary adjustments and deviations from the standard**

- There is a common industrial standard for building, testing and calculation of pollutant emission levels for residential wood stoves in the European Union, and also in some other European countries, such as the United Kingdom. The current standard is BS EN 13240, which will be superseded by a new one, BS EN 16510-1, with new Ecodesign pollutant emission limits, from 1st January 2022. BS EN 16510-1 is the standard chosen for building and testing the developed stove prototype. The standard is explained in Section 4.1, as well as deviations from the standardised testing process. Deviations were i) omission of  $\text{NO}_x$  recording due to unavailability of the appropriate  $\text{NO}_x$  module for the gas analyser, and ii) omission of drying in a dessicator (as defined by the standard), but only in an oven. Whilst running the statistically designed experiments, an additional deviation was required: the gas sampling was done in the vicinity of the secondary combustion chamber exit, instead of in the flue stack. The change in sampling location was done in order to test the flue gas stream undiluted by air.
- Formulae for the calculation of pollutant emission factors and the thermal efficiency, defined by BS EN 16510-1, were derived in Section 3. Moreover, additional formulae were also derived, e.g. the ones for calculation of instan-

taneous pollutant emission factors, normalised to 13% oxygen - which were needed for assessment of leakage of either the combustion chamber, or a flap seal, in the developed prototype.

- Statistical design of experiments was the research method used to conduct the experiments and to objectively analyse and compare the data.

### **3. Produce a proof-of-concept prototype(s)**

- Overall, five gasification stove prototypes were designed, built and tested. Of these, three prototypes featured a cylindrical secondary chamber geometry with a tangential syngas-air mixture entrainment (such geometry is often referred to as cyclonic). Two prototypes featured a rectangular geometry, such as in extant gasification stoves. Prototypes with a cyclonic chamber had an inherent flaw, where the entire flow of the burning gaseous syngas-air mixture hit the secondary glass surface which then failed after several burning cycles. Hence, such a design was not considered for further optimisation and development. On the other hand, stoves with a rectangular secondary chamber do not experience such issues with failed secondary glass. Subsequently, the second of the two rectangular prototypes was then optimised through the statistical design of experiments method.

### **4. Identification of important design factors that influence performance of the stove prototype**

- The four highest influencing factors that affect pollutant emission levels were identified as: i) char bed surface area in the primary chamber (as factor A), ii) nozzle inlet geometry (as factor B), iii) secondary window surface area (as factor C) and iv) secondary chamber outlet geometry (as factor D). Details about the factor levels (variations) are explained in section [5.3.2](#).

### **5. Conduct a statistically designed factorial experiment**

- The experiment was designed to be an unreplicated completely randomised one-half fractional factorial with four factors, two levels each and eight runs:  $2^{4-1}_{IV}$ . This is a resolution IV design, which means that main factor effect estimates are aliased with only 3 or more factor interactions, while two-factor interactions are aliased with each other. The basic experimental unit was one day of testing, rather than one single charge, in order to avoid auto-correlation of results between the firewood charges of the same burn cycle. High independence of main factor effect estimates provides a high level of confidence about the possible system - which is also important for potential further optimisation.

- Experiments were conducted at Hunter Stoves' testing facility in Exeter, United Kingdom during January and February 2021. The testing equipment used is listed in section [4.2](#).

## 6. Analyse and compare the experimental data; make recommendations on designing a low polluting stove

- The observations, results, analyses and recommendations will be discussed in the following sections.

# 7.1 Discussion of Experimental Observations, Results, Analyses and Recommendations

There are two possible ways, that are explored in this project, to minimise pollutant emission levels from a wood stove: i) optimisation of a conventional (updraft) stove design, or ii) development of a new gasification type stove. The latter was the main approach, to which the majority of the effort in the project was dedicated, due to the greater potential for design improvement. Experimental results for the final gasification stove are presented in section [6.3](#). However, the former approach was also partly explored in section [6.2](#), by analysing the test results, obtained during testing by the DTI, of seven conventional stoves. The comparison of test data from conventional and gasification stoves is given in section [6.1](#).

## 7.1.1 Comparison of Conventional and Gasification Stove Models

In section [6.1](#) testing data from all seven conventional stoves and all eight gasification stove variants were compared. It is evident from the graphs in Figures [6.1](#), [6.2](#) and [6.3](#) that gasification stove design features a middle combustion phase (featuring intermediate  $CO_2$  values) with  $CO$  and  $THC$  emission levels lower by one order of magnitude compared with the corresponding levels for conventional stoves. Charge averaged data is shown in Figure [6.4](#) which also shows overall lower  $CO$  and  $THC$  emission levels in gasification stove cases than in conventional ones. Emission levels in gasification stove designs being lower compared to conventional ones is in agreement with the literature (e.g. [[28](#), [20](#), [29](#)] or Tables [2.3](#) and [2.4](#)).

In addition to the observed overall superiority of gasification over conventional stove design in terms of PIC emissions, the following observations are of importance:

- Tested gasification stove designs feature increased sensitivity of PIC levels on  $CO_2$ , at an upper limit of  $CO_2 > 15\%$
- All presented data (from both the gasification and conventional design) show characteristic 'U' - shaped  $CO_2-CO$  and  $CO_2-THC$  relations - where  $CO$  and  $THC$  emission levels are lowest at intermediate levels of  $CO_2$

### 7.1.2 Discussion of Test Results from Conventional Stove Models

An alternative approach to lower the pollutant emission levels is to optimise the conventional stove design. This approach is also partially explored in section 6.2 by comparison of experimental data from seven different commercial stoves, produced by Hunter Stoves and tested by the DTI.

It was shown in Section 6.2 that by analysing the  $CO_2-CO$ ,  $CO_2-THC$  and  $CO_{2,max}-PM^1$  relations, two distinct groups of stoves can be identified: stoves a, b and f as one group, and stoves c, d and e as another group. One metric was found to explain this grouping -  $h/A$  ratio (that can also be called 'slimness'),  $h$  being the combustion chamber height and  $A$  being the surface area of the combustion chamber base. Slimmer stoves (a and f) at elevated  $CO_2$  and  $CO_{2,max}$  values emitted lower  $CO$ ,  $THC$  and  $PM$  levels, compared to their counterparts (stoves c and g). Analogously, when comparing only gaseous pollutants ( $CO$  and  $THC$ ), the same stoves were grouped at low  $CO_2$  levels - but in this case with flipped emission levels - slimmer stoves featured higher  $CO$  and  $THC$  levels. Such analysis implies that the entire  $CO_2-CO$  and  $CO_2-THC$  'U' shaped relations are shifted to the high  $CO_2$  end in case of the slim stove group, compared to the other one.

When analysing  $PM$  emission levels through  $CO_{2,max}-PM$  relations, as presented in Figure 6.6, all tested stoves featured comparable  $PM$  levels when the  $CO_{2,max}$  values were at around 12%. The difference in  $PM$  emission levels between different stoves becomes evident at higher  $CO_{2,max}$  values. It was shown that slimmer stoves (a and f) feature lower sensitivity on increased  $CO_{2,max}$  compared to their counterparts (stoves c and g). Such a trend is in accordance to the gaseous pollutant emissions ( $CO$  and  $THC$ ), as stated in the paragraph above. Influence of stove's slimness, which is quantified by the  $h/A$  ratio, on PIC emission levels at elevated  $CO_2^2$ , can be explained as follows. Slimmer stoves (the ones with comparatively higher  $h/A$  ratio) enable either

<sup>1</sup> $CO_{2,max}$  is a maximum recorded value of  $CO_2$  for a given charge cycle.

<sup>2</sup>which is one of possible measures for oxygen deficiency quantification; the other measure being air excess ratio  $\lambda$  - equations (3.17) and (3.18) show the mutual dependency of  $O_2$ ,  $CO_2$  and  $\lambda$

better mixing, or longer residence time of the mixed reactants in the flame, or both. Hence, the initial emission regime of a charge cycle for a high  $h/A$  ratio stove, when oxygen levels are lowest, provides comparatively lower  $CO$  and  $THC$  than a low  $h/A$  ratio stove. This phenomenon could be studied further, through the  $h/A$  or some similar variable, by conducting a regression analysis.

The difference in  $CO_{2,max}$  values for an average charge cycle between individual stove models can be explained through the corresponding combustion chamber volume; that is, smaller stoves usually feature higher  $CO_{2,max}$  values. This trend is obvious from Figures 6.7 and 6.8, and could be explained by the radiation intensity from flames into the firewood: in smaller volume stoves, the flames are located closer to the firewood, and such stoves feature a smaller window glass area, when compared to the larger volume stoves. Higher radiation intensity leads to a higher pyrolysis rate, which then feeds back into the radiating flames. Hence, smaller volume stoves feature higher  $CO_{2,max}$  and PIC levels during the initial 5 to 10 minute time period of a charge cycle. A more detailed explanation is given in section 6.2.3.

## 7.1.3 Discussion of Test Results from Gasification Stove Variations

### 7.1.3.1 Significant Features of a Gasification Stove

Several significant features, or issues, that are distinct from a conventional stove were identified in the gasification stove models, namely: i) primary chamber sooting, ii) blow-back, iii) channel creation in the char bed, iv) secondary flame ignition stability, v) flap leakage and vi) missed weld leakage. These have been presented earlier in Section 6.3.1 and will be discussed here, where proposed solutions, recommendations and opinions will be provided.

#### **Primary chamber sooting, blow-backs and char bed channels**

Primary chamber sooting refers to the regime in the primary chamber when the soot production rate is elevated which causes the primary door glass surface to darken due to deposition of soot. Blow-back is another issue related to the primary chamber, when the gaseous reactant mixture in the primary chamber burns in a very short period of time (e.g. less than 1 second) thus effectively causing a small explosion. Blow-backs often occur intermittently, e.g. every one or two minutes. Char bed channels are the char-free connections within the char bed between the nozzle and the region above



the char bed.

Primary chamber sooting, blow-back and channel creation in char bed are three distinct issues, but related to each other, with sooting and blow-back issue having a common source. Whenever the radiation intensity from the char into the gas phase of the primary chamber was diminished, soot production was first observed, and in some cases followed by blow-backs. Both the soot production and blow-backs occurred whenever the flame within the primary chamber was diminished or lost. It was observed that lowered radiative heat transfer from the char occurred in two cases:

1. When the char bed is fully covered by firewood, in more than one layer - in such case the primary flame is very diminished or even non-existent. Hence the gas phase above the firewood is not being heated by the char, and probably becomes very fuel rich, which creates soot when in contact with the comparatively cool window glass surface. In contrast to a fully covered char bed, the opposite extreme is the case when a single log is placed onto the char bed which is then only partly covered. In such a case, pyrolysed gases from the entire log surface are heated by the char (either directly or via reflection from vermiculite bricks) and are ignited very close to the log surface.
2. When the char bed contains channels through which most of gas flow takes place, since it is the path of least resistance (i.e. lowest pressure drop). Hence, there is less gas flow through the micro-pores of the packed parts of the char bed, less surface oxidation of char, and thus less heat being generated and radiated into the gas phase.

In both cases the soot production and blow back issues were exacerbated if the firewood contained more moisture.

Char bed channels will always be created after a certain period of time after refuelling. The objective is to maximize this period to beyond the time mark when refuelling criteria are reached<sup>3</sup>. That way, the channels cannot reach a size that would cause the elevated PIC levels. It was found that creation of char bed channels is postponed by i) burning firewood with optimum moisture content, by ii) burning smaller pieces of firewood (e.g. less than 700 g each), by iii) ensuring that firewood - 2 to 3 pieces - is tightly packed directly on top of nozzle inlet and by iv) having a smaller char base surface area. In the following list each step is explained:

---

<sup>3</sup>Out of the two refuelling criteria, the 50 g initial fuel bed mass increment criterion was always reached first.

1. **Optimum moisture content of firewood (cca 12 to 20% M.C.)** - It was found that wetter firewood takes more time to decompose when burning. Drying and decomposition probably occur unevenly across the wood log volume. When a once wet piece of wood splits into 2 or 3 (bigger) pieces of char, the decomposition of each piece takes longer compared to the drier wood log. These bigger char pieces then provide structural support for the firewood above, thus creating channels. The reason for the prolonged time for further char splitting might be that the internal volume of those char pieces still contains virgin (i.e. not fully pyrolysed) wood. This delay in pyrolysis might be due to the higher moisture content of the firewood, whose prolonged drying delayed the pyrolysis.
2. **Smaller pieces of firewood** - Burning bigger firewood pieces, in lower number, results in similar effects, in terms of char bed channel creation, as burning wet firewood. The decomposition of one or two bigger wood logs into smaller char pieces is considerably delayed in comparison to burning three smaller logs. As explained above, delayed char splitting results in a prolonged burn time, char bed channel creation and thus elevated PIC levels.

On the other hand, if the wood logs are smaller, the log count needs to be higher in order to maintain the charge cycle for at least 45 minutes, a requirement of the BS EN 16510-1 methodology. However, with more pieces of firewood, the surface area increases, which causes higher rates of pyrolysis at the beginning of the charge cycle. Since the air inflow rate is fixed, the air excess ratio can drop to below the effective mixing limit of the nozzle (which is at circa  $CO_2 = 15\%$  for tested nozzles). In such an oxygen deficient regime, it was observed that PIC production, including PM, rises at a progressively increasing rate as  $CO_2$  increases. This behaviour can be seen in Figure 6.1 (b).

3. **Tight packing of firewood above the nozzle** - Tight packing of firewood increases the probability of it staying packed once it decomposes into char. Moreover, the char thus created further decomposes right on top and around the nozzle inlet. It was found that such firewood packing delays the creation of char bed channels, and thus the elevated PIC regime.
4. **Small char base surface area** - The start of the elevated PIC regime due to char bed channels is delayed in the case of a smaller primary chamber base area compared to a greater area (tested  $337\text{ cm}^2$  versus  $472\text{ cm}^2$ ). This is evident from the graphs shown in Figure 6.17. Both  $CO$  and  $THC$  data show elevated emissions during the middle and end part of some charge cycles, in cases of a big char base. This fact could be explained as follows. Due to similar firewood consumption rates in all tested cases, which is evident from similar values of calculated

heat output and thermal efficiency, it can be assumed that char creation also occurs at similar rates. Hence, assuming equal char volumes at the same time marks of a charge cycle, a smaller char base leads to a thicker (or taller) char bed. In order for a char bed channel to start to noticeably affect the recorded PIC levels, it needs to connect the nozzle inlet and the top of the char bed. In case of a thicker char bed, the channel needs to be longer, which takes more time to create. However, it is more likely for the fuel bed to collapse before the channel becomes long enough to affect the PIC levels. Therefore, thicker char beds (in smaller stove base cases) in most cases feature fewer channels that would noticeably affect the stove's performance.

Hence, there are several objectives and limits, some of which are conflicting, summarised here:

- A low amount of firewood per charge needed to minimise soot production and to decrease chances of blow-backs,
- A high amount of firewood needed to maintain the minimum charge cycle time of 45 minutes,
- More, smaller firewood pieces needed for delayed char bed channel creation, and
- Fewer, bigger firewood pieces needed to avoid the initial oxygen deficient regime.

Therefore it is clear that finding a solution that addresses all issues is not trivial. One of the possible solutions was tested - a primary chamber in which the dimensions have been selected according to the following rules:

- The depth of the chamber is restricted to ensure that the logs are stacked, and
- the width of the chamber is greater than the length of the logs thus creating clearances on each side, to allow for continuous primary flame.

The geometry of this chamber, including the location of the inlet nozzle, is shown in Figure 7.1.

- **Restricted depth of primary chamber** - The importance of primary chamber depth restriction is twofold: i) it limits the amount of firewood in direct contact with the char at the beginning of a charge cycle, when the pyrolysis occurs at maximum rate (due to the very dry outermost layers of firewood being in contact with

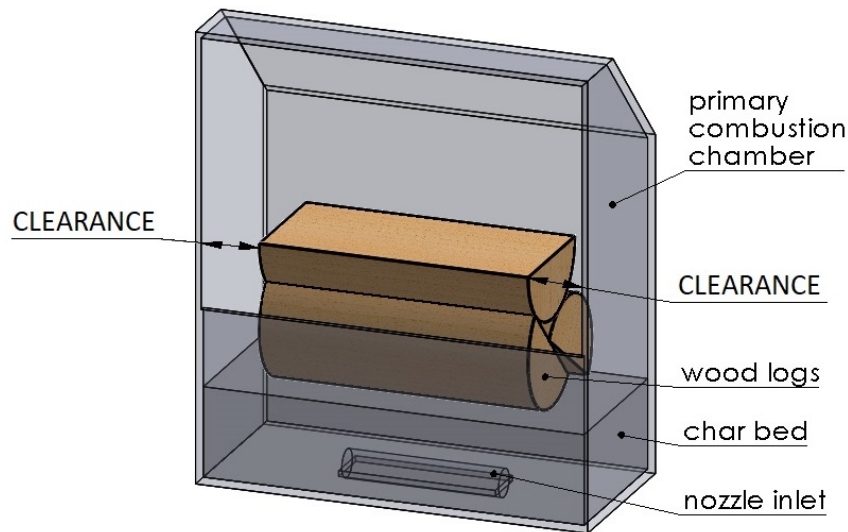


Figure 7.1: Primary chamber geometry, with restricted depth and side clearances between the firewood and walls.

the hot char), and ii) it ensures that some piece(s) of firewood are stacked and separated from the char, thus delaying the majority of the decomposition process to periods when the pyrolysis of the bottom logs diminishes. That way (i.e. by firewood stacking) the temporal variation of overall pyrolysis can be reduced - thus allowing for the stove to be optimised in a way to maximise the time period of the optimum emission regime.

Firewood stacking is also beneficial for delaying the char bed channel creation. As firewood decomposes from the bottom upwards, it shrinks and splits, thus allowing for an upper log to fill the otherwise empty volume, i.e. a char bed channel.

- **Side clearances** are important because they allow for an effective heat transfer from the char bed into the fuel rich gas phase. That way the ignition conditions can be continuously present, thus allowing for a continuous primary flame (which is crucial for avoiding sooting and blow-backs). It was observed that after a certain period of time the side char parts, which are radiating into the gas phase, are consumed and the radiation diminishes. However, due to the continuous flame present in the gas phase, new char regions are being created directly on the upper firewood surface layers, thus continuing to maintain adequate ignition conditions. On the other hand, if the side char layers are consumed without the presence of a continuous primary flame and no upper newly formed char layers, it is likely that soot production would increase, resulting in darkened primary glass, and that blow-backs would follow.

A primary chamber with such features was observed to ensure frequent small movements of char and firewood, driven by regular char splitting and gravity. That way the pores in the char never grow to form channels of prohibitively large size.

Additionally to the correct dimensioning of the primary chamber, the firewood needs to be the right size, i.e. 400 to 700 g, depending on the specific moisture content.

### **Secondary flame ignition stability**

It was found that the stability of the secondary flame ignition largely depends on the nozzle inlet geometry. Although only the inlet was varied in the conducted experiments, it can be assumed that the overall geometry of the nozzle also affects the ignition stability. In case of a tubular inlet cover (level -1 of factor B) it took 15 - 25 minutes for successful ignition, counting from the lighting of the initial batch. On the other hand, the alternative, flat cover (level +1 of factor B) featured a prolonged ignition time (30 to beyond 45 minutes).

Secondary flame ignition stability was not researched in detail, and is therefore not fully understood. However, for the tested cases, one possible explanation will be provided in the following paragraph.

Longer updraft burn time creates more char. Thus, when a secondary flame is ignited within the first 15 minutes, this occurs when the char bed is smaller, than the case when ignition occurs after 30 or 40 minutes. The hypothesis is that in the former case a flame stretches from the primary chamber into the nozzle, thus providing ignition conditions when the syngas and the secondary air stream meet, both comparatively cool. Flame stretching is enabled by good fluid dynamic conditions around the cylindrical cover, which creates less turbulence and recirculation than for the flat cover. In the case of the flat cover and within first 15 to 25 minutes, the flame, stretched from the primary chamber into the nozzle, is being blown-off due to high turbulence conditions. However, when the char bed is much thicker after a prolonged period of time, the incoming syngas stream is being preheated by the char bed and, in spite of the unfavourable turbulent regime at the nozzle inlet, and due to elevated temperature of syngas and air<sup>4</sup> mixture, secondary flame ignition can occur. Computational Fluid Dynamics (CFD) could be a good candidate as a method for testing this hypothesis.

---

<sup>4</sup>Which, by that time, is also preheated due to thermal conduction of steel body of the stove.

### 7.1.3.2 Statistical Analysis of Test Results from Gasification Stove Prototype Variations

Eight unreplicated (but repeated<sup>5</sup>) and completely randomised experimental runs were conducted over eight days of testing, as shown in Table 6.2, whose results were statistically analysed in Section 6.3.4, and are discussed in this section.

It was noticed that the stove conditions in one charge cycle often influence the PIC levels during the following charge cycle. Hence, instead of a single firewood charge, a single day of testing (i.e. one burn cycle consisting of overall four consecutive charges) was defined as an experimental unit, in order to avoid autocorrelation of results.

Two independent sources of elevated PIC emissions were identified: i) a source due to initial oxygen deficiency (i.e. at low air excess ratios) of a charge cycle and ii) a source due to the effects of char bed channels.

With the aim of capturing the individual sources of PIC levels, four data sets were statistically analysed: i) the original, unfiltered, data (data set 1), ii) the first 15 minutes of every tested charge (data set 2), iii) data after the initial 15 minutes of a charge (data set 3), and iv) data where  $CO_2 < 15\%$  (data set 4). Data set 2 was analysed with the aim of capturing the initial elevated PIC regime due to oxygen deficiency. On the other hand, since  $CO_2 > 15\%$  occurs mostly within the first 15 minutes of a charge, data sets 3 and 4 both aim to capture other PIC sources, the biggest of which are char bed channel effects.

$PM$ ,  $CO$  and  $THC$  emission levels were used as response variables for all four data sets. 5% was used as the standard significance limit. Since the  $PM$  was measured only for a given charge, not continuously like  $CO$  and  $THC$ , it was only considered in the analysis of original data set. Hence, 9 individual sets of statistical analyses were made, with the following response variables and corresponding data sets:  $PM_{orig}$ ,  $CO_{orig}$ ,  $THC_{orig}$ ,  $CO_{data1}$ ,  $THC_{data1}$ ,  $CO_{data2}$ ,  $THC_{data2}$ ,  $CO_{data3}$  and  $THC_{data3}$ . Out of these 9 models, 6 were found to be significant (shown in Figure 6.18), listed in ascending order of model significance:  $THC_{data3}$ ,  $CO_{data4}$ ,  $PM_{orig}$ ,  $CO_{data3}$ ,  $THC_{data4}$  and  $CO_{orig}$ . The details regarding the statistical analyses are given in the Appendix A.

The data set with only the initial 15 minutes of every charge cycle (data set 2) did not produce any significant regression models -  $CO_{data2}$  or  $THC_{data2}$ . This is due to the high magnitude of the residuals, i.e. the high influence of some factor(s) not accounted

<sup>5</sup>Measurements were repeated in sense that four consecutive batches, following identical testing procedure, were tested.

for in the model. This influence arises most probably from variation in the firewood (either its size, shape or moisture content in the outermost layers) and variation in how the log is being placed into the primary chamber by the operator. This variation has an especially high influence during the initial stages of the charge cycle, when oxygen levels drop to a certain mixing limit, beyond which the  $CO_2$ - $CO$  and  $CO_2$ - $THC$  relations are very steep. It is also evident that even though the overall PIC emissions from a gasification appliance can be much lower than from a conventional one, the tested gasification appliances feature higher  $CO$  and  $THC$  sensitivity on  $CO_2$  increase between  $CO_2 = 15\%$  to  $16\%$  than is the case for conventional appliances. This can be seen from plot (b) in Figure 6.1.

Analysis of gaseous PIC levels ( $CO$  and  $THC$ ) yielded significant regression models, with good fit to the data, for the two filtered data sets aiming to capture char bed channel effects (data 3 and 4):  $CO_{data3}$  ( $R_{adj}^2 = 0.714$ ,  $p = 0.0189$ ),  $THC_{data3}$  ( $R_{adj}^2 = 0.989$ ,  $p = 0.00086$ ),  $CO_{data4}$  ( $R_{adj}^2 = 0.976$ ,  $p = 0.0026$ ) and  $THC_{data4}$  ( $R_{adj}^2 = 0.809$ ,  $p = 0.0215$ ). This implies that there is a clear effect of different geometric stove features (represented through the four factors and the corresponding levels) on creation of char bed channels and, thus, on  $CO$  and  $THC$  emission levels. Moreover, analysis of coefficients and their magnitudes in the aforementioned models implies that factors A and B (char base surface area and nozzle geometry) and, possibly, their interaction effect, play the most influential roles on emission of pollutants. Therefore, should the stove design be optimised further in some future project, it would be reasonable to focus on factors A and B - where B addresses nozzle geometry more generally, not only through inlet geometry. One possibility for such an optimisation approach would be a *response surface method*.

Analyses on the original data set yielded significant regression models for  $PM$  ( $p = 0.012$ ) and  $CO$  ( $p = 0.0372$ ), but not  $THC$ . Moreover, the  $PM$  model fits the data well ( $R_{adj}^2 = 0.858$ ), but the  $CO$  model less so ( $R_{adj}^2 = 0.625$ ). The reason for less significant and less fitting  $CO$  and, especially,  $THC$  models in the original data set compared to the corresponding models for the third and fourth data sets is probably due to the fact that the original data set accounts for both sources of elevated PIC levels. Models for gaseous PIC levels ( $CO$  and  $THC$ ) in the original data set are inferior to the  $PM$  model probably because the oxygen deficient regime affects the  $PM$  emissions more than the char bed channel regime, compared to  $CO$  and  $THC$  levels. Moreover, as  $PM$  is being sampled only during the first 30 minutes of a charge cycle (as opposed to the continuous measurement of gaseous emissions), it does not often account for  $PM$  emission during the second part of a charge cycle, when the majority of the char bed channels are being created.



Additional evidence supporting the conclusion that *PM* is being very affected by the oxygen deficient regime is in the colour of the deposits on particulate matter sample filters, shown in Table 6.3, which correspond in all presented cases to the initial elevated *CO* regimes, as presented in Figures 6.9 to 6.12.

If *PM* is being compared to the maximum recorded value of carbon dioxide  $CO_{2,max}$  for a corresponding charge, analogously to the conventional stoves (see results section 6.2.2 and discussion section 7.1.2), no clear correlation is observed. However, comparing *PM* to charge averaged *CO* (Figure 6.21) and *THC* (Figure 6.22) levels, with adequate data transformation, trends become visible; with correlation coefficients of  $R^2 = 0.29$  in the case of  $\log(PM)-\log(CO @ 13\% O_2)$  and  $R^2 = 0.37$  in the case of  $\log(PM)-\log(THC @ 13\% O_2)$ .

Regarding the influential factor effects in the *PM* regression model, only the secondary window surface area is significant, where less area gives less *PM*. It is to be noted, however, that the secondary window area in a *PM* model has a lower coefficient, relative to the corresponding mean of response, than the coefficients of significant factors in other regression models (i.e.  $CO_{data3}$ ,  $CO_{data4}$ ,  $THC_{data3}$  and  $THC_{data4}$ ). In other words, the secondary window area has less influence on *PM* than the primary chamber base area and nozzle inlet type on *CO* and *THC* emissions related to the channeling effects.

The fact remains that, even though the final  $PM_{orig}$  model is statistically significant, the model coefficient of a two-factor interaction is highest, which implies weak heredity and is generally regarded as unlikely. Moreover, the highest model effects (A:D, or B:C, interaction) account for only 30% of the mean of the response. On the other hand, alternative (simple) regression models, ones with charge averaged *CO* and *THC* as regressors, explain only 29% and 37% of the *PM* variation. Hence, in order to have more clear and higher fidelity results, an improved experiment should be conducted:

- The experiment should be replicated.
- The EN 16510-1 *PM* testing procedure should be completely followed.

It is to be noted that the range in *PM* emissions for all gasification stove variants (5.62 to 12.06 mgPM/Nm<sup>3</sup><sup>6</sup>, see Table 6.2) compared to other wood burning devices<sup>7</sup> (see Figure 7.2) is much smaller than the range of *CO* or *THC* emissions (43 to 585 ppm, and 1.79 to 12.51 mgC/Nm<sup>3</sup>, respectively). Such a restricted range in *PM* emissions

<sup>6</sup>which lies well within the Ecodesign limit of 40 mg/Nm<sup>3</sup>

<sup>7</sup>Other wood burning devices include conventional stove range tested by the DTI, list of conventional stoves representative for the European market, or wood gasification boilers.



implies that factor variations are not as influential on PM levels as they are on *CO* or *THC* levels. Hence, even if the experimental procedure is corrected and the experiment replicated, the *PM* regression model could still predict relatively low influence of tested factors, compared to *CO* or *THC* models.

### 7.1.3.3 Issue of leakage of PIC and air

Pressure inside the primary chamber is around 9 to 10 Pa higher than in the adjacent flue way. Hence, any leakage of fuel rich gases from the primary chamber into the flue way represents significant pollution. Such leakage can occur through either a flap seal, or through a missed weld between the primary chamber and heat exchanger (i.e. the flue way). The latter can mainly be solved by designing a stove with an air supply cavity between the primary chamber and the flue way. That way a leakage of PIC can be replaced by a leakage of air which is not a pollutant gas, as explained earlier in section 6.3.1.6. Leakage through the flap seal was minimised by utilising a high diameter ceramic sealing rope ( $\Phi 15$  mm) and by a higher sealing pressure, achieved through a specially developed tightening mechanism.

Figure 6.23 in section 6.3.5 shows the comparison of  $CO_2$  levels between the two sampling locations - one in the heat exchanger, near the exit of the secondary combustion chamber, and one in the flue stack, located according to the BS EN 16510-1 standard. From the difference in  $CO_2$  values, and thus oxygen levels, of the two sampling streams, where the upstream probe reads lower values of  $CO_2$ , stream dilution by air is evident. The source of such dilution is unknown at the time of writing. However, its impact on the PIC emission levels is mitigated by value normalisation to 13% oxygen content.

The difference in *CO* levels between the two sampling points is shown through graphs in Figures 6.24, 6.25 and 6.26. *CO* levels plotted in these figures are normalised to the 13% oxygen content, using instantaneous corresponding  $CO_2$  level, according to the equation (3.29). It is to be noted that this formula is different to the one defined by BS EN 16510-1, i.e. for charge averaged  $CO_2$  (equation (3.31)). This alternative formula for value normalisation was used in order to make objective comparisons of instantaneous *CO* levels possible. As explained in the last two paragraphs in section 6.3.5, all three figures show that if *CO* levels are higher than circa 50 ppm, the undiluted sampling probe (the one in the heat exchanger) registers higher *CO* levels, whereas if  $CO < 50$  ppm, the EN sampling probe (the one in the flue stack) registers higher *CO* values. Such results can be explained as follows. There is probably constant leakage through the flap, contributing to up to 20 ppm of *CO* increase in the flue stream - hence

the  $\Delta CO = 20$  ppm in low  $CO$  limit (see Figure 6.26). However, at elevated  $CO$  levels in the vicinity of the secondary combustion chamber exit, where the undiluted sampling point is located and where gas temperatures are still high enough for reactions to occur (which is evident from temperature plots in Figures 6.24 and 6.25), the oxidation of  $CO$  continues in the region past the secondary combustion chamber, thus lowering  $CO$  levels already registered at the undiluted sampling point. Hence, as  $CO$  rises,  $\Delta CO$  moves in the opposite direction (see Figure 6.26), meaning the EN sampling probe registers lower  $CO$  values than the undiluted one.

#### 7.1.4 Optimal Configuration of a Developed Gasification Stove

The optimal configuration of the developed gasification stove was the following: small char bed surface area (factor A, level -1), tubular nozzle inlet (factor B, level -1), small secondary glass area (factor C, level -1) and slotted secondary brick (factor D, level -1). When tested in accordance with the BS EN 16510-1, i.e. with the correct gas sampling location, the averaged and normalised performance data reads:  $CO = 36.1$  ppm,  $THC = 4.58$  mgC/Nm<sup>3</sup>,  $CO_2 = 6.68$  %, efficiency = 92% and heat output = 6.38 kW, as shown in Table 6.4.

#### 7.1.5 Comparison of PIC Levels of a Developed Gasification Stove to Other Stoves from the Literature & Industry

In this section the emission and efficiency values will be graphically compared between the gasification stove developed for this project (the optimal configuration) and other wood burning devices:

- The list of representative conventional stoves on the European market, presented in Table 2.3. All stoves are tested according to EN 13240 standard. The data are labeled as 'Repr.Conv.'
- The range of conventional stoves presented in this thesis (sections 6.1 and 6.2), which have been built by Hunter Stoves and tested by the DTI. Their performance data is shown according to both the EN 13240 and the EN 16510-1 standards. The data are labeled as 'Conv.13240' and 'Conv.16510-1', respectively.
- The list of commercially available natural draft gasification stoves, presented in Table 2.4. Most are tested according to EN 13240. The data is labeled as 'Repr.Gasif.'

- The representative list of induced draft gasification boilers, presented in Table 2.5. Testing standards are EN ISO 17225-5 and DIN EN 303-5. The data is labeled as 'Repr.Boiler'

Figure 7.2 shows this comparison where the developed gasification stove is labeled as 'Dev.Gasif.' and other devices are labeled as defined in the bulleted list above. There are four plots in the figure, each showing performance data for  $CO$ ,  $THC$ ,  $PM$  and efficiency, respectively. On the three graphs showing the PIC emission data, the horizontal dotted line shows the corresponding Ecodesign limit. By comparing the performance data from all graphs, it can be observed that the developed gasification stove is superior to most other devices. Comparing the data of  $CO$ ,  $THC$  and efficiency, the developed stove is comparable with the gasification boilers, but superior to other wood stoves. When the  $PM$  data is compared, the trend is not as clear as in other performance criteria between the compared categories.

As a final note regarding comparing the sources of elevated PIC emissions between the tested gasification and conventional stoves, the following can be stated. While both stove types feature elevated PIC levels during the oxygen deficient regime, there is a difference in the second elevated PIC emission regime. Conventional stoves inherently feature elevated  $CO$  and  $THC$  during the charring regime - which is indicated by the decreased  $CO_2$  levels. On the other hand, in gasification stoves, the regime with decreased  $CO_2$  levels is almost always related to the char bed channels, which, given adequate measures, can be avoided. Such non-existence of elevated PIC levels due to the decreased  $CO_2$  in gasification stoves is evident when analysing the following parts from Figures 6.9 to 6.12: all batches in run 1; batches 2, 3 and 4 in run 2; batches 2 and 4 in run 3; batches 2, 3 and 5 in run 5; batches 1 and 2 in run 6; batch 3 in run 7 and batch 1 in run 8. The author's hypothesis is that from the perspective of the thermochemistry of a char bed, the charring regime in a conventional stove and the char bed channeling regime in a gasification stove are probably the same regimes. Such a statement is supported by the fact that in both regimes the values and trends in  $CO_2$ ,  $CO$  and  $THC$  are very similar. Decreased  $CO_2$  levels during the charring regime in conventional stoves occur due to a low inflow rate of air directly into the char bed and thus low oxidation rate of char. Low char oxidation and thus gasification rates, in absence of a sufficient pyrolysis rate, probably leads to spatially uneven char gasification, decreased flame temperature and poor ignition conditions across the entire combustible gas stream. A low air inflow rate is needed in order to minimise the PIC emissions during the main pyrolysis stage of a charge cycle. Similarly, decreased  $CO_2$  levels during the char bed channeling regime in gasification stoves probably occurs due to an analogous chain of events described above: low char oxidation and gasification rates

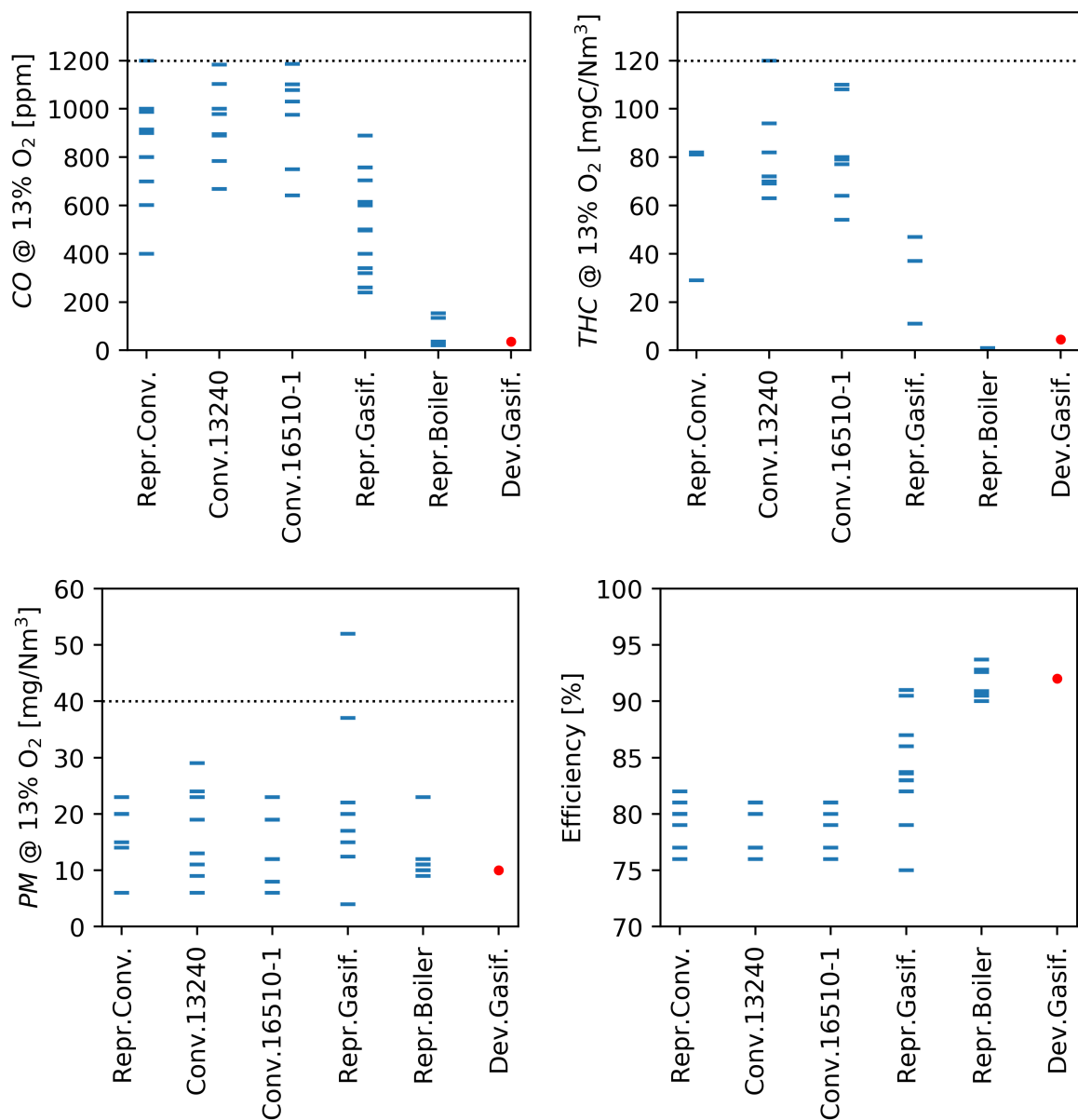


Figure 7.2: Comparison of PIC emission data and efficiency values between the developed gasification stove and other stoves and boilers

due to increased air flow through the channels and thus a decreased air flow through pores in the compact parts of the char bed, decreased  $CO_2$  and decreased flame temperatures. On the other hand, if the char bed is frequently being packed through char decomposition and firewood movement, even under decreased pyrolysis rates at the end of a charge cycle, air, not being consumed by the flame in the primary chamber, is then consumed through char oxidation by passing through numerous pores of a packed char bed, and  $CO_2$  levels stay sufficiently high until the end of the charge cycle.

### 7.1.6 Limitations of the reviewed scientific articles

As stated in section 2.5, most peer-reviewed scientific articles do not report either the used industrial standard for conducting the experiments (if any), or the exact step-by-step method they use. Moreover, most reported PIC emission levels do not satisfy the Ecodesign limits. As such, any comparison of PIC emission data between different articles or between articles and technical brochures of commercial stoves is not objective. Hence, the information supplied in most scientific articles cannot be used as a benchmark for development of a commercial stove.

On the other hand, PIC emission data, reported in the technical brochures for corresponding commercial stoves, did come from certification tests conducted in accordance with the adequate industrial standards (mostly EN 13240) and are within Ecodesign limits. Hence, all quantitative comparisons between the developed gasification stove and other wood burning devices are done with emission data from the technical brochures, rather than from scientific articles.

### 7.1.7 Downsides of BS EN 16510-1, or similar, standard

In the author's opinion there are two main downsides to the BS EN 16510-1 standard: i) *The disparity in PIC emission levels between the certification tests and real world usage*, and ii) *The standard motivates manufacturers to design stoves with compromised performance robustness*.

#### 7.1.7.1 Disparity between certification tests and real world stove usage

Research has shown that PIC emission levels produced in the certification tests largely underestimate the emission levels from real life, i.e. from stoves installed in users' homes and operated by them [94, 95, 96, 97]. Such disparity in emission levels probably arises due to two main factors: *the amount of firewood per batch* and *sub-optimal positioning of air controls (air valves)*. The objective of a stove user is often to prolong the unattended time with the stove, i.e. to prolong the time between refuelling. This is often done by a simultaneous increase in the firewood refuelling weight and decrease of openings in the air controls, in order to maintain the required heat output. However, such management of the burning process very often results in highly elevated PIC emission levels. The elevated PIC sources can be:

- **Smoldering of fresh firewood.** This can arise due to restricted air inflow rate at the beginning of a charge cycle and, thus, poor ignition conditions for fresh firewood.
- **High temporal variation in pyrolysis rates.** Once ignited, a high amount of firewood per charge cycle can result in either
  - severe initial pyrolysis rates and, thus, a highly polluting oxygen deficient regime - due to elevated air inflow rate into the char layer, or
  - a prolonged charring regime, with decreased  $CO_2$  levels, and elevated  $CO$  and  $THC$  - due to the decreased air inflow rate.

In the case of the developed gasification stove, the aforementioned disparity between the laboratory tests and real world PIC data is yet to be assessed. However, the author's expectation is that the disparity should be lower, due to following reasons:

- The developed gasification stove does not feature adjustable air controls
- The primary chamber is designed in such way that it is physically impossible to excessively fill the stove with firewood due to the reduced depth of the chamber. Any attempt in overfilling the chamber with firewood would result in wood logs falling over the log retainer.

In addition to aforementioned sources of disparity, an additional great source of pollution is the burning of the ignition batch (due to cold start conditions), which is not accounted for by current certification tests. Adequate lighting methods for wood stoves have been and still are being researched by e.g. Nussbaumer et al [98] and others.

The issue of the described disparity between the certification tests and real world tests is being addressed by Reichert and Schmidl in their research [99].

#### 7.1.7.2 Compromised robustness of stove's performance

Performance robustness refers to how sensitive the PIC emission levels are, especially  $PM$ , to variations in stove operation. Variations accounted for are different orientation or amount of firewood per batch, or different openings of the air controls.

The BS EN 16510-1 standard does not require testing of a stove under the regime of reduced heat output by adjusting the air controls, like the Norwegian standard NS 3058

or Defra - AEA<sup>8</sup> do. By limiting PIC emissions under the reduced air inflow regime, the testing procedure becomes more representative of the real world operation of wood stoves. However, in both cases (NS 3058 and Defra - AEA standards) the only pollutant being measured is PM, without CO or THC. This might be the case because these two standards concentrate on optimising only *PM* emission levels.

If a priority is given to reducing the *PM* levels, over the *CO* and *THC* levels, as in the Norwegian standard, the optimisation process becomes single-objective. In the case of conventional stoves, when considering the graph in Figure 6.6,  $CO_{2,max}$  is the only regressor, meaning that reducing *PM* can be mostly achieved by limiting the maximum value of  $CO_2$  for a given charge in a specific stove. This can be achieved by increasing the flow rate of air through secondary air holes (shown in Figure 5.1 (a)). However, increasing the secondary air flow rate will necessarily increase the average air excess ratio and, thus, lower the average  $CO_2$ . Increased air excess ratio will then negatively affect *CO* and *THC* during the charring regime (left part of a 'U'-curve in *CO-CO<sub>2</sub>* and *THC-CO<sub>2</sub>* graphs in Figures 6.1 and 6.2). However, given the hierarchy of optimisation priorities (which favour dealing with the initial PM spike over any negative consequences of the charring regime on *CO* or *THC*) this may still be advantageous. An example of such PM versus gaseous PIC trade-off is evident from PIC emission values of a conventional stove e (presented in section 6.2), which featured on average lowest values of maximum  $CO_2$  within an individual charge cycle. When averaging according to the EN 16510-1 standard, PIC emission levels normalised to 13% O<sub>2</sub> were:  $PM = 6 \text{ mg/Nm}^3$ ,  $CO = 976 \text{ ppm}$  and  $THC = 77 \text{ mg/Nm}^3$ . By comparing these values to the PIC values of other stoves on the market (shown in Figure 7.2 and in Tables 2.3, 2.4 and 2.5) it can be seen that in terms of *PM* emission, stove e is superior to the vast majority of other stoves, while in terms of *CO* and *THC*, stove e is within the average, or slightly inferior, of other stoves.

To summarise, by having a single optimisation objective, that is minimisation of *PM* alone - which corresponds to the NS 3058 testing procedure - a stove can be robustly designed in such way that it is less likely that an average stove user operates the stove in an oxygen deficient regime, i.e. in a regime where all PIC emission levels can be very high; *PM* can be at least several times higher compared to the charring regime. The cost of designing such a stove with an increased secondary air flow rate is elevated *CO* and *THC* during the charring regime, *PM* not as much.

Therefore, one could question whether measuring and limiting different pollutant gases by an industrial standard really ensures lower pollutant emission levels emitted by an

---

<sup>8</sup>The Agricultural Engineers Association

average stove installed in households and operated by an average user. It is to be noted that such an argument is based on several premises: i) a stove is of conventional type (single chamber and up draft), ii) a stove has air controls, iii) an average user is able to excessively overfill the stove with firewood, iv) a stove does not feature any kind of automated air valve system.



# Chapter 8

## Conclusions & Recommendations

The aim of this engineering doctorate project was to minimise pollutant emissions from residential wood log burning stoves by numerical and experimental methods. The goal was to surpass the EU Ecodesign limits on pollutant emission levels and, if possible, to surpass the emission levels of stoves presently on the market. Numerical methods were reviewed and evaluated in earlier project reports. The conclusion was that a development of a low polluting commercial wood stove by using numerical methods, CFD in particular, as a main methodology is not feasible, mainly due to the large amount of physical and chemical phenomena needed to be accounted for by the numerical model. The main methodology in this thesis was conducting physical experiments on wood stoves.

The proximate objectives towards achieving the aim of the thesis were i) to produce a literature review of scientific and industrial state-of-the-art in wood stove technology, ii) to identify the appropriate industrial standards for building and testing the stove - and as a by-product to derive and define formulae for analysis of the test results, iii) to manufacture a proof-of-concept prototype(s), iv) to identify important factors that influence the performance of the stove prototype, v) to conduct a statistically designed experiment with previously identified factors and corresponding levels, and vi) to analyse, compare and discuss the experimental data.

Two different routes towards the stove's performance optimisation were explored: i) optimisation of a conventional (single chamber, up draft) stove, and ii) design development and optimisation of a gasification stove (dual chamber, down draft). The latter route was confirmed by both the literature and experimental data comparisons within this thesis to be superior and with a greater possible design space. Hence the majority of the work was devoted to the gasification stove design development and optimisation.

The following three lists summarise the project conclusions, recommendations and future publications, respectively.

### *Conclusions*

- The formulae defined by the BS EN 16510-1:2018 standard were derived in this thesis. To the author's knowledge this is the first instance that these derivations have been presented in a single source.
- The data and information presented in the peer-reviewed scientific articles cannot be used as benchmark for the development of a commercial wood stove. This is because: i) articles rarely state the industrial standards used for testing and calculations, and ii) pollutant emission values very often exceed current Ecodesign limits.
- It was concluded from both the literature and in-house testing that natural draft gasification stoves are superior to conventional stoves in terms of pollutant emission values.
- Conventional stoves feature two possible regimes of elevated pollutant emission levels: *oxygen deficient regime* and *charring regime*. While the oxygen deficient regime can be avoided by ensuring adequate air inflow rates in adequate places at adequate times within the combustion chamber, the charring regime is inherently present in conventional stoves.
- Particulate matter emission levels from different conventional stove geometries can be low (2 to 15 mg/Nm<sup>3</sup> @ 13% O<sub>2</sub>) if the maximum value of CO<sub>2</sub><sup>1</sup> is kept below 12%.
- The geometry of the combustion chamber in a conventional stove significantly affects CO, THC and PM emission levels at increased maximum CO<sub>2</sub> values (e.g. more than 14%). It was found that slimmer<sup>2</sup> stoves generate less pollutants at decreased oxygen levels.
- Conventional stoves with bigger combustion chambers feature lower maximum values of CO<sub>2</sub>, than conventional stoves with small combustion chamber volumes.
- Gasification stoves with cylindrical secondary combustion chamber and tangential entrainment of syngas-air mixture were tested as preliminary prototypes. Such

---

<sup>1</sup>High CO<sub>2</sub> value corresponds to low O<sub>2</sub> value

<sup>2</sup>Slimness was quantified by the quotient of the mean height and base surface area of the combustion chamber.

particular design resulted in failed glass on secondary chamber door. Hence its was not considered for further development.

- Gasification stoves also feature two possible regimes of elevated pollutant emission levels: *oxygen deficient regime* and *char bed channeling regime*. In this case both regimes can be avoided or, at least, minimised. The oxygen deficient regime can be avoided by ensuring that  $CO_2$  does not increase beyond the effective mixing limit of a nozzle. Moreover, this limit can be offset to higher  $CO_2$  values. The char bed channeling regime can be minimised through the specific design of a primary chamber.
- There are several significant features of gasification stoves that differ from conventional ones: primary chamber sooting regime, blow-back, char bed channeling, instability of secondary flame ignition, and the potential for leakage of air and, more importantly, of fuel rich pyrolytic gases into the otherwise clean flue gas stream.
- Nozzle cover type and, probably, the entire nozzle geometry, significantly influence the stability of the secondary flame. It was observed that the time period for successful secondary flame ignition (counting from initial lighting firewood batch), depending on nozzle cover type, ranges from 15 to more than 45 minutes.
- There is a limit on effective mixing in a gasification stove which depends largely on the nozzle design. It can be quantified through  $CO_2$  volume fraction and was observed to be around  $CO_2 = 15\%$ . Beyond this value the pollutant emission levels increase at a progressive rate to above the pollutant emission levels of a conventional stoves, at the same  $CO_2$ .
- Statistical analysis on the gasification stoves' test data, filtered to capture only char bed channel effects, produced regression models in which the surface area of the primary chamber base and type of nozzle were the most significant and influential factors.
- Statistical analysis on the gasification stoves' test data, filtered to capture only the oxygen deficient regime, did not produce any significant regression model.
- Statistical analysis on the unfiltered gasification stoves' test data produced a statistically significant model for predicting particulate matter emission levels. Secondary window glass area was the only significant factor, but this was not as influential as those factors mentioned above in their respective models.
- An optimum gasification stove configuration, tested according to the BS EN 16510-1:2018 standard, exhibits the following performance data:  $CO = 36.1$  vol ppm,

$THC = 4.58 \text{ mgC/Nm}^3$ , efficiency = 92% and heat output = 6.4 kW. Considering these values, it is believed that this stove, in terms of pollutant emission levels and efficiency, surpasses all other wood stoves present on the market to date. Considering  $PM$ , the tested configuration featured  $PM = 10.02 \text{ mg/Nm}^3$ , whereas the  $PM$  range from all tested gasification stove variants was  $PM = 5.62$  to  $12.06 \text{ mg/Nm}^3$ . Therefore, the  $PM$  emission levels are comparable to the extant conventional and gasification stoves. Taking into account this information, it can be stated that the overall aim of this thesis has been achieved.

### *Recommendations & Future Research*

- Statistical design of experiments methodology can be used for future optimisation of a conventional stove design.
- Secondary flame ignition stability and effective mixing limits both depend on a nozzle design. Hence further research into better nozzle geometries is needed.
- Further research into new and innovative flap mechanism designs or, possibly, into a different overall combustion system design, is needed in order to minimise the leakage of pollutant gases from the primary chamber into the flue way.
- Further optimisation of the gasification stove design is possible through a *response surface method* and a central composite factorial design.

### *Future Publications*

Several research papers are in preparation for publication:

- Analysis of dependance of gaseous PIC and PM emissions on  $CO_{2,max}$  and geometry features of a conventional stove
- Quantification of importance of design factors of developed gasification stove designs through the statistical Design of Experiments methodology
- Comparative study of pollutant emission levels from conventional and gasification natural draft stove designs

The journals to which the papers will be submitted include options, such as *Applied Energy*, *Applied Thermal Engineering*, *Fuel Processing Technology*, or similar.

## Acknowledgements

The author would like to acknowledge

- the EPSRC Centre for Doctoral Training in Sustainable Materials and Manufacturing (EP/L016389/1) and Hunter Stoves Limited for funding this research and
- the Danish Technological Institute for providing the test data of the seven conventional wood stoves.

# Bibliography

- [1] “Emissions of air pollutants in the UK – Particulate matter (PM10 and PM2.5).” <https://www.gov.uk/government/statistics/emissions-of-air-pollutants/emissions-of-air-pollutants-in-the-uk-particulate-matter-pm10-and-pm25>.
- [2] M. Wöhler, J. S. Andersen, G. Becker, H. Persson, G. Reichert, C. Schön, C. Schmidl, D. Jaeger, and S. K. Pelz, “Investigation of real life operation of biomass room heating appliances - Results of a European survey,” *Applied Energy*, vol. 169, pp. 240–249, 5 2016.
- [3] J. D. Mcdonald, B. Zielinska, E. M. Fujita, J. C. Sagebiel, J. C. Chow, and J. G. Watson, “Fine particle and gaseous emission rates from residential wood combustion,” *Environmental Science and Technology*, vol. 34, pp. 2080–2091, 6 2000.
- [4] C. Fountoukis, T. Butler, M. G. Lawrence, H. A. Denier van der Gon, A. J. Visschedijk, P. Charalampidis, C. Pilinis, and S. N. Pandis, “Impacts of controlling biomass burning emissions on wintertime carbonaceous aerosol in Europe,” *Atmospheric Environment*, vol. 87, pp. 175–182, 4 2014.
- [5] “Commission Regulation (EU) 2015/1185 of 24 April 2015 implementing Directive 2009/125/EC of the European Parliament and of the Council with regard to ecodesign requirements for solid fuel local space heaters.” <https://eur-lex.europa.eu/legal-content/EN/TXT/?uri=CELEX%3A02015R1185-20170109>, last accessed on 01/03/2021.
- [6] “BS EN 16510-1 Explained.” <https://www.hetas.co.uk/bsen16510-1-explained/>, last accessed on 01/03/2021.
- [7] “SIA. Ecodesign legislation & implications..” <https://stoveindustryalliance.com/sia-ecodesign-ready-appliances/ecodesign-legislation-implications/>.
- [8] “Bonfire. Eco Design Stoves 2022..” <https://bonfire.co.uk/eco-design-2022/>.

- [9] “Commission regulation (EU) 2015/1185 of 24 April 2015 implementing Directive 2009/125/EC of the European Parliament and of the Council with regard to ecodesign requirements for solid fuel local heaters,” *Official Journal of the European Union*, 2015.
- [10] P. Basu, “Chapter 1 - Introduction,” in *Biomass Gasification and Pyrolysis* (P. Basu, ed.), pp. 1–25, Boston: Academic Press, 2010.
- [11] A. Azenic, “Review of Theoretical Fundamentals and Numerical Models of Wood Combustion in Residential Stoves - 1st EngD Portfolio Submission,” 2019.
- [12] A. Azenic, “Collaborative Project between University of Exeter, Hunter Stoves Ltd and Bioenergy 2020+ GmbH - 2nd EngD Portfolio Submission,” 2019.
- [13] E. J. S. Mitchell, *Emissions from Residential Solid Fuel Combustion and Implications for Air Quality and Climate Change*. PhD thesis, University of Leeds, 2017.
- [14] “BS EN 13284-1:2017 - Stationary source emissions. Determination of low range mass concentration of dust. Manual gravimetric method.”
- [15] J. Warnatz, U. Maas, and R. W. Dibble, *Combustion. Physical and Chemical Fundamentals, Modeling and Simulation, Experiments, Pollutant Formation*. 2006.
- [16] “BS EN 12619:2013 - Stationary source emissions. Determination of the mass concentration of total gaseous organic carbon. Continuous flame ionisation detector method.”
- [17] H. Lamberg, O. Sippula, J. Tissari, A. Virén, T. Kaivosoja, A. Aarinen, V. Salminen, and J. Jokiniemi, “Operation and Emissions of a Hybrid Stove Fueled by Pellets and Log Wood,” *Energy and Fuels*, vol. 31, no. 2, pp. 1961–1968, 2017.
- [18] E. Pettersson, C. Boman, R. Westerholm, D. Boström, and A. Nordin, “Stove performance and emission characteristics in residential wood log and pellet combustion, part 2: Wood stove,” *Energy and Fuels*, vol. 25, no. 1, pp. 315–323, 2011.
- [19] A. I. Calvo, L. A. Tarelho, C. A. Alves, M. Duarte, and T. Nunes, “Characterization of operating conditions of two residential wood combustion appliances,” *Fuel Processing Technology*, vol. 126, pp. 222–232, 2014.
- [20] T. Brunner, I. Obernberger, and R. Scharler, “Primary measures for low-emission residential wood combustion - comparison of old with optimised modern systems,” *Proceedings of the 17th European Biomass Conference & Exhibition*, no. July 2009, pp. 1319–1328, 2009.

- [21] R. Trojanowski and V. Fthenakis, "Nanoparticle emissions from residential wood combustion: A critical literature review, characterization, and recommendations," *Renewable and Sustainable Energy Reviews*, vol. 103, no. December 2018, pp. 515–528, 2019.
- [22] M. Olsson and J. Kjällstrand, "Low emissions from wood burning in an ecolabelled residential boiler," *Atmospheric Environment*, vol. 40, no. 6, pp. 1148–1158, 2006.
- [23] K. L. Bignal, S. Langridge, and J. L. Zhou, "Release of polycyclic aromatic hydrocarbons, carbon monoxide and particulate matter from biomass combustion in a wood-fired boiler under varying boiler conditions," *Atmospheric Environment*, vol. 42, no. 39, pp. 8863–8871, 2008.
- [24] F. Cereceda-Balic, M. Toledo, V. Vidal, F. Guerrero, L. A. Diaz-Robles, X. Petit-Breuilh, and M. Lapuerta, "Emission factors for PM<sub>2.5</sub>, CO, CO<sub>2</sub>, NO<sub>x</sub>, SO<sub>2</sub> and particle size distributions from the combustion of wood species using a new controlled combustion chamber 3CE," *Science of the Total Environment*, vol. 584-585, pp. 901–910, 4 2017.
- [25] G. Shen, M. Xue, S. Wei, Y. Chen, Q. Zhao, B. Li, H. Wu, and S. Tao, "Influence of fuel moisture, charge size, feeding rate and air ventilation conditions on the emissions of PM, OC, EC, parent PAHs, and their derivatives from residential wood combustion," *Journal of Environmental Sciences (China)*, vol. 25, pp. 1808–1816, 9 2013.
- [26] E. J. Mitchell, A. R. Lea-Langton, J. M. Jones, A. Williams, P. Layden, and R. Johnson, "The impact of fuel properties on the emissions from the combustion of biomass and other solid fuels in a fixed bed domestic stove," *Fuel Processing Technology*, vol. 142, pp. 115–123, 2 2016.
- [27] K. Krpec, J. Horák, V. Laciok, F. Hopan, P. Kubesa, H. Lamberg, J. Jokiniemi, and Š. Tomšejová, "Impact of Boiler Type, Heat Output, and Combusted Fuel on Emission Factors for Gaseous and Particulate Pollutants," *Energy and Fuels*, vol. 30, pp. 8448–8456, 10 2016.
- [28] L. S. Johansson, B. Leckner, L. Gustavsson, D. Cooper, C. Tullin, and A. Potter, "Emission characteristics of modern and old-type residential boilers fired with wood logs and wood pellets," *Atmospheric Environment*, vol. 38, no. 25, pp. 4183–4195, 2004.
- [29] I. Obernberger, T. Brunner, and G. Barnthaler, "Fine particulate emissions from modern austrian small-scale biomass combustion plants," in *15th European*



- Biomass Conference & Exhibition, 7 - 11 May 2007, Berlin, Germany*, pp. 1546–1557, 2007.
- [30] M. Obaidullah, S. Bram, V. K. Verma, and J. De Ruyck, “A review on particle emissions from small scale biomass combustion,” *International Journal of Renewable Energy Research*, vol. 2, no. 1, pp. 147–159, 2012.
- [31] C. Boman, E. Pettersson, R. Westerholm, D. Boström, and A. Nordin, “Stove performance and emission characteristics in residential wood log and pellet combustion, part 1: Pellet stoves,” *Energy and Fuels*, vol. 25, no. 1, pp. 307–314, 2011.
- [32] C. Boman, E. Petterson, F. Lindmark, M. Ohman, A. Nordin, and R. Westerholm, “Emissions from small-scale combustion of biomass fuels - extensive quantification and characterization: Effects of Temperature and Residence Time on Emission Characteristics during Fixed-Bed Combustion of Conifer Stem-wood Pellets,” *Energy Technology and Thermal Process Chemistry, Umea University, Analytical Chemistry, Arrhenius Laboratory, Stockholm University*, 2005.
- [33] J. Tissari, *Fine Particle Emissions from Residential Wood Combustion, University of Kuopio*. PhD thesis, 2008.
- [34] “Choose a Catalytic Converter.” <https://whitebeam.net/products/choose-a-catalytic-converter/>.
- [35] G. Reichbert, C. Schmidl, W. Haslinger, H. Stressler, R. Sturmlechner, M. Schwabl, N. Kienzl, and C. Hochenauer, “Long term durability and safety aspects of oxidizing honeycomb catalysts integrated in firewood stoves,” *Biomass and Bioenergy*, no. 105, pp. 428–442, 2017.
- [36] A. Hukkanen, T. Kaivosoja, O. Sippula, K. Nuutinen, J. Jokiniemi, and J. Tissari, “Reduction of gaseous and particulate emissions from small-scale wood combustion with a catalytic combustor,” *Atmospheric Environment*, vol. 50, pp. 16–23, 2012.
- [37] “Blackthorn Environmental Ltd.” <https://www.blackthorn.net/>.
- [38] “Installation Manual: Contura C310, Contura C310G.” <https://www.contura.eu/en-gb/stove-collection/wood-burning-stoves/Contura-310--3668>.
- [39] “Installation Manual: Contura C510.” <https://www.contura.eu/en-gb/stove-collection/wood-burning-stoves/Contura-510-Style--3732>.
- [40] “Installation Manual: Contura C510.” <https://www.contura.eu/en-gb/stove-collection/wood-burning-stoves/Contura-810-Style--4900>.

- [41] “Installation Manual: Rais 600 MAX, Rais 600 MAX/E.” <https://www.rais.com/en/wood-burning-stoves/600-max>.
- [42] “Installation Manual: Rais Q-Tee, Rais Q-Tee C.” <https://www.rais.com/en/wood-burning-stoves/rais-q-tee-new>.
- [43] “Installation Manual: Rais Viva L series.” <https://www.rais.com/en/wood-burning-stoves/rais-viva-l-120>.
- [44] “Scan 41-1.” <https://www.scan-stoves.co.uk/products/wood-stoves/scan-41-1>.
- [45] “Scan 41-2.” <https://www.scan-stoves.co.uk/products/wood-stoves/scan-41-2>.
- [46] “UK - Assembly and instructions manual: Scan 83.” <https://www.scan-stoves.co.uk/products/wood-stoves/scan-83-4-maxi>.
- [47] “Scan 68-14.” <https://www.scan-stoves.co.uk/products/wood-stoves/scan-68-14>.
- [48] “User manual: Rais Bionic Fire.” <https://www.rais.com/en/wood-burning-stoves/rais-bionic-fire>.
- [49] “Explanation of the performance 5kW [PDF].” <https://www.xeoes.de/en/technology.html>.
- [50] “Explanation of the performance 8kW [PDF].” <https://www.xeoes.de/en/technology.html>.
- [51] “Brochure; Walltherm AIR, pp. 11.” <https://www.wallnoefer.it/en/products/wallthermr-wood-stoves/air-woodstove.html>.
- [52] “Walltherm Vajolet Manual, pp.18.” <https://www.manualslib.com/manual/1824098/Wallnoefer-Walltherm-Vajolet.html?page=18#manual>.
- [53] “Pyro Nemo 6 kW.” <https://www.ls-stoves.com/p/pyrolytic-glowing-stove-pyro-nemo-6-kw>.
- [54] “Pyro Nemo 9 kW.” <https://www.ls-stoves.com/p/pyrolytic-glowing-stove-pyro-nemo-9-kw>.
- [55] “Pyro Nemo 12 kW.” <https://www.ls-stoves.com/p/pyrolytic-glowing-stove-pyro-nemo-12-kw>.

- [56] “Pyro Magic 6 kW.” <https://www.ls-stoves.com/p/pyrolytic-glowing-stove-pyro-magic-6-kww>.
- [57] “Pyro Magic 10 kW.” <https://www.ls-stoves.com/p/pyrolytic-glowing-stove-pyro-magic-10-kww>.
- [58] “Pyro Magic 14 kW.” <https://www.ls-stoves.com/p/pyrolytic-glowing-stove-pyro-magic-14-kww>.
- [59] “Oranier Hektos Aqua II, User Manual, pp. 9.” <https://oranier.com/en/heating/products/wood-stoves/wood-stoves-with-boiler-function/wood-gasification-stove-hektos-aqua/>.
- [60] “LUUMA Luvano Touch.” <https://www.tegernsee-solar.de/ofenshop-wasserfuehrende-holzoefen-kaminoefen-holzvergaser-kaminofen-luuma-luvano.html>.
- [61] “Pertinger 100 Reverse Flame, Technical Data Sheet.” <https://www.pertinger.com/en/heating-stoves/heating-stoves-reverse-flame/19-7.html>.
- [62] “Jayline UL200, Specifications.” [https://www.jayline.co.nz/wp-content/uploads/2016/12/Jayline-UL200\\_spec-sheet\\_Sep18.pdf](https://www.jayline.co.nz/wp-content/uploads/2016/12/Jayline-UL200_spec-sheet_Sep18.pdf).
- [63] British Standards Institution, “BS EN 16510-1:2018 - Residential solid fuel burning appliances. Part 1. General requirements and test methods,” 2018.
- [64] “Brochure: Hargassner Wood Log Boiler.” <https://www.hargassner.at/en/wood-log/neo-hv-carburetor-boiler.html>.
- [65] “Certifications BioX Download, Solarbayer.” <https://www.solarbayer.com/Wood-boiler-BioX.html>.
- [66] Y. A. Cengel, M. A. Boles, and M. Kanoglu, *Thermodynamics: An Engineering Approach*. McGraw-Hill Education, 9 ed., 2019.
- [67] “3.6: Thermochemistry - Chemistry LibreTexts.”
- [68] “Wood as Fuel. A Guide to Choosing and Drying Logs. Biomass Energy Centre. Forestry Commission England.” [https://www.forestresearch.gov.uk/documents/1959/FR\\_BEC\\_Wood\\_as\\_Fuel\\_2012.pdf](https://www.forestresearch.gov.uk/documents/1959/FR_BEC_Wood_as_Fuel_2012.pdf).
- [69] British Standards Institution, “BS EN 16510-2-1:2013: Residential solid fuel burning appliances. Part 2-1 Roomheater,” 2013.
- [70] “Danish Technological Institute.” <https://www.dti.dk/>.

- [71] “Advanced Optima Continuous Gas Analyzers.” <https://library.e.abb.com/public/db3096bae2566231c1257b0c005468b9/10-24-120-01-EN.pdf>.
- [72] “Keysight 34970A.” <https://www.keysight.com/gb/en/product/34970A/34970a-data-acquisition-control-mainframe-modules.html>.
- [73] “Plane filter device.” [https://www.paulgothe.com/epages/62307369.sf/en\\_GB/?ObjectPath=/Shops/62307369/Products/7.2](https://www.paulgothe.com/epages/62307369.sf/en_GB/?ObjectPath=/Shops/62307369/Products/7.2).
- [74] “Glasfaser Planfilter ET/MG 160.” <https://www.paulgothe.com/Planfilter-aus-Glasfasern>.
- [75] “Small filter device heater.” [https://www.paulgothe.com/epages/62307369.sf/en\\_GB/?ObjectPath=/Shops/62307369/Products/35.03](https://www.paulgothe.com/epages/62307369.sf/en_GB/?ObjectPath=/Shops/62307369/Products/35.03).
- [76] “Complete equipment for volume measurement.” [https://www.paulgothe.com/epages/62307369.sf/en\\_GB/?ObjectPath=/Shops/62307369/Products/22.0K-1](https://www.paulgothe.com/epages/62307369.sf/en_GB/?ObjectPath=/Shops/62307369/Products/22.0K-1).
- [77] “Hand-pressure instrument HMG B.” <https://www.paulgothe.com/Hand-pressure-instrument-HMG-B>.
- [78] “Hand-pressure instrument HMG 03.” <https://www.paulgothe.com/Hand-pressure-instrument-HMG-03>.
- [79] “Ohaus Defender 3000.” <https://us.ohaus.com/en-US/Defender3000>.
- [80] “Adoner 300.” [https://www.amazon.co.uk/gp/product/B082FG3ZYM/ref=ox\\_sc\\_saved\\_title\\_3?smid=A386Z5J71EAFY&psc=1](https://www.amazon.co.uk/gp/product/B082FG3ZYM/ref=ox_sc_saved_title_3?smid=A386Z5J71EAFY&psc=1).
- [81] D. C. Montgomery, *Design and Analysis of Experiments, International Student Version*. John Wiley, 8 ed., 2013.
- [82] “Down-draft wood log gasification appliance.” <http://www.williamsrenewables.co.uk/biomass/log-boilers/>.
- [83] “Side-draft wood log gasification appliance.” <https://www.edergruppe.at/en/eder-produkte/scheitholzessel-biovent-slc/>.
- [84] “Rais | Stoves & Inserts.” <http://www.rais.com/en/>.
- [85] “BIONIC FIRE | Moog Kaminstudio | Kamine, Öfen und Zubehör in Paderborn und Umgebung.” <http://www.moog-kaminstudio.de/bionic-fire>.
- [86] “Wittus - Fire by Design.” <http://www.wittus.com/>.

- [87] “Twinfire Solo - Azure Magazine.” <http://www.azuremagazine.com/product-guide/twinfire-solo/>.
- [88] “Wallnoefer - solar thermal collectors and Walltherm® stove.” <http://www.wallnoefer.it/en.html>.
- [89] “Eco2all Walltherm Vajolet CV-houtvergasserkachel - Product in beeld - Startpagina voor haarden en kachels ideeën | UW-haard.nl.” <https://www.uw-haard.nl/product-eco2all-walltherm-vajolet-cv-houtvergasserkachel/>.
- [90] “Polar Furnace G Class Models.” <https://www.polarfurnace.com/products/gclass>.
- [91] “Wood gasification boiler firestar 18-40.” [https://www.herz-energie.at/en/products/boiler-for-log-wood/herz-firestar-gasification-boiler-18-40/?noredirect=en\\_US](https://www.herz-energie.at/en/products/boiler-for-log-wood/herz-firestar-gasification-boiler-18-40/?noredirect=en_US).
- [92] A. Azenic, “Introduction to Selected Principles and Technologies for Combustion of Wood,” 2019.
- [93] T. Nussbaumer, “Combustion and Co-combustion of Biomass: Fundamentals, Technologies, and Primary Measures for Emission Reduction,” *Energy and Fuels*, vol. 17, pp. 1510–1521, 11 2003.
- [94] “Pollution from residential burning. Danish experience in an international perspective..” <https://www.clean-heat.eu/en/actions/info-material/download/danish-case-study-uk-11.html>.
- [95] Skreiberg, E. Karlsvik, J. E. Hustad, and O. K. Sønju, “Round robin test of a wood stove: The influence of standards, test procedures and calculation procedures on the emission level,” *Biomass and Bioenergy*, vol. 12, no. 6, pp. 439–452, 1997.
- [96] “Real-life emissions from residential wood burning appliances in New Zealand..” <http://citeseerx.ist.psu.edu/viewdoc/download?doi=10.1.1.615.2369&rep=rep1&type=pdf>.
- [97] “Long-term performance of EPA-Certified Phase 2 Woodstoves, Klamath Falls and Portland, Oregon: 1998/1999..” <https://www.omni-test.com/publications/Long-Term.pdf>.
- [98] T. Nussbaumer, A. Doberer, N. Klippel, R. Bühler, and W. Vock, “Influence of ignition and operation type on particle emissions from residential wood combustion,” in *16th European Biomass Conference and Exhibition*, pp. 2–6, Valencia Spain, 2008.

- [99] “G. Reichert and C. Schmidl. Advanced Test Methods for Firewood Stoves. Report on consequences of real-life operation on stove performance. IEA Bioenergy Task 32. Wieselburg, September 2018..” [https://www.ieabioenergy.com/wp-content/uploads/2018/11/IEA\\_Bioenergy\\_Task32\\_Test-Methods.pdf](https://www.ieabioenergy.com/wp-content/uploads/2018/11/IEA_Bioenergy_Task32_Test-Methods.pdf).

# Appendix A

## Results of Statistical Analyses

### A.1 Original Data Set - Data Set 1

#### A.1.1 Carbon Monoxide - Data Set 1

Table A.1: Effect estimates, aliases, regression coefficients and % contribution with  $CO$  as response variable in data set 1

| Source   | Alias      | Regression coefficient | Effect estimate | % contribution |
|----------|------------|------------------------|-----------------|----------------|
| A        | BCD        | 35.50                  | 71.0            | 9.4            |
| <b>B</b> | <b>ACD</b> | <b>110.50</b>          | <b>221.0</b>    | <b>29.3</b>    |
| <b>C</b> | <b>ABD</b> | <b>91.75</b>           | <b>183.5</b>    | <b>24.4</b>    |
| D        | ABC        | -63.25                 | -126.5          | 16.8           |
| AB       | CD         | -12.75                 | -25.5           | 3.4            |
| AC       | BD         | -23.00                 | -46.0           | 6.1            |
| AD       | BC         | 40.00                  | 80.0            | 10.6           |

Reduced model equation reads:

$$\widehat{CO}_{\text{data1}} = 287.25 + 110.5 \cdot B - 91.75 \cdot C \quad (\text{A.1})$$

Table A.2: ANOVA table with *CO* as response variable in data set 1

| Source   | Regression coefficient | Sum of Squares | DoF | F    | Pr(>F) |
|----------|------------------------|----------------|-----|------|--------|
| B        | 110.5                  | 97682.0        | 1   | 8.08 | 0.0361 |
| C        | -91.75                 | 67344.5        | 1   | 5.57 | 0.0647 |
| Residual |                        | 60419          | 5   |      |        |
| Totals   |                        | 225445.5       | 7   |      |        |

Table A.3: Regression model summary - *CO* - data set 1

| $R^2$ | Adjusted $R^2$ | F     | P(F)   | Mean of Response |
|-------|----------------|-------|--------|------------------|
| 0.732 | 0.625          | 6.828 | 0.0372 | 287.25           |

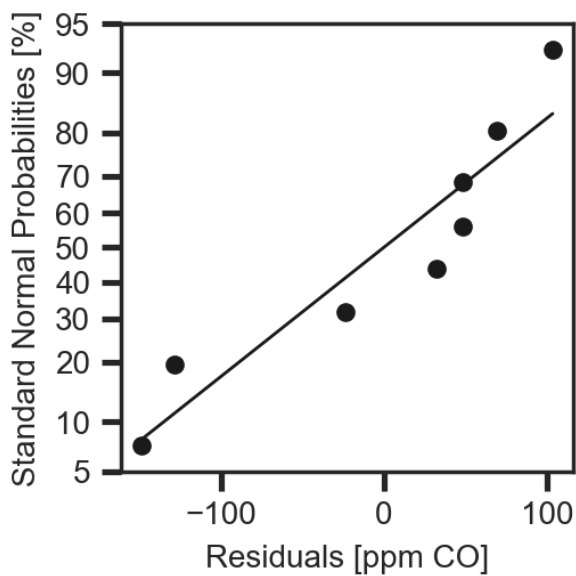


Figure A.1: Normal probability plot

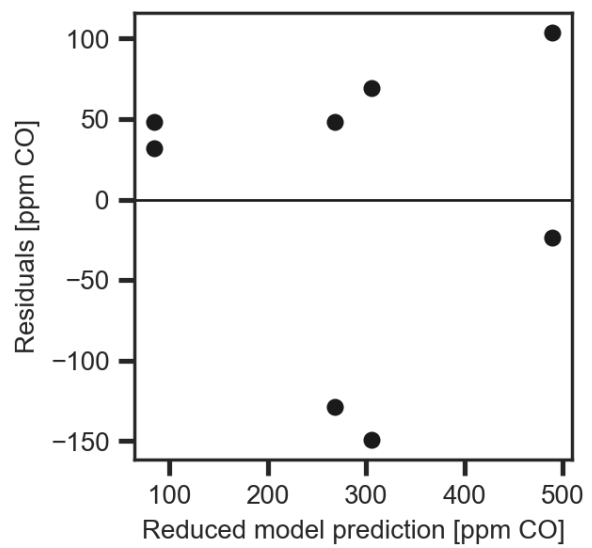


Figure A.2: Residual plot



### A.1.2 Particulate Matter - Data Set 1

Table A.4: Effect estimates, aliases, regression coefficients and % contribution with *PM* as response variable in data set 1

| Source    | Alias      | Regression coefficient | Effect estimate | % contribution |
|-----------|------------|------------------------|-----------------|----------------|
| A         | BCD        | 0.407                  | 0.81            | 9.2            |
| B         | ACD        | -0.023                 | -0.04           | 0.5            |
| <b>C</b>  | <b>ABD</b> | <b>1.207</b>           | <b>2.41</b>     | <b>27.4</b>    |
| <b>D</b>  | <b>ABC</b> | <b>-0.794</b>          | <b>-1.59</b>    | <b>18</b>      |
| AB        | CD         | -0.4                   | -0.8            | 9.1            |
| AC        | BD         | 0.177                  | 0.35            | 4              |
| <b>AD</b> | <b>BC</b>  | <b>1.398</b>           | <b>2.79</b>     | <b>31.7</b>    |

Table A.5: ANOVA table with *PM* as response variable in data set 1

| Source   | Regression coefficient | Sum of Squares | DoF | F     | Pr(>F) |
|----------|------------------------|----------------|-----|-------|--------|
| C        | 1.207                  | 11.66          | 1   | 16.33 | 0.0156 |
| D        | -0.794                 | 5.05           | 1   | 7.07  | 0.0564 |
| AD       | 1.398                  | 15.63          | 1   | 21.90 | 0.0094 |
| Residual |                        | 2.85           | 4   |       |        |
| Totals   |                        | 35.19          | 7   |       |        |

Table A.6: Regression model summary - *THC* - data set 1

| R <sup>2</sup> | Adjusted R <sup>2</sup> | F    | P(F)  | Mean of Response |
|----------------|-------------------------|------|-------|------------------|
| 0.919          | 0.858                   | 15.1 | 0.012 | 8.87             |

Reduced model equation reads:

$$\widehat{PM}_{\text{data1}} = 8.87 + 1.207 \cdot C - 0.794 \cdot D + 1.398 \cdot AD \quad (\text{A.2})$$

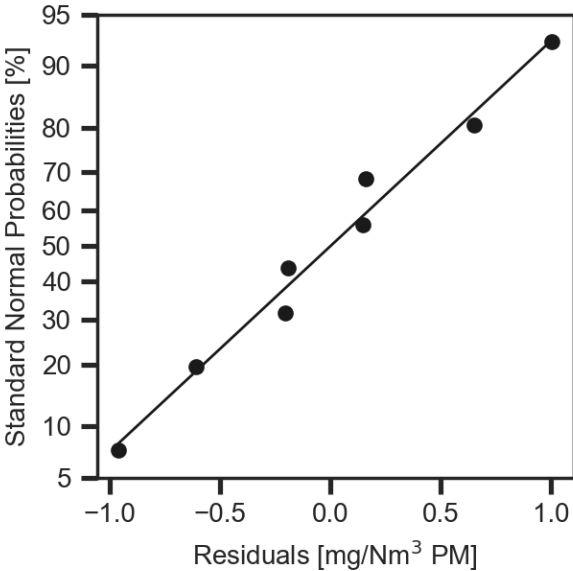


Figure A.3: Normal probability plot

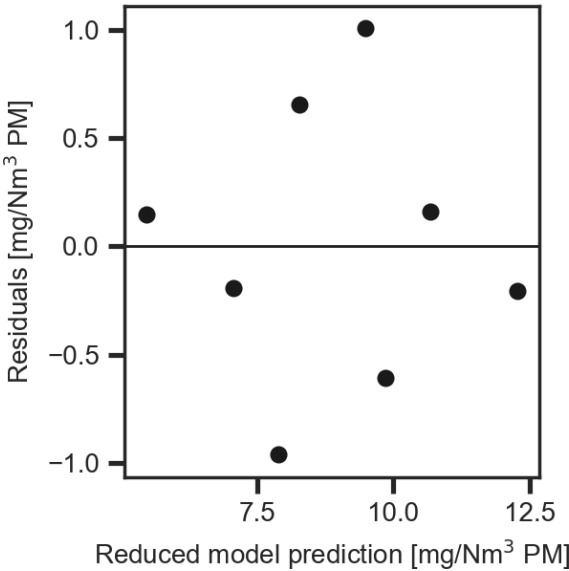


Figure A.4: Residual plot

## **A.2 Data from Initial 15 Minutes of Every Charge - Data Set 2**

From this data set neither *CO* nor *THC* analysis gave any significant results.

## A.3 Data Without Initial 15 Minutes of Every Charge - Data Set 3

### A.3.1 Carbon Monoxide - Data Set 3

Table A.7: Effect estimates, aliases, regression coefficients and % contribution with *CO* as response variable in data set 3

| Source   | Alias      | Regression coefficient | Effect estimate | % contribution |
|----------|------------|------------------------|-----------------|----------------|
| <b>A</b> | <b>BCD</b> | <b>121.5</b>           | <b>243</b>      | <b>32.5</b>    |
| <b>B</b> | <b>ACD</b> | <b>93.25</b>           | <b>186.5</b>    | <b>24.9</b>    |
| C        | ABD        | 39.75                  | 79.5            | 10.6           |
| D        | ABC        | 16.50                  | 33.0            | 4.4            |
| AB       | CD         | 54.50                  | 109.0           | 14.6           |
| AC       | BD         | 29.00                  | 58.0            | 7.8            |
| AD       | BC         | -19.25                 | -38.5           | 5.2            |

Table A.8: ANOVA table with *CO* as response variable in data set 3

| Source   | Regression coefficient | Sum of Squares | DoF | F         | Pr(>F) |
|----------|------------------------|----------------|-----|-----------|--------|
| A        | 121.5                  | 118098.0       | 1   | 12.232304 | 0.0173 |
| B        | 93.2500                | 69564.5        | 1   | 7.205322  | 0.0436 |
| Residual |                        | 48273.0        | 5   |           |        |
| Totals   |                        | 235935.5       | 7   |           |        |

Table A.9: Regression model summary - *CO* - data set 3

| $R^2$ | Adjusted $R^2$ | F     | P(F)   | Mean of Response |
|-------|----------------|-------|--------|------------------|
| 0.795 | 0.714          | 9.719 | 0.0189 | 249.75           |

Reduced model equation reads:

$$\widehat{CO}_{data3} = 249.75 + 121.5 \cdot A + 93.25 \cdot B \tag{A.3}$$

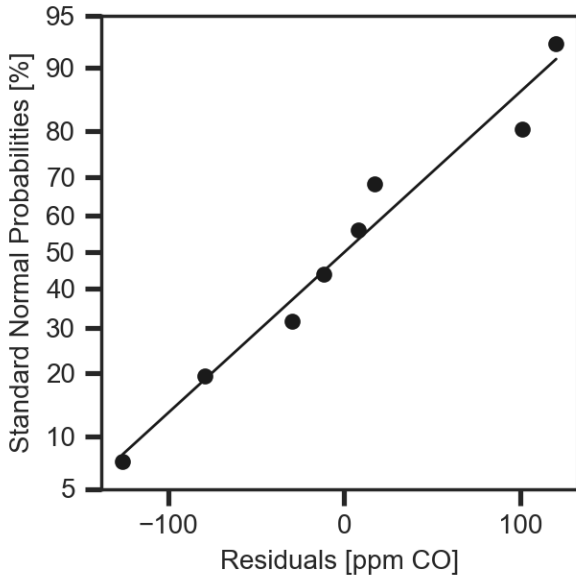


Figure A.5: Normal probability plot

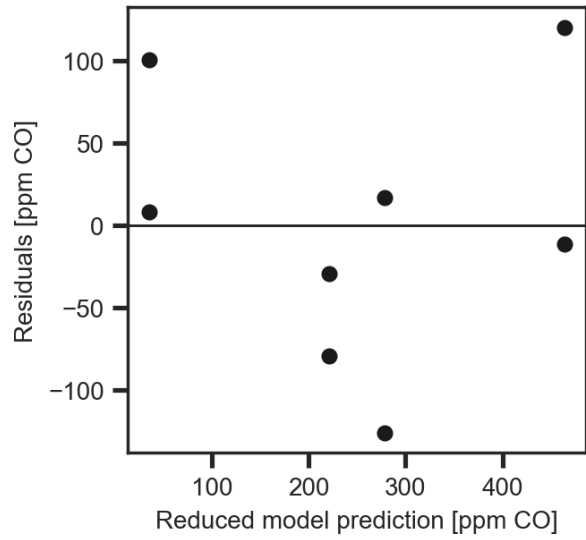


Figure A.6: Residual plot

### A.3.2 Total Hydrocarbons - Data Set 3

Table A.10: Effect estimates, aliases, regression coefficients and % contribution with *THC* as response variable in data set 3

| Source    | Alias      | Regression coefficient | Effect estimate | % contribution |
|-----------|------------|------------------------|-----------------|----------------|
| <b>A</b>  | <b>BCD</b> | <b>3.2275</b>          | <b>6.455</b>    | <b>43.6</b>    |
| <b>B</b>  | <b>ACD</b> | <b>1.7575</b>          | <b>3.515</b>    | <b>23.8</b>    |
| C         | ABD        | 0.2375                 | 0.475           | 3.2            |
| <b>D</b>  | <b>ABC</b> | <b>-0.6125</b>         | <b>-1.225</b>   | <b>8.3</b>     |
| <b>AB</b> | <b>CD</b>  | <b>1.3825</b>          | <b>2.765</b>    | <b>18.7</b>    |
| AC        | BD         | -0.0375                | -0.075          | 0.5            |
| AD        | BC         | 0.1425                 | 0.285           | 1.9            |

Table A.11: ANOVA table with *THC* as response variable in data set 3

| Source   | Regression coefficient | Sum of Squares | DoF | F          | Pr(>F) |
|----------|------------------------|----------------|-----|------------|--------|
| A        | 3.2275                 | 83.33405       | 1   | 400.035443 | 0.0003 |
| B        | 1.7575                 | 24.71045       | 1   | 118.619650 | 0.0017 |
| D        | -0.6125                | 3.00125        | 1   | 14.407153  | 0.0321 |
| AB       | 1.3825                 | 15.29045       | 1   | 73.400032  | 0.0033 |
| Residual |                        | 0.62495        | 3   |            |        |
| Totals   |                        | 126.96115      | 7   |            |        |

Table A.12: Regression model summary - *THC* - data set 3

| R <sup>2</sup> | Adjusted R <sup>2</sup> | F     | P(F)     | Mean of Response |
|----------------|-------------------------|-------|----------|------------------|
| 0.995          | 0.989                   | 151.6 | 0.000861 | 5.8725           |

Reduced model equation reads:

$$\widehat{THC}_{\text{data3}} = 5.8725 + 3.2275 \cdot A + 1.7575 \cdot B - 0.6125 \cdot D + 1.3825 \cdot AB \quad (\text{A.4})$$

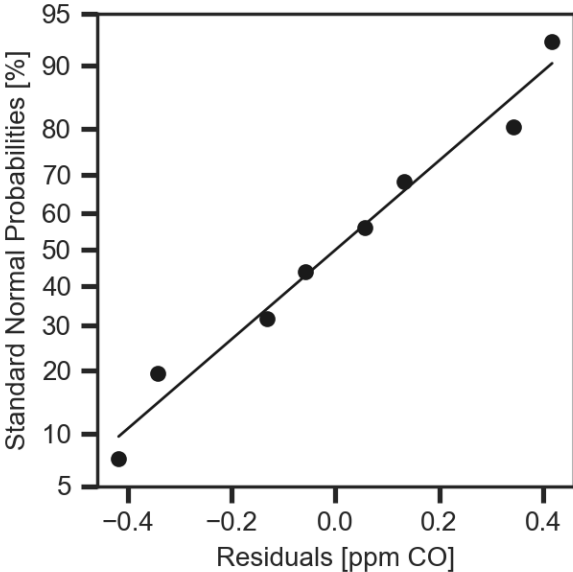


Figure A.7: Normal probability plot

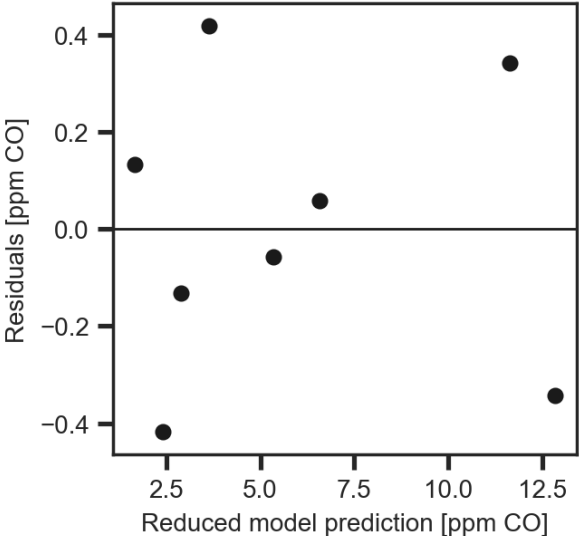


Figure A.8: Residual plot

## A.4 Data Without $CO_2 > 15\%$ - Data Set 4

### A.4.1 Carbon Monoxide - Data Set 4

Table A.13: Effect estimates, aliases, regression coefficients and % contribution with  $CO$  as response variable in data set 4

| Source    | Alias      | Regression coefficient | Effect estimate | % contribution |
|-----------|------------|------------------------|-----------------|----------------|
| <b>A</b>  | <b>BCD</b> | <b>85.125</b>          | <b>170.25</b>   | <b>32.9</b>    |
| <b>B</b>  | <b>ACD</b> | <b>79.875</b>          | <b>159.75</b>   | <b>30.9</b>    |
| <b>C</b>  | <b>ABD</b> | <b>47.875</b>          | <b>95.75</b>    | <b>18.5</b>    |
| D         | ABC        | -1.875                 | -3.75           | 0.7            |
| <b>AB</b> | <b>CD</b>  | <b>26.875</b>          | <b>53.75</b>    | <b>10.4</b>    |
| AC        | BD         | 11.875                 | 23.75           | 4.6            |
| AD        | BC         | -5.375                 | -10.75          | 2.1            |

Table A.14: ANOVA table with  $CO$  as response variable in data set 4

| Source   | Regression coefficient | Sum of Squares | DoF | F          | Pr(>F) |
|----------|------------------------|----------------|-----|------------|--------|
| A        | 85.125                 | 57970.125      | 1   | 125.352104 | 0.0015 |
| B        | 79.875                 | 51040.125      | 1   | 110.366970 | 0.0018 |
| C        | 47.875                 | 18336.125      | 1   | 39.649248  | 0.0081 |
| AB       | 26.875                 | 5778.125       | 1   | 12.494369  | 0.0385 |
| Residual |                        | 1387.375       | 3   |            |        |
| Totals   |                        | 134511         | 7   |            |        |

Reduced model equation reads:

$$\widehat{CO}_{\text{data4}} = 221.625 + 85.125 \cdot A + 79.875 \cdot B + 47.875 \cdot C + 26.875 \cdot AB \quad (\text{A.5})$$



Table A.15: Regression model summary - *CO* - data set 4

| $R^2$ | Adjusted $R^2$ | F     | P(F)    | Mean of Response |
|-------|----------------|-------|---------|------------------|
| 0.990 | 0.976          | 71.97 | 0.00260 | 221.625          |

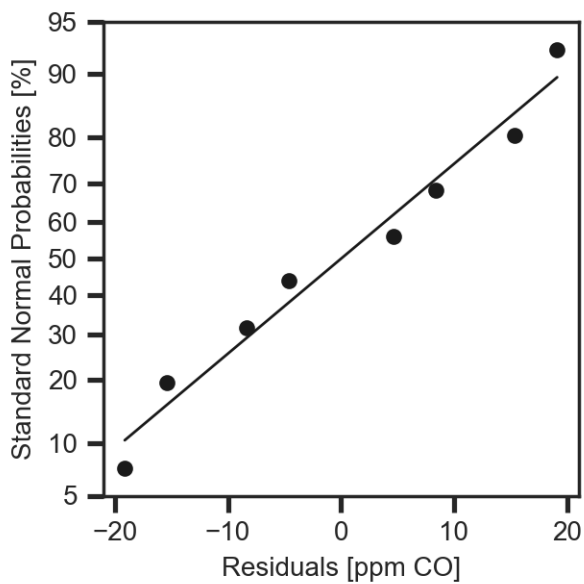


Figure A.9: Normal probability plot of the residuals.

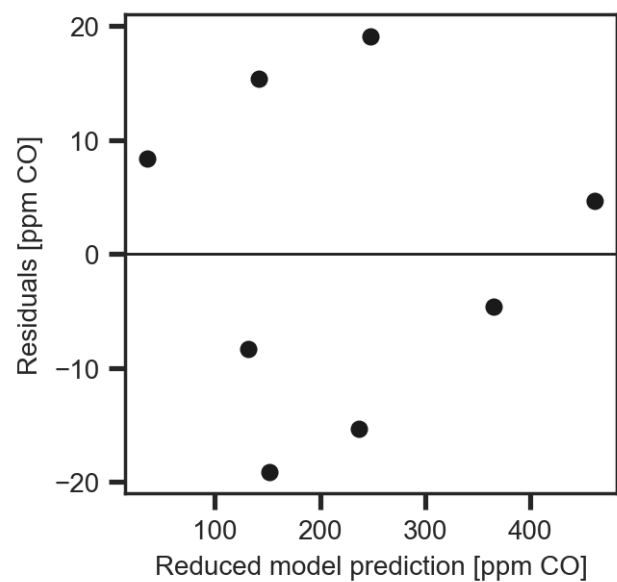


Figure A.10: Plot of residuals versus predicted yield.

### A.4.2 Total Hydrocarbons - Data Set 4

Table A.16: Effect estimates, aliases, regression coefficients and % contribution with *THC* as response variable in data set 4

| Source   | Alias      | Regression coefficient | Effect estimate | % contribution |
|----------|------------|------------------------|-----------------|----------------|
| <b>A</b> | <b>BCD</b> | <b>2.369125</b>        | <b>4.73825</b>  | <b>31.3</b>    |
| <b>B</b> | <b>ACD</b> | <b>1.692625</b>        | <b>3.38525</b>  | <b>22.4</b>    |
| C        | ABD        | 0.855625               | 1.71125         | 11.3           |
| <b>D</b> | <b>ABC</b> | <b>-1.381375</b>       | <b>-2.76275</b> | <b>18.3</b>    |
| AB       | CD         | 0.460625               | 0.92125         | 6.1            |
| AC       | BD         | -0.355875              | -0.71175        | 4.7            |
| AD       | BC         | 0.448125               | 0.89625         | 5.9            |

Table A.17: ANOVA table with *THC* as response variable in data set 4

| Source   | Regression coefficient | Sum of Squares | DoF | F         | Pr(>F) |
|----------|------------------------|----------------|-----|-----------|--------|
| A        | 2.3691                 | 44.902026      | 1   | 17.653879 | 0.0137 |
| B        | 1.6926                 | 22.919835      | 1   | 9.011264  | 0.0399 |
| D        | -1.3814                | 15.265575      | 1   | 6.001881  | 0.0705 |
| Residual |                        | 0.62495        | 4   |           |        |
| Totals   |                        | 126.96115      | 7   |           |        |

Table A.18: Regression model summary - *THC* - data set 4

| R <sup>2</sup> | Adjusted R <sup>2</sup> | F     | P(F)   | Mean of Response |
|----------------|-------------------------|-------|--------|------------------|
| 0.891          | 0.809                   | 10.89 | 0.0215 | 6.2601           |

Reduced model equation reads:

$$\widehat{THC}_{\text{data4}} = 6.2601 + 2.3691 \cdot A + 1.6926 \cdot B - 1.3814 \cdot D \quad (\text{A.6})$$

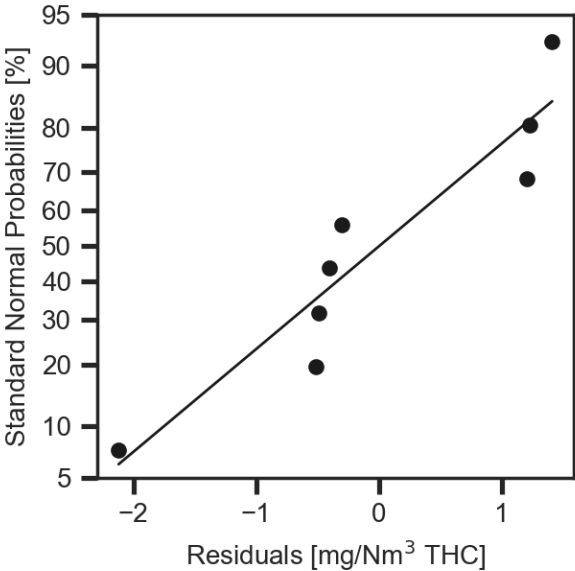


Figure A.11: Normal probability plot

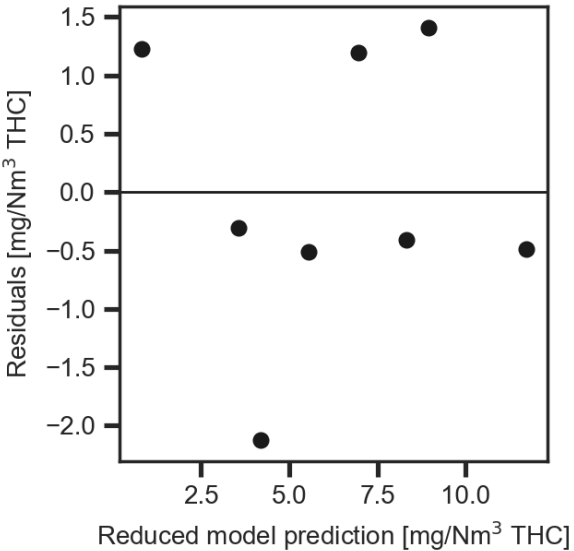


Figure A.12: Residual plot